

Geology, mineralogy and geochemistry of the L-D mine,  
Chelan County, Washington

by

Thomas T. Roberts

Submitted in Partial Fulfillment  
of the Requirements for the degree of  
Master of Science  
in  
Geology

NEW MEXICO INSTITUTE OF MINING AND TECHNOLOGY

Socorro, New Mexico

May, 1990

## TABLE OF CONTENTS

	Page
LIST OF FIGURES	iv
LIST OF TABLES	x
ACKNOWLEDGEMENTS	xi
ABSTRACT	xiii
INTRODUCTION	1
METHODS	5
HISTORY AND PRODUCTION	8
PREVIOUS INVESTIGATIONS	11
<u>Regional studies</u>	11
<u>Local studies</u>	14
<u>L-D mine studies</u>	19
GEOLOGIC SETTING	21
<u>Structure</u>	24
<u>Sedimentary rocks</u>	29
<u>Igneous rocks</u>	31
MINE GEOLOGY	35
<u>Structure</u>	36
Footwall Fissure	36
North-south Faults	39
Bedding Attitudes	42
Small-scale Structures	44
Joints	45
Vein Structures	46
<u>Interpretation of structures</u>	49
<u>Sediments</u>	52
Wenatchee Formation	52
Chumstick Formation	55
Mine Sequence	61
<u>Assesment of stratigraphic relationships</u>	70
<u>Igneous Rocks</u>	74
Andesite	74
Rhyodacite	79
Other Felsic Volcanics	82
Basalt	82
<u>Geologic history</u>	85

ALTERATION	90
<u>Types of alteration</u>	90
Diagenesis	90
Propylitization	93
Silicification	98
Sericitization	104
Argillization	107
Supergene Alteration	109
MINERALIZATION	119
<u>Types of mineralization</u>	119
Major Veins	119
Sheeted Veins	122
Stockwork	122
Breccias	123
<u>Gangue mineralogy</u>	123
Quartz	123
Calcite	132
Adularia	136
<u>Metallic mineralogy</u>	136
Pyrite	138
Arsenopyrite	140
Chalcopyrite	141
Electrum	141
Native Gold	142
Marcasite	147
Acanthite	147
Sulfosalts	147
Native Silver	150
Naumannite/Aguilarite	152
Sphalerite	152
<u>Paragenesis</u>	154
<u>Fluid inclusions</u>	156
TRACE-ELEMENT GEOCHEMISTRY	161
DISCUSSION	170
<u>Setting</u>	170
<u>Hostrock characteristics</u>	171
<u>Alteration</u>	173
<u>Mineralization</u>	174
<u>Supergene processes</u>	177
<u>Considerations on ore genesis</u>	178
CONCLUSIONS	186
REFERENCES	188
APPENDIX I-- THIN-SECTIONS	198
APPENDIX II-- GEOCHEMICAL DATA	204

## LIST OF FIGURES

Figure	Title	Page
1	Map showing the location of Wenatchee.	2
2	Map of the Wenatchee district showing the locations of the mines and silicified outcrops or "reefs".	4
3	A chart showing the progression of stratigraphic nomenclature as applied to the Chiwaukum graben.	16
4	Regional structure map of the Pacific Northwest. (modified from Evans, 1988)	22
5	General geology of the Chiwaukum graben and surrounding region.	25
6	Schematic stratigraphy of the Chiwaukum graben and adjacent Swauk Basin. (modified from Evans and Johnson, 1989)	33
7	General stratigraphic column of sediments in the Chiwaukum graben.	34
8	Surface geologic map of the L-D mine based on surface exposures and limited projection from underground mapping. Mapping by Lovitt Mining, Cyprus Minerals and Asamera Minerals.	37
9	Cross-section of the L-D mine along A-A' oriented N 40 E and looking towards the northwest.	38
10	Photograph of the east strand of the Footwall Fissure exposed in a cut at the 1645 level. The fault separates conglomerate of the Chumstick Formation from mineralized mine sediments.	40
11	Sketch map showing the offset of the L-D mine orebody into three segments by north trending faults. (modified from Patton and Cheney, 1971)	41

12	Contoured stereonet plot of poles to bedding.	43
13	Contoured stereonet plot of poles to joint surfaces in Block One.	47
14	Contoured stereonet plot of poles to veins.	48
15	Cross-section sketch of the Footwall Fissure and the "Flat Fault" of Lovitt and Skerl (1958) (top) and the reinterpretation of the Footwall Fissure (bottom).	50
16	Photograph of the type section of the Wenatchee Formation in Squilchuck Canyon, taken from the L-D mine.	54
17	Photograph of the boulder conglomerate on the east side of the L-D mine, taken from the 1250 level.	60
18	Photograph of the thick, cross-bedded sandstones, and shales of the mixed-load facies of the Chumstick Formation, 120 meters east of the L-D mine.	62
19	Photograph of unaltered mine sequence sediments exposed in a cut 200 meters southwest of the L-D mine.	63
20	Stratigraphic sections of the L-D mine sediments. The sections were measured from drifts and drill holes oriented perpendicular to bedding. Measured by T. Roberts, L. Ott, and M. Klisch.	64
21	QFL diagram of mine sequence sediments in comparison with sandstones from the Swauk Formation.	72
22	Revised schematic stratigraphy of the Chiwaukum graben and adjacent Swauk Basin. This is a more simplified stratigraphy than that proposed by Evans and Johnson (1989).	73
23	Photograph of the andesitic unit adjacent to C-reef. Taken from the top of Block 3.	75
24	Photomicrograph of an unaltered andesite ash-flow tuff at Old Butte. Sample OB-1.	78

25	Photograph of the rhyodacite of Rooster Comb taken from the top of Block 3.	80
26	Photomicrograph of propylitically altered basalt from sample SR-4a 646'.	84
27	Photomicrograph of diagenetically altered sediments from sample I88-2a 32'.	92
28	Photomicrograph of chloritized biotite from the propylitic zone in sample C88-7m 380'.	94
29	Photomicrograph of pyrite replacing biotite in propylitized sediments from sample C88-7m 380'.	97
30	Photomicrograph of hydrothermal quartz overgrowth on detrital quartz in sample C88-7n 16'	100
31	Photomicrograph of early quartz veinlet. Note that the vein is going around detrital grains. Sample C88-8b 121'.	101
32	Photomicrograph of arsenopyrite replacing pyrite in sample C87-2v 293'	103
33	Photomicrograph of sericitized biotite in sample C88-7n 101'.	105
34	Photomicrograph of weakly illitized plagioclase in sample C88-7m 256'.	106
35	Photomicrograph of strongly illitized and sericitized plagioclase in sample 28-10.	108
36	Sketch of fracture controlled oxidation with thin selvage of bleached wall rock from sample C87-2z 42'.	111
37	Photomicrograph of strongly oxidized sediments. Note the absence of phyllosilicates which are normally 10 % of the wall rock. Sample C87-1q 83'.	113
38	Photomicrograph of goethite and hematite in matrix of oxidized wall rock from sample C88-7n 16'.	114

39	Photomicrograph of jarosite in a fracture cross-cutting sediments from sample C88-7m 97'.	115
40	Histogram plot of gold values in ppb for samples of intervals with less than 50 % oxidation (top) and greater than or equal to 50 % oxidation (bottom). n = 299.	116
41	Histogram plot of silver values in ppm for samples of intervals with less than 50 % oxidation (top) and greater than or equal to 50 % oxidation (bottom). n = 299	117
42	Cross-sectional sketch of the distribution of alteration types in the L-D mine. Zones are defined by drill hole information.	118
43	Photograph of the outcrop of the L-D mine looking northeast.	120
44	Sketch of typical vein in Block One. From drill hole C88-8h.	124
45	Cross-section of 49 stope in Block Three. Note the sheeted veins. (from Lovitt and Skerl, 1958).	125
46	Photomicrograph of chalcedonic quartz in sample 12-34 from Block One. Note that it is rimming earlier quartz (top) and a wall rock fragment (bottom).	127
47	Photomicrograph of recrystallized chalcedonic quartz in sample 13E-20. Note the continuous bands of fluid inclusions cutting across grain boundaries.	128
48	Photomicrograph of quartz pseudomorphs after bladed calcite in sample C88-7k 34'.	129
49	Photomicrograph of "stratified quartz" in sample 19-52.	130
50	Photomicrograph of quartz spheres in sample 10-9.	131
51	Photomicrograph of bladed calcite in sample 22-101. Note the boxwork texture and drusy quartz.	133

52	Photomicrograph of blocky calcite filling a vug in sample 19-52.	135
53	Photomicrograph of euhedral adularia in sample 13B-1.	137
54	Photomicrograph of discontinuous veinlet composed exclusively of pyrite in sample C87-2x 115'.	139
55	Histogram plots of electrum grain sizes in samples C88-8A 47' and 1550-2, from Blocks One and Two respectively.	143
56	Histogram plots of electrum grain sizes in samples C88-6A 3' and C88-6A 50' from Block Two.	144
57	Photomicrograph of a large native gold grain in a sample of the 2.5 vein from the 1250 level of Block One.	145
58	Histogram plots of gold grain sizes in samples 5-20 and C87-2C 95' from Block One.	146
59	Photomicrograph of marcasite occupying a fracture in arkosic wall rock from sample C87-1j 178'.	148
60	Photomicrograph of an acanthite grain from sample C87-4m 33'. Note how the grain is partially wrapped around the vein fragment.	149
61	Photomicrograph of pearcite and proustite in sample C87-4m 33'.	151
62	Diagram showing the paragenetic sequence of hydrothermal minerals in the L-D mine.	157
63	Sketches of fluid inclusion textures in quartz.	159
64	Photomicrograph of fluid inclusions in a calcite blade from sample 22-101. in Block Two. Note the coexistence of vapor and liquid-rich inclusions.	160
65	Sketch map of the Wenatchee district showing the general distribution of average trace-element concentration.	169



- 66 Oxygen activity-pH diagram calculated at 285 C and 100 bars.  $a_{Na}/a_K = 6$ ,  $a_{Cl} = 0.05$ , total S = 0.02 molal. Modified from Klisch, 1989. The cross-hatched area is the environment of L-D main stage fluids. 175
- 67 Calculated oxygen activity-sulfur activity diagram for the system Fe-As-NaCl-S-H<sub>2</sub>O at 250 C, pH = 5, and 1.0 m NaCl. Modified from Romberger, 1988. The cross-hatched area is the environment of L-D main stage fluids. 176
- 68 Eh-pH diagram for some iron compounds at 25 C and 1 atm, calculated from the activities of ions in acid water (from Brown, 1971). The cross-hatched area is the environment of L-D supergene fluids. 179
- The Ag-AgCl and Au-AuCl<sub>4</sub> fields are from Mann (1984).
- 69 Conceptual model for the L-D mine. Cross-section is along the Eagle Creek structure. Looking southwest. No scale. 185

## LIST OF TABLES

Table	Title	Page
1	L-D mine production from 1949 to 1967, in ounces per short ton. Compiled by Ott (1988) from Lovitt Mining Co. records. Grade is given as Au/Ag.	10
2	Composition and relative percentages in a sample from the conglomerate member of the Wenatchee Formation. Percentages were determined by the Gazzi-Dickenson method. (from Klish, unpub. data).	56
3	Composition of sediments from the L-D mine.	66
4	Criteria for distinguishing Swauk Fm. from Chumstick Fm.. (from Gresens, 1983).	68
5	List of minerals and their idealized compositions, found in the L-D mine during the course of this study.	153
6	Summary of trace-element variation in several epithermal deposits from around the globe. All values in ppm.	166
7	Characteristics that classify a hydrothermal system as being epithermal (after Lindgren, 1933).	182
8	Characteristics of low-sulfur or adularia-sericite type epithermal systems (after Bonham, 1986 and Heald and others, 1987).	183

## ACKNOWLEDGEMENTS

There are a great many people without whom this thesis would have been impossible. First and foremost, I would like to thank my wife, Jeanice and son, Taylor for encouraging me through the difficult times and not complaining when they never see me, thanks for hanging in there ! A special thank you to my father, who got me interested in geology in the first place and taught me more about it than any other person, and to my mother, who's never ending optimism is a source of inspiration. Larry Ott also deserves a big thanks for his suggestions during the frequent discussions we had on the geology of the district, and for providing much of the entertainment during my first summer in Wenatchee.

I would like to thank Asamera Minerals for their financial and professional support and for putting up with me for three summers. I would especially like to thank Thomas Alexander, Bill Bond, Carl Hale, Eric McCulloch, and John Whitehorn, the geology staff at Asamera, for their friendship, encouragement, and many useful discussions.

Finally, I would like to thank my advisor, Bill Chavez, who took me on as a graduate student and is the sole reason I stayed at Tech. Thanks Bill for your friendship and valuable professional advice. Thanks go to the other member of my committee, Andy Campbell, for his patience and

very helpful comments. There are many other professors and students, to numerous to mention here, who have unknowingly contributed to this thesis, and I thank them.

## ABSTRACT

Epithermal precious metal mineralization of the Wenatchee district and the L-D mine therein, is located in the southern portion of the northwest trending Chiwaukum graben, a major non-marine pull-apart or wrench-fault basin in central Washington. The Chiwaukum graben was active throughout the Eocene, during the Challis volcanic episode, where it occupied an intra-arc setting. Regional wrench-faulting is the product of oblique subduction of the Kula plate beneath the North American plate during this time. The primary structural control on mineralization in the Wenatchee district is the Eagle Creek structure, a major northwest trending wrench-fault within the graben. Local tensional fractures within this structure are the sites of vein hosted mineralization. Mineralization is spatially and temporally associated with the calc-alkalic arc magmatism generated during this period. Sedimentary rocks infilling the graben are the host for mineralization in the L-D mine, specifically, arkosic sandstones of the middle Swauk Formation.

Alteration in the L-D mine is pervasive and is controlled by permeability of the sediments. Most intense alteration consists of silica flooding of the sediments accompanied by sericitic alteration, and is spatially associated with veining. This zone consists of quartz,

sericite, illite, and arsenopyrite. Distal to this, is a zone of weak sericitization characterized by mixed layer illite-smectite. Finally, a broad halo of propylitic alteration occurs throughout the district and consists of chlorite, pyrite, and calcite. The pervasive silicification affected a good seal on the sediments and increased their competence, allowing for brittle deformation and maintenance of tensional openings. Supergene oxidation is prevalent in the upper portions of the mine, but has had no effect on precious metal grades. The supergene assemblage consists of kaolinite, jarosite, goethite, and hematite.

In contrast to alteration, mineralization is strictly structure controlled and is characterized by wide veins, sheeted veins and stockwork. Vein gangue mineralogy consists chiefly of quartz and calcite with subordinate adularia, pyrite, arsenopyrite, and chalcopyrite. Ore minerals include electrum, native gold, sulfosalts, acanthite, and rare native silver, naumannite, and aguilarite. Overall, metallic minerals make-up no more than 2 % of vein material.

Geochemically, the L-D system was rather dilute in terms of associated trace-elements compared to other Au-Ag epithermal systems, with averages as follows: As - 114 ppm, Sb - 8 ppm, Hg - 82 ppb, Se - 4 ppm, Cu - 22 ppm, and Zn - 17 ppm. Conversely, gold and silver average 2.3 ppm and 6.5

ppm respectively, which translates into a Ag to Au ratio of 3:1.

On the basis of vein and alteration mineralogy, it is suggested that the hydrothermal fluids responsible for mineralization were neutral to weakly acidic, potassium metasomatic, low in Cl<sup>-</sup> , low total S, low fO<sub>2</sub>, high CO<sub>2</sub>, dilute, meteoric dominated fluids. From this the L-D system can be classified as a low-sulfur type or adularia-sericite type, epithermal precious metal deposit. On the district scale it is hypothesized that the L-D mine represents deposition from a lateral outflow plume of a convective hydrothermal system centered under Wenatchee Heights.

## INTRODUCTION

The town of Wenatchee is situated at the eastern edge of the Cascade Range, along the Columbia River in Chelan County, Washington. The northwest edge of the Columbia Plateau passes within 2 km east of the city (figure 1). Adjacent to the southern and western city limits, in the foothills of the Cascades, lies the Wenatchee district. The L-D mine is three miles south of Wenatchee, in the southern end of the district (figure 2).

Gold and silver mineralization in the Wenatchee district has been exploited intermittently for one hundred years. Until recently, the only successful operation was the Lovitt mine (later renamed the L-D mine), which was in production from 1949 to 1967. Asamera's Cannon mine, the only current producer, has been in operation since mid-1985. Gold was, and still remains, the principal commodity; silver is the only by-product.

Tertiary age arkosic, fluvial sediments within the Chiwaukum graben are the host of the epithermal, gold-bearing quartz veins in the district. Pre-mineral structures associated with wrench fault activity are the locus of precious metal mineralization and associated alteration. Permeable lithologies play a local role in the pervasiveness of alteration: coarser grained units are generally more silicified than finer grained units. Post-mineral structures play an important part in present-day



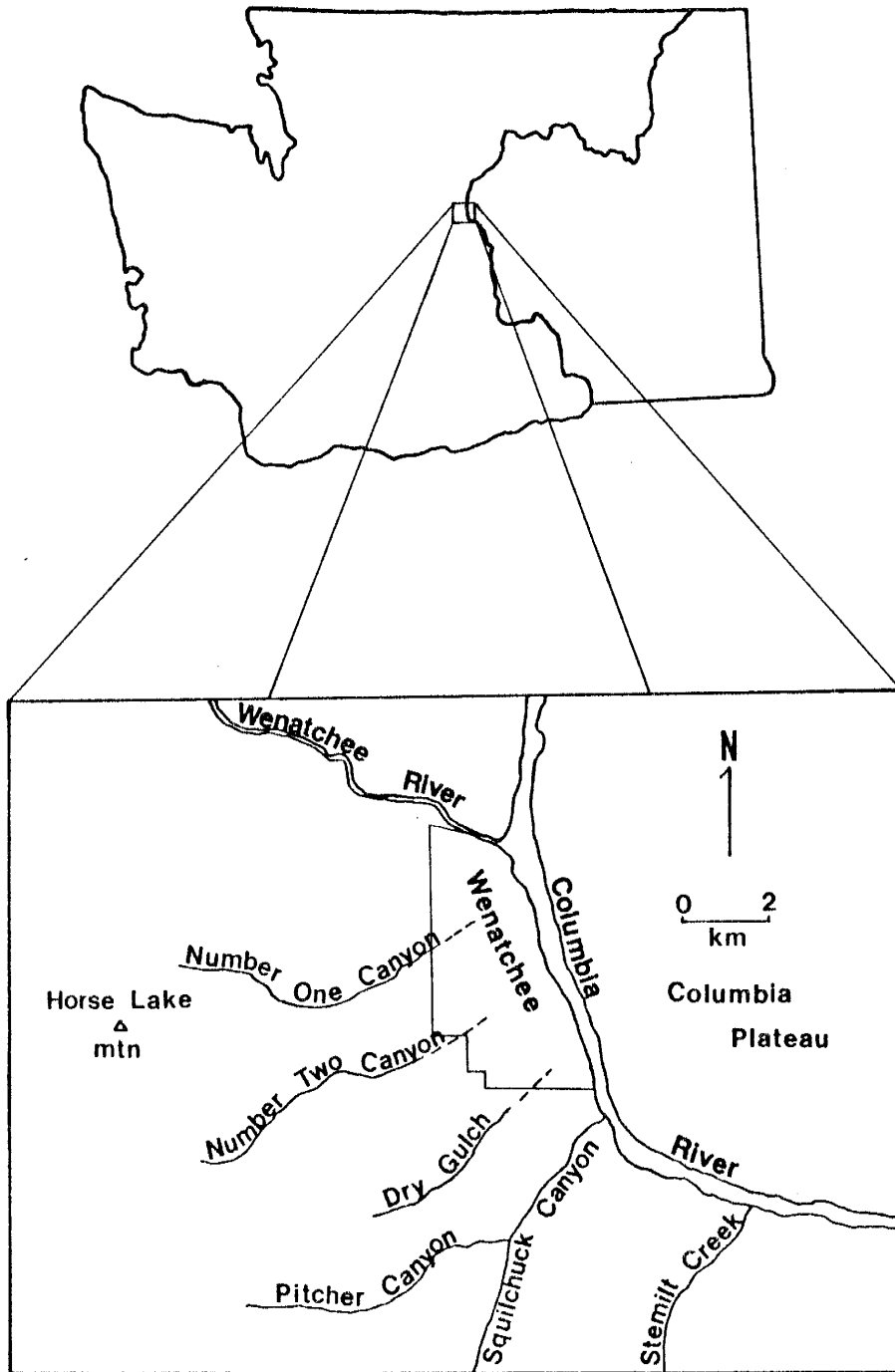


Figure 1- Map showing the location of Wenatchee.

position of mineralized areas and have been the main focus of exploration efforts. In addition to structure, current exploration is focusing on the complicated stratigraphic problems which are only now close to being solved.

The objective of this study is to develop a descriptive model of the L-D mine vein system based on its geologic, geochemical and mineralogic features. This model will be used along with other studies of the Wenatchee district to further exploration efforts in the district by defining structural, lithologic and geochemical relationships between the mineralized areas.

Field work for this study was completed during three consecutive summers (1987 through 1989) while in the employ of Asamera Minerals (U.S.) Inc. Laboratory work was accomplished during the intervening periods at the New Mexico Institute of Mining and Technology.

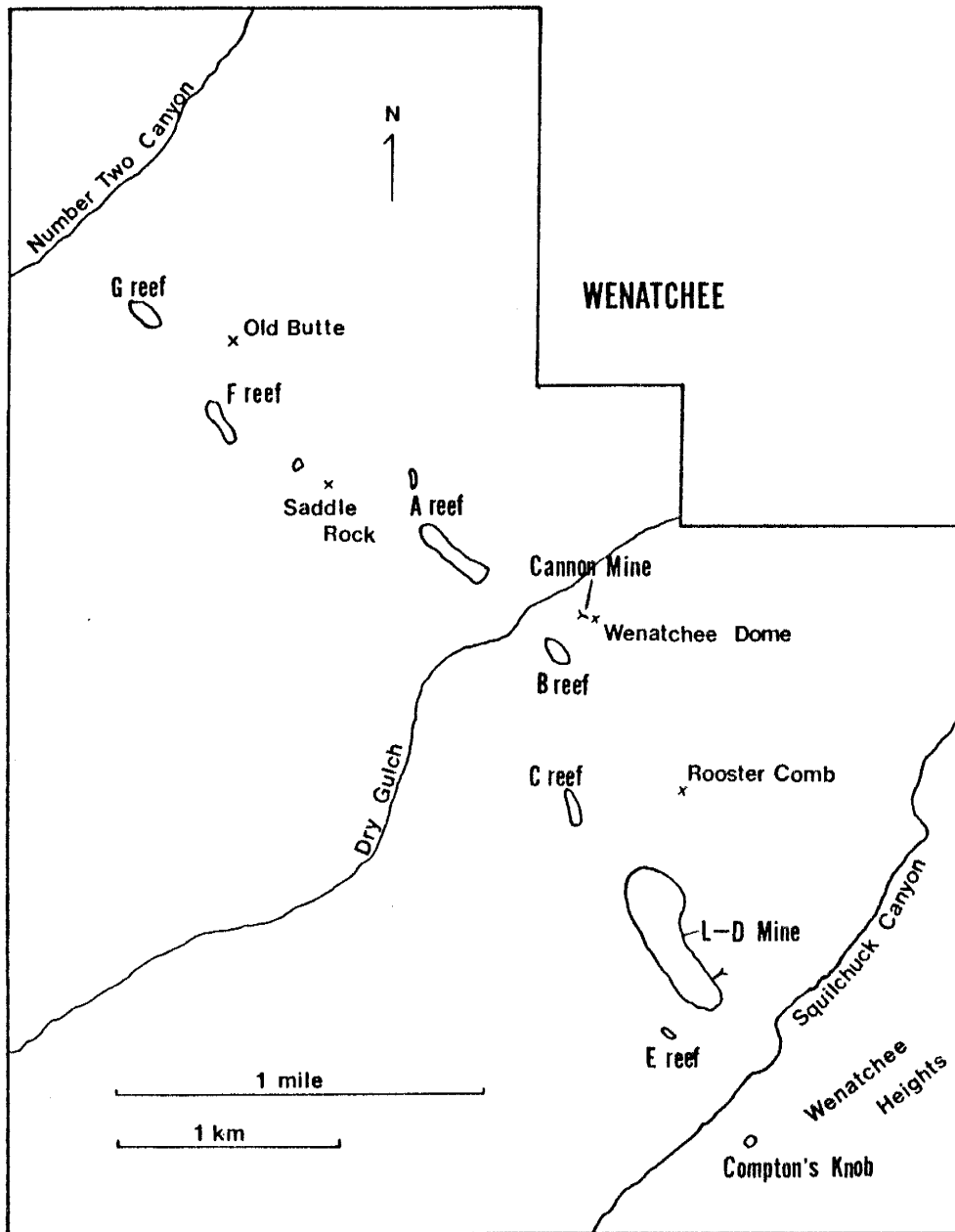


Figure 2- Map of the Wenatchee district showing the locations of the mines and silicified outcrops or "reefs".

## METHODS

My research concentrated on the geologic, mineralogic and geochemical aspects of the L-D mine system. It is designed to answer questions about the chemistry of the hydrothermal fluid(s), stratigraphic position of the host sediments, structural evolution of the mine area, spatial and temporal relationships of mineralization to the geologic evolution of the district, and the influence of structure and host lithology on the position and composition of mineralization. To answer these questions I employed ore petrography, trace-element geochemistry, and interpretation of geologic data collected by myself and many other workers past and present in the region, including mapping done by the Lovitt Mining Company and Asamera Minerals, and diamond drill hole information collected by three companies over the past 16 years.

For this study, quartz vein and host rock samples were collected from various locations in the mine and from diamond drill holes (Appendix I). Because of limited access most of the samples are from the 1250 level and from drill holes. Some samples are from the 1450 and 1550 levels, and the 1645 dump. Block One has received the most coverage as the result of concentrated drilling and because it is the most accessible block. Sampling on the 1450 level is in Block One as well. Block Two was sampled from the 1250 and

1550 levels and from hole C88-6A. Lastly, several surface samples, from the 1645 dump and from the 1250 level, are from Block Three.

Ore microscopy was a major part of my research on the L-D mine. Importantly, ore, gangue and alteration mineralogy and assemblages, and paragenetic sequence were assessed. In addition, the number of periods of mineralization, timing of precious metal deposition, and the chemical evolution of the system can be surmised from petrographic studies. An important result of the detailed petrographic study was recognition of the distribution of alteration minerals and metal phases around the deposit; halos that indicate the direction of fluid flow, and the effect of structure and lithology on localizing mineralization. In addition to the petrographic study, X-ray analysis was employed to identify unknown alteration phases, specifically clays, and microprobe methods to identify unknown mineral phases.

Another significant portion of my work was devoted to the general geology of the L-D mine system. Detailed geologic descriptions and interpretations such as stratigraphic position of the host sequence, structural setting and evolution, relative age of events, and the distribution and attitude of veins were derived from data collected by Asamera Minerals, Lovitt Mining Co., Cyprus Minerals, Anaconda, Tenneco and my own observations made

during nine months of work in the district.

Finally, trace-element geochemistry of wall rock in the mineralizing system comprises another integral part of my research. The trace-element make-up is a key to understanding potential sources for the elements and the chemistry of the fluids responsible for mineralization. In addition, distribution of trace-elements related to mineralization is another indicator of fluid flow. Data for this study was compiled from United Mining Corporation and Asamera Minerals exploration programs, completed in 1983 and 1988, respectively.

## HISTORY AND PRODUCTION

In 1885 a prospector by the name of V. Carkeek staked the Gold King and McBeth claims on the prominent ridge of silicified sandstone that eventually became the L-D mine. To the old timers the obtrusive outcrops of silicified rock were known as "reefs". This particular outcrop was and often still is referred to as the D-reef. Very little work was done on the claims prior to 1894. At that time the Golden King Mining Co. built a five stamp mill and began to drive drifts into the D-reef outcrop (Ott, 1988). Mining and milling was sporadic and eventually the Wenatchee Mining Co. took over around the turn of the century. They also met with little success and decided to abandon the project in 1911 (Lovitt and McDowall, 1954). Poor recovery and low overall grade are cited as the reasons for failure.

The claims laid dormant until 1928, when they were purchased by J.J. Keegan. During the period from 1928 to 1949 Keegan attempted to interest large mining companies in the property. Several companies did evaluate the claims, including the Knob Hill Mining Co. from 1943 to 1945. Knob Hill determined that the property could be mined as a low-grade orebody using surface mining methods, but they took no action (Ott, 1988). In 1949, the Lovitt Mining Co. examined the property and decided that the gold bearing veins could

be mined profitably using underground methods to extract the veins selectively. Lovitt bought the property and began mining (Anon., 1953a). Ore was shipped directly to the smelter in Tacoma, Washington from 1949 to 1962. A brief lull in activity came in 1952 when Anaconda took an option on the property. After a year of evaluation and some development work, they decided against any action and dropped the option in 1953 (Anon., 1953b).

In 1961, the Lovitt Mining Co. entered into a joint venture with Day Mines Inc. of Wallace, Idaho. The mine was renamed the L-D mine and a 30 ton per day flotation mill was erected (Anon., 1962). From 1962 to 1967, concentrate and some direct shipping ore were sent directly to the smelter in Tacoma. In anticipation of ore depletion, L-D Mines increased exploration efforts not only in and around the L-D mine proper, but also other silicified areas within the district. They were not successful and the mine was shut down in 1967. Total production for the period 1949-1967 is given in Table 1.

The claims were leased by Cyprus Mines in the mid-seventies. They spent a couple of years drilling and evaluating the property and did not find enough reserves to be economic. In the early 1980's, Teck Resources picked up the lease and examined the claims. They too decided the property was not economic and dropped the lease. In 1983, United Mining Corporation, in response to the discovery by



Asamera Minerals at B-reef, began to evaluate their properties which included the L-D mine. After a geochemical and drilling program they decided not to proceed. A joint venture between Asamera Minerals (U.S.) Inc. and Breakwater Resources acquired the lease in 1985 and geologists from Asamera are currently evaluating the property as a potential low-grade, heap leach orebody amenable to open-pit methods.

Table 1-- L-D Mine production from 1949 to 1967 in ounces per short ton. Compiled by Ott (1988) from Lovitt Mining Co. records. Grade is given as Au/Ag.

Year	Tons to smelter	Grade	Tons milled	Grade	Total tons	Grade
1949	9,351	.557/.53	----	----	9,351	.557/.53
1950	43,417	.744/.66	----	----	43,417	.744/.66
1951	52,704	.490/.63	----	----	52,704	.490/.63
1952	38,850	.385/.49	----	----	38,850	.385/.49
1953	57,689	.422/.59	----	----	57,689	.422/.59
1954	52,747	.419/.52	----	----	57,747	.419/.52
1955	60,756	.407/.41	----	----	60,756	.407/.41
1956	61,602	.398/.45	----	----	61,602	.398/.45
1957	68,909	.368/.42	----	----	68,909	.368/.42
1958	62,972	.351/.44	----	----	62,972	.351/.44
1959	31,810	.961/1.73	----	----	31,810	.961/1.73
1960	40,339	.859/1.76	----	----	40,339	.859/1.76
1961	40,752	.584/1.14	----	----	40,752	.584/1.14
1962	3,622	.348/.71	40,554	.393/.34	44,176	.389/.37
1963	5,867	.155/.27	82,861	.290/.30	88,728	.281/.30
1964	6,229	.266/.74	88,034	.193/.61	94,263	.198/.62
1965	2,344	.101/.25	85,716	.226/.59	88,060	.223/.58
1966	1,512	.230/.38	90,984	.190/.46	92,496	.191/.46
1967	----	----	6,951	.227/.25	6,951	.227/.25

Total short tons from 1949 to 1967: 1,036,572

Total ounces: Au- 410,482 Ag- 625,849

Average grade: Au- 0.396 oz/ton Ag- 0.60 oz/ton

Silver to gold ratio: 1.525:1

## PREVIOUS INVESTIGATIONS

There are a number of excellent studies done on both the regional and local levels in the Pacific Northwest. Regional studies encompass the broad spectrum of tectonic activity and associated structural, volcanic and sedimentological features that characterize the geological evolution of this part of the country during the Cenozoic era. Local studies are quite thorough and provide excellent documentation of the rock record in and around the Wenatchee district. Studies related specifically to the L-D mine are not as numerous or thorough, but provide an adequate background for this study.

### Regional studies

Early attempts to decipher the igneous history of the Pacific Northwest, in particular the Cenozoic era, were made by Van Houten (1961) and Waters (1962). Their work, although pioneering, lacked the advantage of isotopically determined ages, making absolute timing and correlation difficult. Lipman and others (1971), ten years later, provided a compilation of ages, distribution, and chemical data of volcanic rocks in the western United States. Followed by more data from Lipman and others (1972) and Christiansen and Lipman (1972), these studies served as the basis for all subsequent work. They were the first to

recognize patterns in volcanic activity through time over a large regional area.

Incorporating the above data, Armstrong (1979) provided the first regional synthesis of the igneous history of the Pacific Northwest during the Cenozoic era. His work placed all known volcanic activity into a context of time and related it to motions and interactions of crustal plates that existed during this era. He defined periods of high volcanic activity and periods of relative quiescence. Armstrong concluded that the first 10 m.y. of the Cenozoic was a time of inactivity. Beginning at about 54 ma and ending at 40 ma, the northwest experienced an episode of intense volcanic activity, referred to as the Challis Volcanic Episode. It was during this episode that mineralization occurred in the Wenatchee district. Another period of igneous quiescence began at about 38 ma and lasted until 18 ma. The Columbia Volcanic Episode started at 16 ma and exists today in the Cascade Range.

Ewing's (1980) work dealt with the tectonic evolution of the Pacific Northwest during the early Tertiary. He defined episodes of high tectonic activity and those of relative inactivity. He went as far as to break down tectonic activity into periods of compressive stress and extensional stress by using examples derived from local geologic studies. Ewing, as did Armstrong, then related his observations to the motions and interactions of the crustal

plates. He defined the period from 65-53 ma as one of crustal shortening. Extensional tectonics, characterized by strike-slip and normal faulting, dominated the period from 53-42 ma. This period of extension overlaps the Challis Episode and is responsible for the structural preparation essential for mineralization. Tectonic inactivity characterized the period from 42-30 ma.

Johnson's (1985) publication looked specifically at non-marine sedimentary basins in Washington. He looked at several Tertiary aged basins including the Chiwaukum graben. Johnson concluded that Eocene strike-slip faulting was the mechanism responsible for basin formation and was generated by oblique convergence between the Kula and North American plates during this period. He also concluded that these basins occupied forearc or intra-arc settings.

The work of Heller and others (1987) is similar to Ewing, except that it focused specifically on Washington and Oregon. Their work is also the most recent, and it draws on local studies completed in the interim. This work defined both igneous and tectonic episodes that occurred in early Tertiary time, and defines a transition from a compressional to an extensional regime occurring at approximately 50 ma. As a result, marine and non-marine basins opened up, filling rapidly with sediments during subsidence. The Chiwaukum graben is an example of a non-marine basin formed during this period and the Chumstick

Formation represents basin fill.

The aforementioned regional studies have drawn on voluminous literature concerning the geology at local levels. The following are some of these local studies completed on the Wenatchee area.

#### Local studies

The first recorded geologic descriptions of the Wenatchee area were made by Gibbs (1855). His Pacific Railway exploration party passed through the area of the future city of Wenatchee and described the sequence of lava and interbedded conglomerate near the mouth of the Wenatchee River. Forty-five years later, Russell (1900) working for the United States Geological Survey, did a reconnaissance of the North Cascade Mountains. He defined the Swauk Formation near the city of Wenatchee. The first descriptions of the district were completed by Smith and Calkins (1904). They described the sediments and reported the occurrence of rhyolite and andesite at the mouth of Dry Gulch. The Chiwaukum graben was later defined and described by Willis (1953).

Stratigraphy in the Chiwaukum graben is complicated at best, but a great deal of detailed work has been completed (figure 3). Waters (1930), who did the first detailed work on the northern part of the graben, grouped all of the sediments into the Swauk Formation. Chappell

(1936) described the Wenatchee area and classified the sediments as Swauk Formation as well. Further work on the sediments in the northern part of the graben by Whetten (1976) redefined the sediments as the Chumstick Formation. Whetten dated the formaion at 45 ma and defined its characteristics. He interpreted the formation as the infilling fluvial sediments deposited during subsidence of the graben. Using sedimentology and paleocurrent directions, Whetten (1977) later substantiated his previous interpretations.

Gresens focused his attention on the southern half of the graben. In an abstract written in 1976, he characterized another formation found in the graben. The Wenatchee Formation, as he named it, is the youngest of the Tertiary sedimentary units at 34 ma. A more detailed study by Gresens and others (1981) further distinguished between the Chumstick and the Wenatchee Formations, as well as providing discussions of contact relationships, age determination, and depositional environment. Gresens (1983) later identified an area in the southern half of the graben where the Swauk Formation is exposed. There is, however, a great deal of disagreement about the occurence of the Swauk Formation in the graben. Evans (1988) defines only two formations in the graben, the Chumstick and the Wenatchee. His descriptions of the Chumstick Formation are the most detailed to date.

Russell (1900)  
 Waters (1930)  
 Chappell (1936)

Whetten (1976)

Gresens (1976)  
 Evans (1988)

Gresens (1983)  
 This Study

		Wenatchee	Wenatchee
Swauk	Chumstick	Chumstick	Chumstick
			Swauk
Swakane Biotite Gneiss			

Figure 3-- A chart showing the progression of stratigraphic nomenclature as applied to the Chiwaukum graben.

Structural studies within the graben are limited. Employing a gravity study, Silling (1979) attempted unsuccessfully to precisely determine the depth of the graben. She concluded it could be anywhere from 2 to 11 kilometers deep. Gresens did a great deal of the pioneering work on the structural history of the graben (1976b, 1980, 1982, 1982b, 1983). Gresens found that deformation of the Wenatchee Formation places a time constraint on activity of the graben. Structural features within the Wenatchee Formation were found by Gresens (1976) to be controlled by structures in the older units. Gresens (1982) presented two alternatives for development of the graben. The first model consisted of rotation and strike-slip movement and the second is a rhombochasm model. Gresens preferred the second model because it better explained the observed geological features. He summarized the geologic history of the graben in detail in an article published in 1982(a).

More recently, Evans (1987, 1988) described the evolution of the Chiwaukum graben based on his detailed studies of the Chumstick Formation. He concluded that graben development occurred in two sub-basin developments. The existence of a structural high within the basin was first alluded to by Whetten (1976) and Buza (1977) through detailed paleocurrent studies. According to Evans, the first sub-basin opened at 48 ma along the Eagle Creek fault zone and the second at 45 ma along the Leavenworth fault



zone. Early Chumstick deposition, known as phase 1, was part of a continuous depositional system with the Swauk Formation prior to activity along the Leavenworth fault. Two other phases of Chumstick deposition were recorded by Evans (1988), all defined by periodic activity along the major wrench-faults.

The igneous rocks are described in some detail by Smith and Calkins (1904), Chappell (1936), Coombs (1950), Gresens (1982a, 1983), Margolis (1987), Ott and others (1986) and Ott, (1988). Chappell and Coombs gave excellent petrographic descriptions of the rhyodacite and andesite that occur in the district. The most thorough and recent descriptions of the igneous rocks in the vicinity of the mines are given by Ott (1988).

The most thorough report to date on the general geology of the Wenatchee area was completed by Gresens (1983). In it, Gresens discussed in detail the stratigraphy of the sedimentary formations, characteristics of the igneous rocks, structural features, mineralization, interpretations, and geologic history.

A trend of mineralization to the south of the L-D mine is discussed by Margolis (1987). He described the geologic setting, alteration, mineralogy, and genesis of the mineralization and suggested a genetic relationship to the L-D mine. An article by Ott and others (1986) is an introduction to the geology of the Cannon mine, located

three quarters of a mile north of the L-D mine. Ott (1988) completed a detailed study of the Wenatchee district. He describes all aspects of the Wenatchee district, but focused most of the detail on the Cannon mine. A fluid inclusion study of the Cannon mine has been completed by Klisch (1989).

### L-D mine studies

Literature on the L-D mine has been quite general and descriptive and has not addressed many significant problems. An early report on the ore mineralogy, by Moody (1958) found abundant pyrite and native gold as well as hessite (Ag Te) in minor amounts. An early and substantial petrographic study was done by Guilbert (1963). His descriptions of the ore and gangue mineralogy are quite detailed, although his conclusions are based on only ten samples. There are also several internal company reports on mineralogy done by geologists from Anaconda and Cyprus (1950's and 1970's, respectively). Most of these reports are unavailable to this author, and those few that are available are quite general. Asamera recently contracted some microprobe work which included a couple of samples from the L-D mine. They reveal some minerals that are rare and comprise only very minor phases in the L-D deposit.

General descriptions of mine geology were done by

Lovitt and McDowall (1954) and Lovitt and Skerl (1958). They discuss the host rocks, vein orientations and structure. Patton (1967) completed the first detailed study of the mine geology. He described in more detail the characteristics of the host rocks, and aspects of structure. The descriptions are quite general and the interpretations have since been modified. Patton and Cheney (1971) published an article on the structural characteristics based on the findings of Patton.

Recently, Ott (1988) has made a significant step toward understanding the complicated geology. He re-mapped some of the accessible mine workings and described in greater detail the structure and stratigraphy of the host rocks.

## GEOLOGIC SETTING

The dominant geologic feature of the region is the Chiwaukum graben. The graben as it is manifested today was originally defined by Willis (1953). The margins of the graben are delineated by the Entiat fault to the northeast and the Leavenworth fault to the southwest (figure 4). The Leavenworth fault merges at the northern end of the graben with the Entiat fault. The Entiat is a major, linear strike-slip fault and is a splay off the Straight Creek fault originating in the north-central Cascade Range (figure 4). The Chiwaukum graben and its bounding faults trend N30W. Covering the southern end of the graben are basalts of the Yakima Subgroup of the Columbia River Basalt Group (Swanson and others, 1979). The total length of the graben is unknown. Bordering the graben to the east and northwest are Mesozoic basement rocks of the Swakane Gneiss terraine, Chiwaukum Schist and the Chelan Complex (Tabor and others, 1977). Rocks of the Mount Stewart batholith and the Ingalls ophiolite complex (Miller, 1985) are situated on the west-central border. Finally, Eocene non-marine sediments and associated volcanics of the Swauk basin comprise the southwestern border (figure 5). The graben itself is filled with Eocene fluvio-lacustrine sediments with associated volcanics and intrusives.

During formation of the graben and deposition of the sediments, the region was situated in the Challis

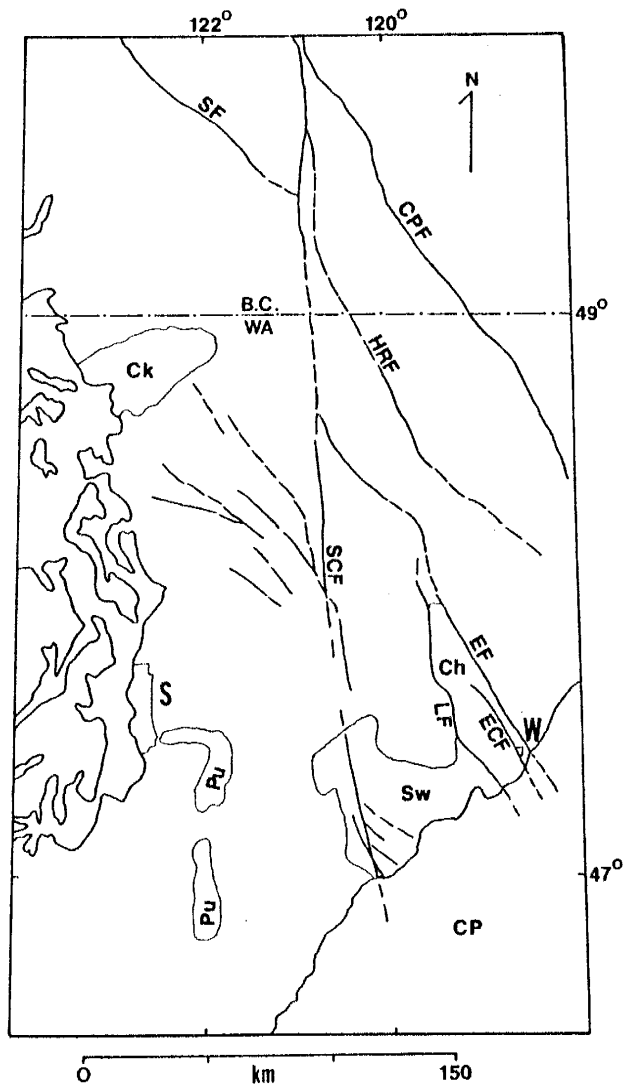


Figure 4- Regional structure map of part of the Pacific Northwest. Sw=Swauk basin, Ch=Chiwaukum graben, Ck=Chuckanut basin, Pu=Puget Group, CP=Columbia Plateau, LF=Leavenworth fault, ECF=Eagle Creek fault, EF=Entiat fault, SCF=Straight Creek fault, HRF=Hozameen-Ross Lake fault, CPF=Chewack-Pasayten fault, SF=Settler fault; S=Seattle, W=Wenatchee. (modified from Evans, 1988)

magmatic arc (Armstrong, 1979). The Challis arc extended from the present Cascade arc to western Montana (Lipman and others, 1972; Armstrong, 1979; Ewing, 1980). Volcanic rocks from this period include andesites and dacites with subordinate rhyolite and basalt. The 52 ma Silver Pass Member of the Swauk Formation and the overlying 47 ma Teanaway Formation are examples. The Challis episode is characterized by non-marine basin formation in an extensional regime (Armstrong, 1979; Vance, 1979; Ewing, 1980; Johnson, 1985; and Heller and others, 1987). The tectonic setting proposed for this period of time is one of slowed convergence between the Kula plate and the North American plate due to subduction of younger, more buoyant crust as the spreading center approached the trench (Engebretson and others, 1984). According to Engebretson, this is the reason for extension in the arc and back-arc areas. Ewing (1980) proposed that the sedimentary basins formed by one of three possible mechanisms: 1) transcurrent faulting due to collision of a continental block, 2) transcurrent faulting due to oblique convergence, or 3) an onland transform similar to the San Andreas fault. Johnson (1985) attributes extension to oblique convergence between the Kula and North American plates. Regardless of the tectonic regime all the authors agree that strike-slip faulting is the mechanism responsible for non-marine basin formation of which the Chiwaukum graben is an example.

In summary, the Chiwaukum graben occupied an extensional intra-arc setting within the Challis magmatic arc during the middle Eocene.

### Structure

Structures within the graben, for the most part, trend at an oblique angle to the bounding faults that define the graben. This northwest structural grain is the most pronounced and seems to have dominated the structural history of the graben. Minor features and inclined bedding were noted by the early geologists during their reconnaissance work. Waters (1930) was the first to describe the structures in detail in the northern part of the graben. He described folding and minor faulting in the Swauk Formation associated with what he defined as the Nahahum graben. The Nahahum graben is actually only a part of the Chiwaukum graben between the Eagle Creek structure and the Entiat fault, corresponding to the eastern sub-basin of Evans (1989).

The Eagle Creek structure is the most important structural feature in the graben. Willis (1953) described the structure as an asymmetrical, open-fold that trends N30W and is closely associated with the Eagle Creek fault zone. The anticline involves sediments of the Chumstick Formation. At the type locality in the northern end of the graben,

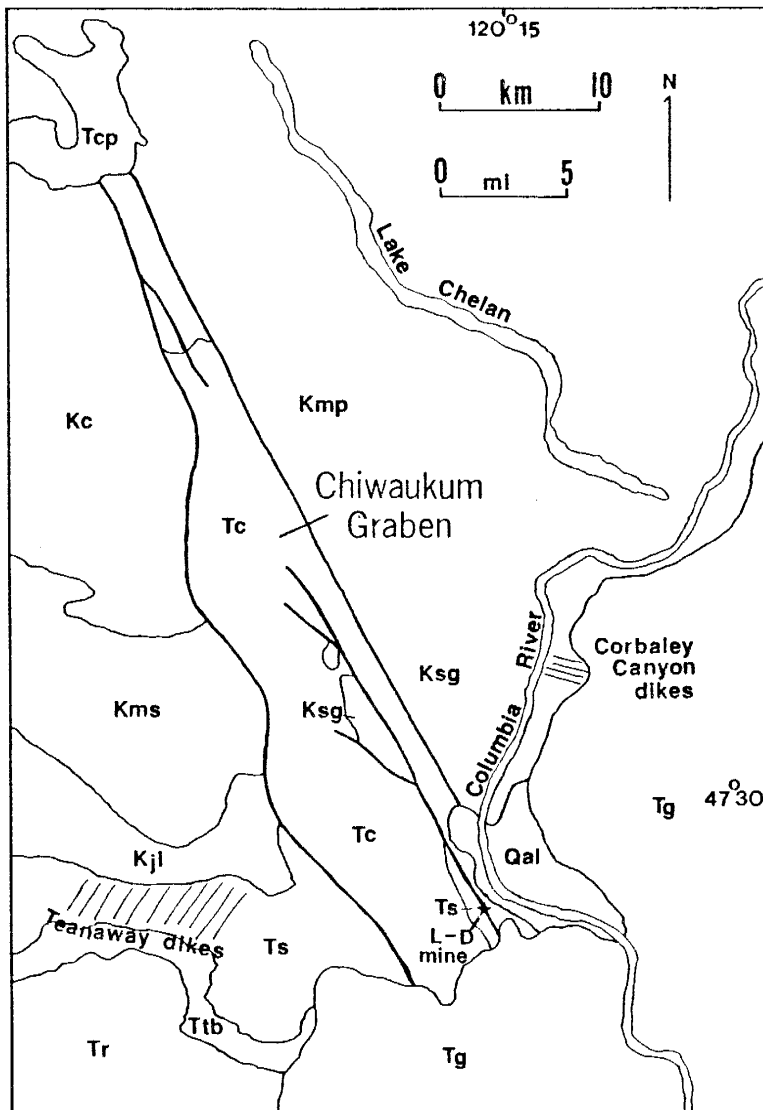


Figure 5- General geology of the Chiwaukum graben and surrounding region. Ts=Swauk Formation, Tc=Chumstick Formation, Ttb=Teaaway Formation, Tr=Roslyn Formation, Tg=Grande Ronde basalts, Tc=Cloudy Pass pluton, Ksg=Swakane Biotite Gneiss, Kji=Ingalls Complex, Kms=Mount Stewart Batholith, Kc=Chiwaukum Schist, Kmp=Chelan Complex.



Swakane Gneiss is exposed in the core. In the southern end of the graben near Wenatchee, the Swauk Formation is exposed in the core of the breached anticline (Gresens 1976). The Eagle Creek fault zone is composed of several, closely spaced, high-angle faults on the northeast limb of the anticline. Willis proposed that the Eagle Creek anticline formed by movement along the fault zone during a period of regional compression, similar to the basement-cored uplifts of the Laramide orogeny in the western United States. Gresens (1983) interpreted the Eagle Creek anticline as a drape fold due to faulting. Ott (1988) referred to the anticline as simply the Eagle Creek structure and interpreted it as a zone of dextral strike-slip faulting. Recently, Evans (1989) defined the Eagle Creek structure as a transtensional step over of the Entait fault. Either way, the structure is an important regional control for localization of igneous rocks and mineralization; and orientation of sedimentary and volcanic units (Chappell, 1936; Gresens, 1983; Margolis, 1987; Ott, 1988).

There are several folds in the Chumstick Fm. within the graben and all roughly exhibit the same N50W trend (Waters, 1930; Chappell, 1936; Willis, 1953; and Gresens, 1976, 1980, 1982a, 1983). These folds are related to the final stage of deformation within the graben from 37-34 ma (Evans, 1988). The Pitcher syncline (Gresens, 1976, 1980, 1983) is also a N50W trending structure, but it is

significantly later than activity associated with deformation of the graben (figure 8). This fold is also an open fold, and is in the Oligocene Wenatchee Formation. The fold axis is parallel to the Eagle Creek anticline, but partially overlies it (Gresens, 1980). The Pitcher syncline is the result of folding during thrust-faulting of the underlying Chumstick Formation during northeast directed compression (Gresens, 1983). The earlier Eagle Creek structure controlled the initial movements during this period of post-Wenatchee compression (Gresens, 1983).

Thrust-faults are another feature of the graben and are described by Gresens (1976, 1980, 1982a, 1983). Notably, drilling by Asamera Minerals does not confirm that some suspected thrust-faults flatten at depth; as such, they may be high-angle reverse faults. These now-suspected reverse faults, although parallel to the graben's structural grain, are post-graben features, but are controlled by earlier graben structures.

Structures that do not exhibit a northwest trend are also observed in the district, and comprise N-S trending strike-slip faults, E-W thrust faults, and west- to southwest-trending folds (Gresens, 1983; Ott, 1988). The set of N-S trending faults were described as important post-mineral structures by Lovitt and Skerl (1953), Patton (1967), Patton and Cheney (1971) and Ott (1988). Mapping by Asamera geologists (Ott, 1988; Klisch and Roberts, 1989) has

revealed several additional N-S faults in the Wenatchee district and they appear to be a common structural feature throughout the district. A set of west- to southwest-trending folds occur in the sediments of the Cannon mine (Ott, 1988). The gold-bearing quartz veins occupy a-c extension joints associated with the folding. This style of folding is not recognized anywhere else in the graben. Finally, E-W trending thrust faults are observed in the Cannon mine (Ott, 1988). They are post-mineral and may be associated with final stages of graben formation/deformation. This unique set of structures observed in the Cannon mine may be due to some local effects not recognized elsewhere in the graben.

Several ideas concerning the development and history of the graben have been put forward. Willis (1953) merely indicates that faulting and shearing in the basement formed the Chiwaukum graben. Whetten (1977) proposed that the graben was made up of two subsidiary grabens separated by the Swakane Gneiss core of the Eagle Creek anticline, suggesting this anticline was a structural high during subsidence of the two sub-grabens. Gresens (1982a, 1983) on the other hand, interpreted graben formation as a single event by one of two mechanisms: 1) clockwise rotation and right-lateral strike-slip movement, or 2) right-lateral strike-slip motion along a fault with an original bend or step, also known simply as a pull-apart basin. A variation

of the Whetten (1977) theme was put forward by Evans (1988). He proposed that the graben developed initially by dextral movement along the Leavenworth fault zone; separation of this single basin having a continuous depositional system between the Straight Creek and Entiat faults, resulted in formation of the Swauk and Chumstick basins. Later, and further to the east, dextral movement along the Eagle Creek-Entiat fault system created a transtensional step-over basin resulting in the formation of two sub-basins within the Chiwaukum graben. Ott (1988) concurs with Evans, based on evidence within the Wenatchee district; Ott (1988) also suggests there was a significant component of rotational strain in the deformation of the Eagle Creek structure, resulting in development of a strong oblique northwest structural grain in the rocks of the graben.

Modern studies of wrench-fault basins reveals these systems exhibit many different structural orientations within the stress regimes that can be attributed to the evolution of a single wrench-fault system (eg. Wilcox and others, 1973).

#### Sedimentary rocks

There are two well-defined sedimentary formations within the graben; one other formation may be distinguished, but its existence is still not agreed upon (figure 6). All

of the sediments in the graben are non-marine, fluvial with deltaic and lacustrine components. The three formations are all Tertiary in age and cover the narrow time span from early Eocene to mid-Oligocene. Sediments constitute by far the greatest volume of the basin fill.

Early to mid Eocene arkosic sediments of the Swauk Formation are found southwest of the Leavenworth fault in the Swauk basin (figure 5). Tabor and others (1982, 1984) describe the Swauk Formation as dominated by dark colored feldspathic to lithofeldspathic subquartzose sandstone, with interbeds of pebbly sandstone, conglomerate, siltstone, and shale. Identification of Swauk Formation within the Eagle Creek structure in the Wenatchee district by Gresens (1983) has been disputed by subsequent workers (Tabor and others, 1984; Margolis, 1987; Evans, 1988). This problem is addressed in a later section.

Mid to late Eocene arkosic sediments of the Chumstick Formation lie entirely within the Chiwaukum graben and is a distinct unit separate from the Swauk Formation (Whetten, 1976). The Chumstick Formation has been described in great detail by Gresens and others (1981) and Evans (1988), but consists generally of feldspathic to lithofeldspathic sandstone, pebbly sandstone, conglomerate, shale and shaly sandstone. Numerous interbedded tuffs occur in the middle of the formation (McClincy, 1986). The Chumstick Formation forms the bulk of the sedimentary basin

fill.

The youngest formation, the early Oligocene Wenatchee Formation, was defined by Gresens (1976) near the town that is its namesake. The Wenatchee Formation is restricted to a relatively small area within a radius of about 10 km around the city of Wenatchee. Quartz sandstone, conglomerate, tuffaceous shale, and thin coal beds comprise the formation (Gresens, 1981).

### Igneous rocks

Two periods of igneous activity characterize the Wenatchee district. An early period of calc-alkaline Eocene igneous rocks are associated with events of the Challis magmatic arc. A final period of calc-alkaline magmatism is late Oligocene and associated with the Cascade arc.

Eocene igneous rocks in the district consist of basalt, gabbro, andesite, rhyodacite, dacite, and rhyolite. Felsic rocks are volumetrically the most abundant followed by andesite, basalt and gabbro. In the southern part of the district, one mile from the L-D mine, Margolis (1987) identified an extensive sequence of felsic volcanic rocks. The NORCO volcanic complex (NVC), as named by Margolis, underlies the Chumstick Formation, is approximately 200 m thick and consists of rhyodacite flows, rhyolite ash-flow tuffs and depositional breccias deposited in a lacustrine environment. In addition, dacite, andesite, rhyolite, and

basaltic andesite dikes are encountered. Margolis identified the NVC as the center of volcanic activity in the area. Ages from the NVC range from 47-40 ma (Margolis, 1987). Further exploration by Asamera Minerals south of Wenatchee Heights indicates that the volcanics may begin to decrease in thickness and extent to the south. It is suggested that a volcanic center exists under Wenatchee Heights, possibly representing a caldera environment.

The Horse Lake Mountain complex, situated just to the west of the Wenatchee district, represents late Oligocene magmatism of the Cascade arc. Hornblende K-Ar dates average 29 ma (Gresens, 1983). Dikes and sills of hornblende andesite porphyry comprise the complex (Bayley, 1965). Mineralization in the Wenatchee district is neither spatially nor temporally associated with this period of activity.

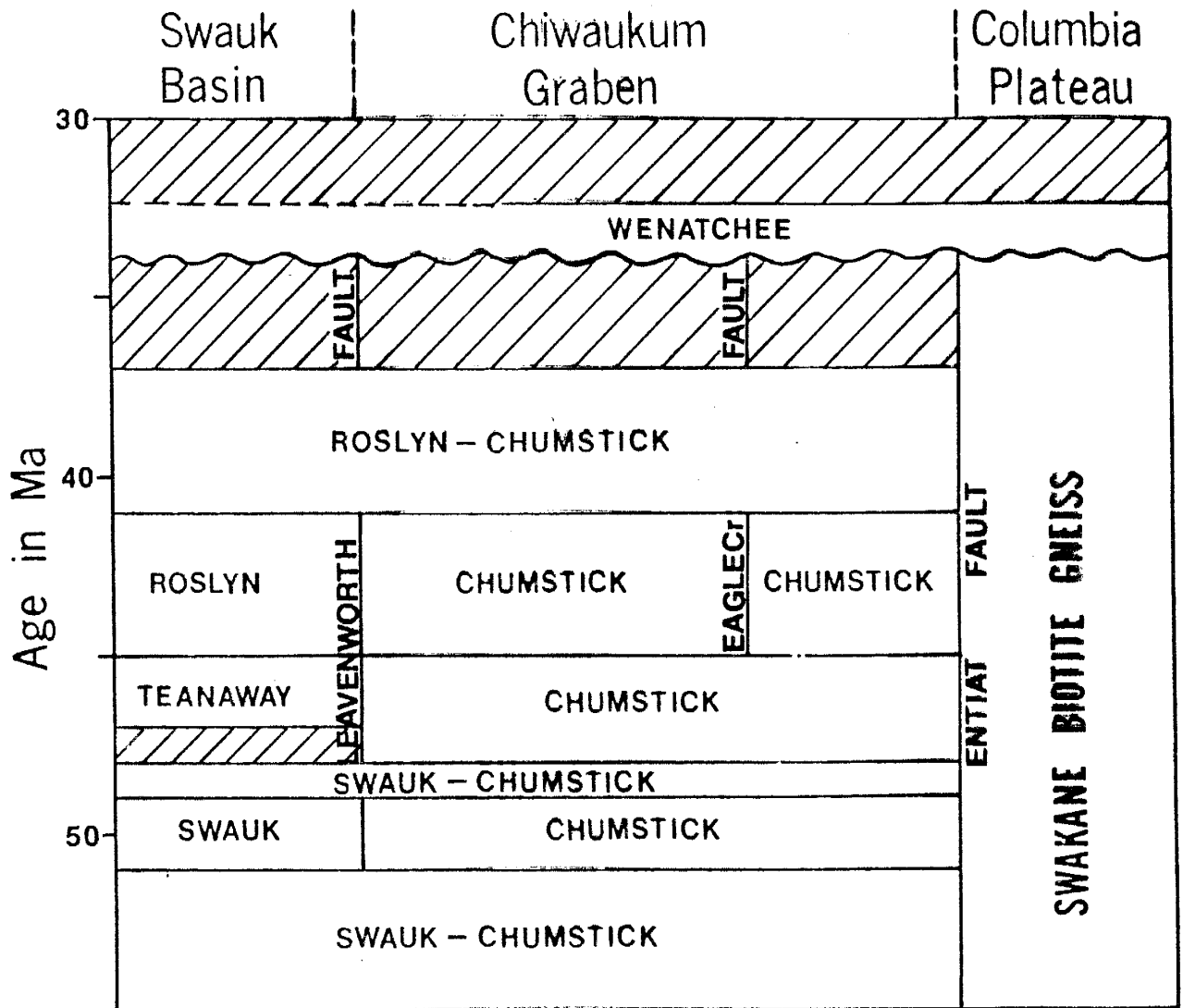


Figure 6-- Schematic stratigraphy of the Chiwaukum Graben and adjacent Swauk Basin. (modified from Evans and Johnson, 1989)



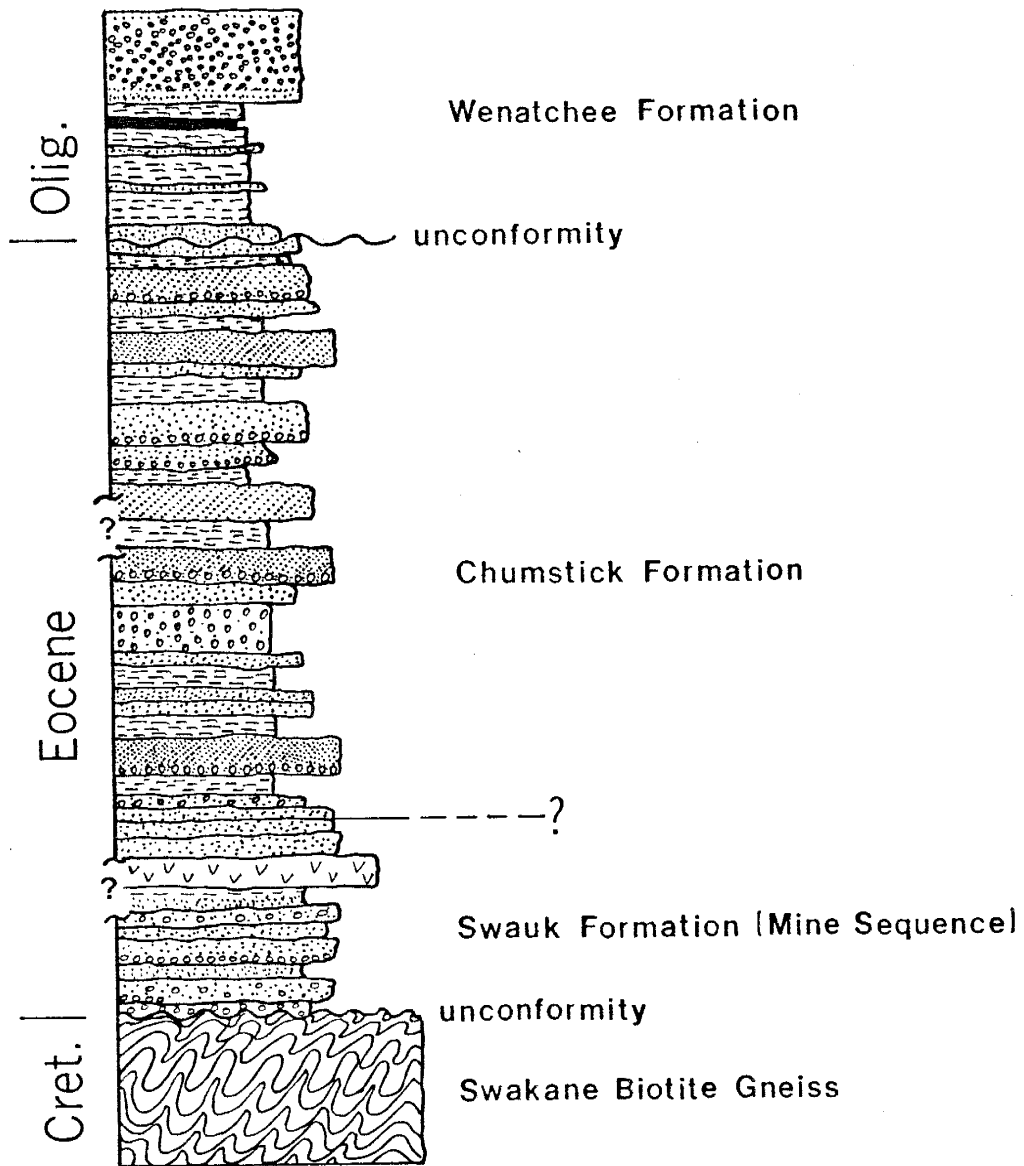


Figure 7-- General stratigraphic column of sediments in the Chiwaukum graben.

## MINE GEOLOGY

The L-D mine is situated in the southern end of the exposed Chiwaukum graben. Basaltic debris and basalt flows of the Columbia Plateau cover the remainder of the graben to the south and southeast. Margolis (1987) interpreted a major northeast trending fault zone under Wenatchee Heights to be the southern bounding fault of the Chiwaukum graben; however, current exploration drilling southeast of Wenatchee Heights has revealed the presence of arkosic sediments and mineralization identical to those within the graben, well outside of Margolis's proposed graben boundary. Exploration over the last five years has indicated the presence of precious metal mineralization as far south as Stemilt Creek (figure 1). The southern projection of the Eagle Creek structure (Gresens, 1983; Ott, 1988; Evans, 1988) passes through the L-D mine, and is the primary control on structural deformation. The mine and surrounding area are exceedingly complex, structurally and stratigraphically. Faulting appears to be the dominant deformational feature.

Rock units of the L-D mine form a prominent, iron-stained and silicified ridge. The ridge strikes N50W and is continuous for 460 meters before intersecting a northeast trending ridge. The mineralized sediments dip steeply to the southwest. Elevation in the area of the mine varies from 268 meters above sea level in Squilchuck Valley to 586 meters above sea level at the top of Rooster Comb.

Topography is relatively steep, but hillsides are generally smooth. Except for the silicified mine rocks and the intrusion of Rooster Comb, outcrops are rare, making geologic mapping and interpretation difficult at best. Figures 8 and 9 are a geologic map and cross-section, respectively, of the L-D mine.

### Structure

#### Footwall Fissure

The most prominent structural feature in the mine is the Footwall fissure. Mapping of the Footwall Fissure is extensive, it is found on old mine maps because of its importance as an ore boundary and has been mapped in detail by Asamera Minerals. The Footwall fissure (FWF) actually consists of two parallel fault strands, the west strand of the Footwall fissure (WFF) and the east strand of the Footwall fissure (EFF). Distance between the two strands varies from 0 to 46 meters and thickness of each individual strand varies from 1.5 to 6 meters. The Footwall fissure is curvilinear along both strike and dip, but overall strike is approximately N50W, and dip averages about 70 SW, roughly parallel to bedding. Displacement along the fault is indicated to be in a reverse direction (Lovitt and Skerl, 1958; Patton, 1967; Patton and Cheney, 1971; Gresens, 1983; Ott, 1988), but the amount of displacement is unknown due

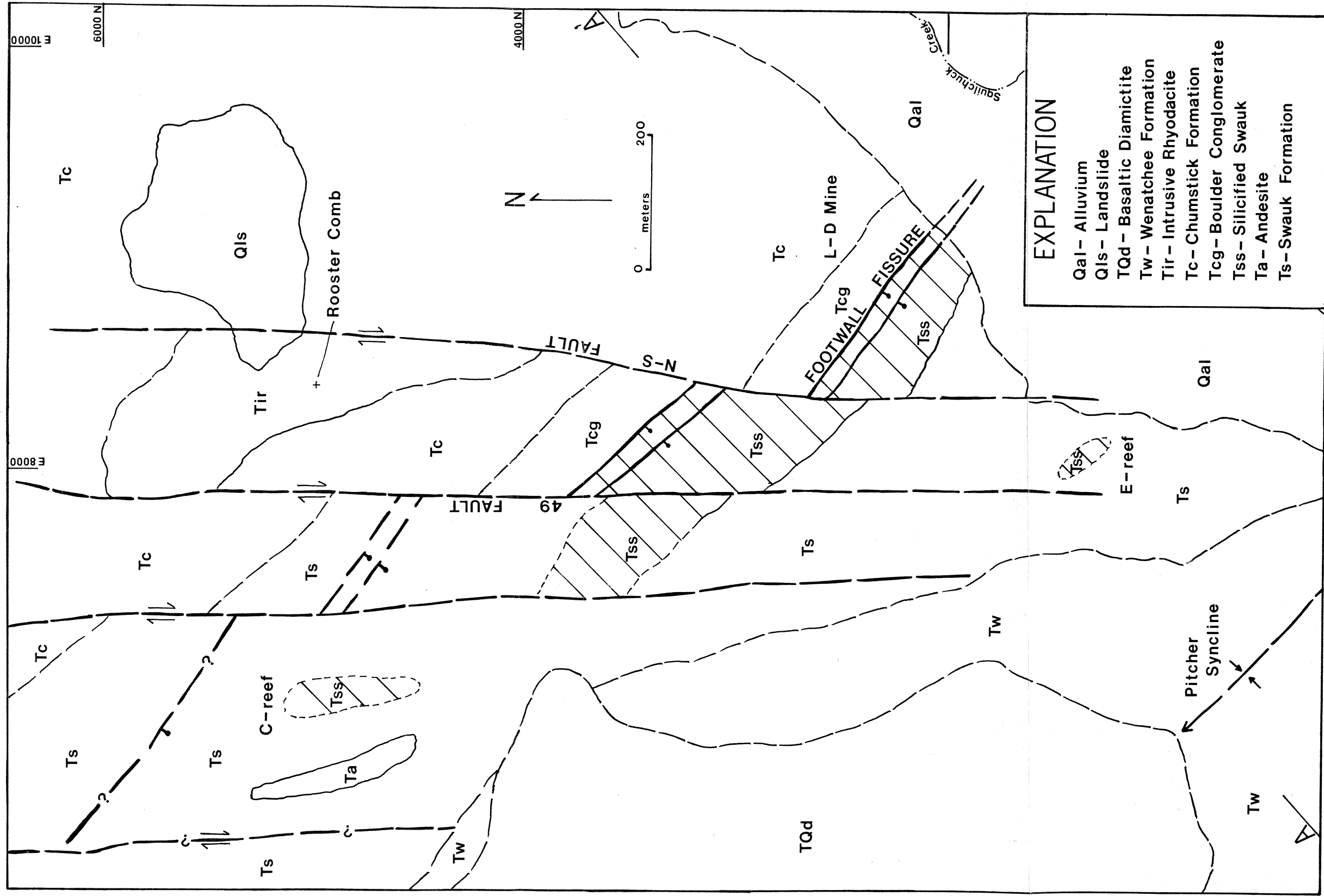


Figure 8 -- Geologic map of the L-D mine.  
Modified from Ott(1988).

to the difficult stratigraphic problems. The EFF separates mineralized Swauk Formation on the west side from unaltered Chumstick Formation conglomerates on the east side (figure 10). The fault zone is characterized by broken unaltered arkose lenses, silicified arkose and vein fragments in a matrix of black, sheared, clayey gouge. Post-mineral movement is suggested by the abrupt termination of major vein structures against the WFF and the termination of silicification against the EFF, as well as the existence of mineralized fragments in the structure.

#### North-south Faults

Another prominent structural feature of the L-D mine is the presence of a set of en echelon, north trending faults that offset the ore body into three blocks (figure 11). The N-S faults are indicated on old mine maps and have recently been mapped in detail (Ott, 1988). Mapping by the author suggests that these structures are important throughout the district. Three faults are identified in the area of the mine, the North-South fault, the 49 fault, and an unnamed fault. The N-S fault separates Block One from Block Two, the 49 fault separates Block Two from Block Three, and the as yet unnamed fault occurs at the west end of Block Three. Strike of the faults varies from due north to N10W, and dips are vertical. Lateral offset on the N-S and 49 faults are 200 and 300 meters respectively,



Figure 10-- Photograph of the east strand of the Footwall  
Fissure exposed in a cut at the 1645 level. The fault  
separates conglomerate of the Chumstick Fm. from  
mineralized mine sediments.

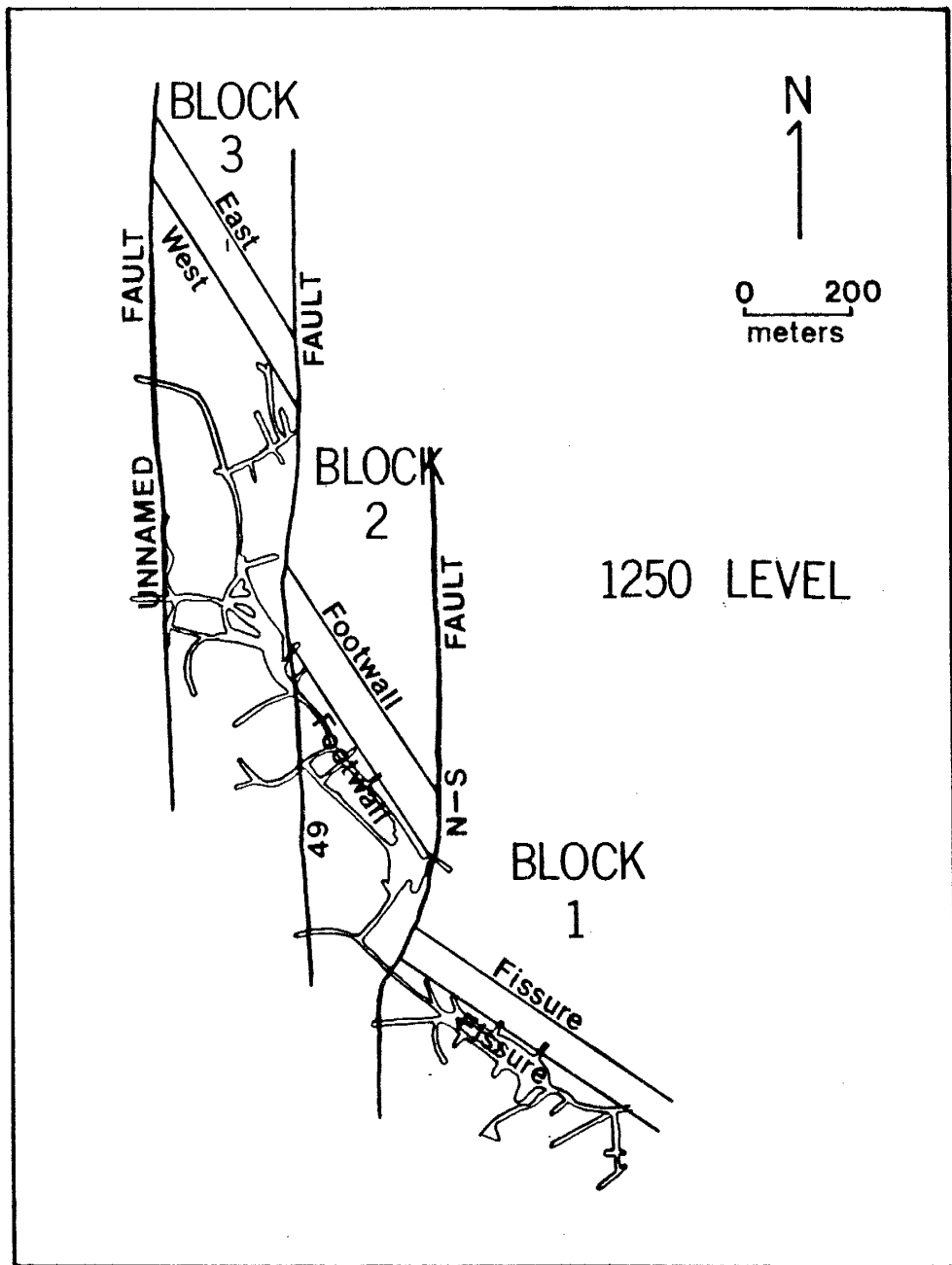


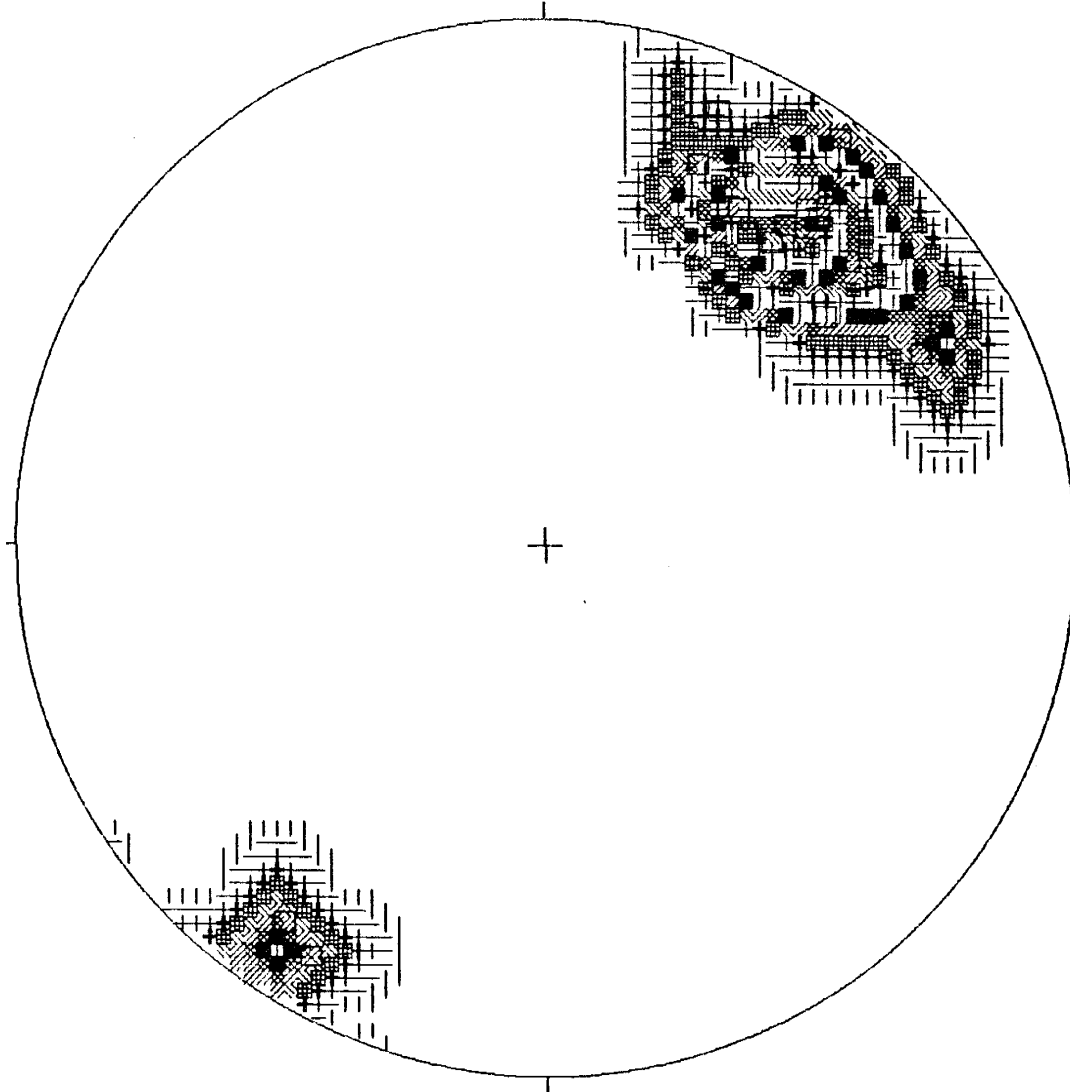
Figure 11-- Sketch map showing the offset of the L-D mine ore body into three segments by north trending faults. (Modified from Patton and Cheney, 1971)

displacement on the unnamed fault is unknown (Ott, 1988). A component of oblique reverse movement is indicated by deformational features within the unnamed fault (Ott, 1988). Reverse movement is clearly the last event, but the amount of dip-slip displacement is unknown. Patton and Cheney (1971) interpreted the faults as high-angle reverse faults. Ott (1988) interpreted them as strike-slip faults that underwent a final stage of reverse movement. Strike-slip displacement is indicated by minor folds in the fault that have near-vertical axes and subhorizontal lineations in the fault gouge (Ott, 1988).

#### Bedding Attitudes

Bedding orientations were measured during underground mapping and taken from old mine maps. The contoured pole diagram constructed from this data (figure 12) indicates two populations. The first, and largest population represents a northwesterly strike with southwesterly dips. The second population is based on only two measurements, and also indicates a northwest strike, but with northeasterly dips. These two bedding orientations were measured between the two strands of the Footwall fissure and probably represents rotation of bedding during differential movement along the faults. Mean pole trend is N 40 E which translates into a mean bedding strike of N 50 W, precisely parallel to the overall internal structural





LEGEND (for first 9 intervals)

□	1- 1	▨	6- 6
▤	2- 2	▩	7- 7
▥	3- 3	▪	8- 8
▦	4- 4	■	9- 9
▧	5- 5		

21 Points

Contour Method: Schmidt (1925)  
 Counting Area: 0.010  
 Contour Interval: 1½ Points per 1% Area  
 Maximum Contour: 29

NOTE: Contour Patterns Repeat Every 9 Intervals

Figure 12-- Contoured stereonet plot of poles to bedding.

grain of the graben, but oblique to the bounding wrench-faults. The mean dip of bedding is 69 degrees. Unlike the west to southwest-trending asymmetric folding prevalent in the Cannon mine, sediments of the L-D mine are folded according to the dominant structural grain in the graben.

#### Small-scale Structures

Small-scale structures are quite common throughout the mine and include low-angle faults (including the "Flat Fault" of Lovitt and Skerl, 1958), strike-slip offsets and bedding-plane slips. Low-angle faults have been mapped on several levels in the mine. These faults strike northwest, dip generally less than 30 degrees southwest and appear as up to 50 cm thick black gouge zones. Offsets along the low-angle faults range from only a meter up to 4 meters in a reverse direction. Both ore bearing and barren veins are offset by these thrust-faults, as well as bedding-plane shears.

Another prominent set of small-scale structures, as indicated on old mine maps and by recent underground mapping, are north to northeast striking faults. These structures are high-angle and offset veins of all attitudes. The faults are characterized by narrow zones of black gouge. Displacement seldom exceeds 3 meters and seems to be strike-slip as suggested by subhorizontal striations in gouge.

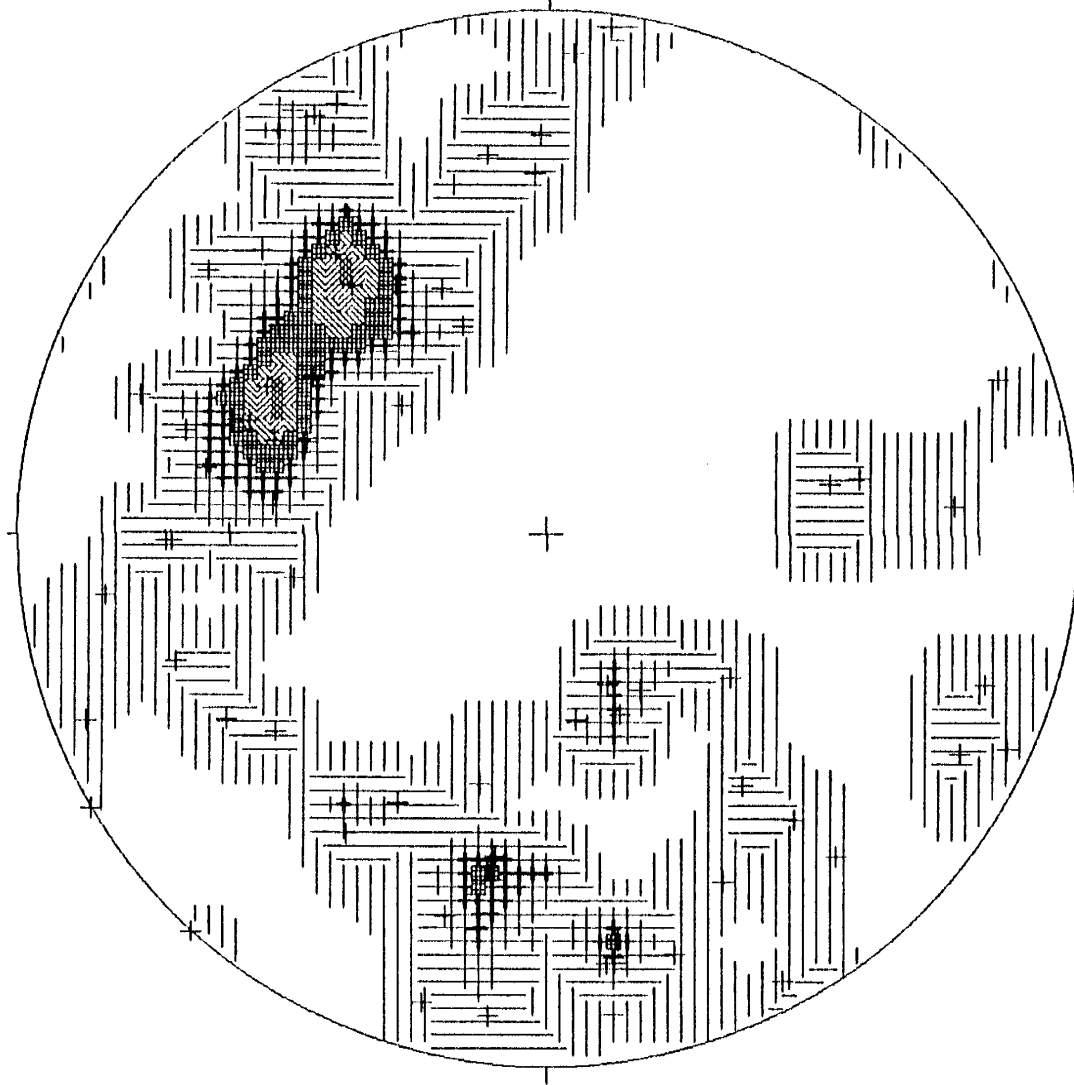
Bedding plane slips are the most common type of structure in the mine. Ott (1988) mapped several of these structures on the 1250 level in Block One and the NW striking, steeply SW dipping structures on the old Lovitt mine maps are also very likely bedding parallel slips. Veins of all orientations are offset by these structures and displacement is generally less than 3 meters, although as much as 9 meters is indicated along some structures. Bedding parallel slips vary in width from as little as a centimeter to as much as 0.5 meters and predominantly occur along black, carbonaceous mudstone beds within the mine sequence.

#### Joints

Jointing is another common feature in the mine. Figure 13 is contour plot of the poles to 84 joints, measured on the 1250 level of Block one. The plot indicates a significant number of joints have a northeast strike and dip moderately to the southeast. Another, less developed joint set strikes northeast and dips moderately northwest. There is an even weaker set of north-west striking joints that dip both southwesterly and northeasterly. Joints are barren of mineralization except for north-dipping joints which are commonly pyritic. Crosscutting relationships between joint sets could not be determined.

## Vein Structures

The most important structural features of the L-D mine are those that host the veins. Vein orientations were measured on the 1250 level and taken from old mine maps for other levels and inaccessible areas. A stereonet plot of poles to veins indicate two well developed populations and one weakly developed set (figure 14). The two well developed vein sets are both northeast striking, but one set dips to the northwest and the other set dips to the southeast. The weaker set strikes northwest and dips to the southwest and are bedding-plane veins. Crosscutting relationships are readily apparent and reveal that the earliest set are the bedding parallel veins, followed by the northwest dipping set and finally the southeast dipping veins. Vein textures, which will be discussed in a later section, indicate the vein hosting structures had to be tensional.



LEGEND (for first 9 intervals)

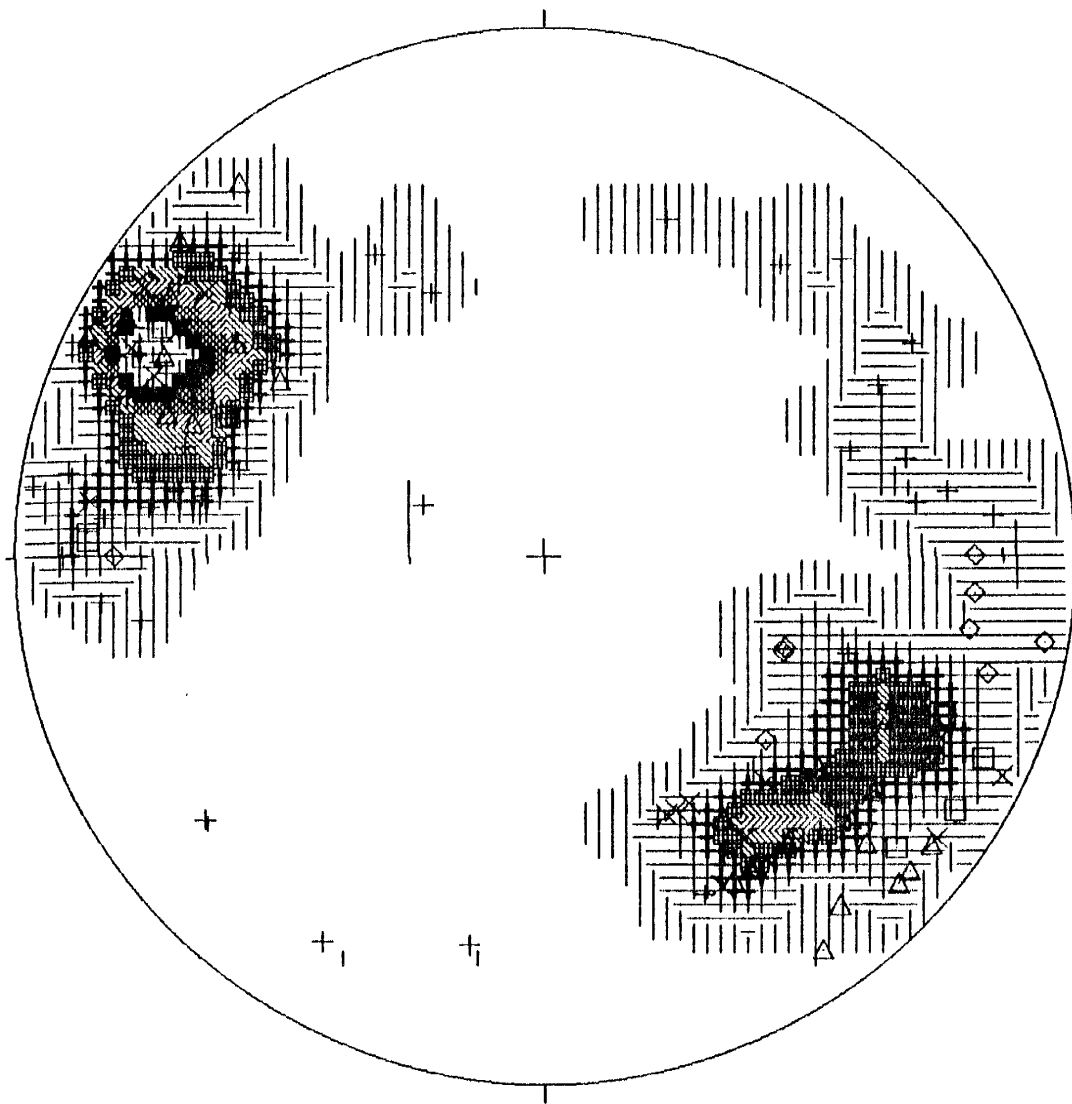
□	1- 1	▨	6- 6
▤	2- 2	▩	7- 7
▥	3- 3	▪	8- 8
▦	4- 4	■	9- 9
▧	5- 5		

84 Points

Contour Method: Schmidt (1925)  
 Counting Area: 0.010  
 Contour Interval: 1% Points per 1% Area  
 Maximum Contour: 8

NOTE: Contour Patterns Repeat Every 9 Intervals

Figure 13-- Contoured stereonet plot of poles to joint surfaces in Block One.



181 Points

LEGEND (for first 9 intervals)

□	1- 1	▨	6- 6
▤	2- 2	▩	7- 7
▥	3- 3	▪	8- 8
▦	4- 4	■	9- 9
▧	5- 5		

Contour Method: Schmidt (1925)  
 Counting Area: 0.010  
 Contour Interval: 1½ Points per 1% Area  
 Maximum Contour: 13

NOTE: Contour Patterns Repeat Every 9 Intervals

Figure 14-- Contoured stereonet plot of poles to veins.

## Interpretation of structures

The Footwall Fissure has been interpreted as a thrust-fault by many previous workers (Lovitt and Skerl, 1958; Patton, 1967; Patton and Cheney, 1971; Gresens, 1983;), but Ott (1988) points out that the "Flat Fault" of Lovitt and Skerl (1958), which was assumed by subsequent workers to be the flattened portion of the FWF (figure 15), may actually be one of the numerous low-angle reverse structures common in the L-D mine (these are small-scale structures and are discussed in a later section). A review of drill logs acquired from the years of drilling by many companies just does not support the idea of a thrust-fault, as no major low-angle fault has ever been recorded in the logs. The Footwall Fissure, therefore, is better termed as a high-angle reverse fault initiated during NE-SW directed compression that occurred during the Oligocene. The Footwall Fissure is the youngest structure in the mine.

Orientation and the en echelon pattern of north-south faults is consistent with their origin as antithetic strike-slip faults generated in response to dextral movement along the Eagle Creek structure. The component of reverse displacement may have occurred during the same Oligocene compressional event that produced the Pitcher syncline in the Wenatchee Formation and initiated the Footwall Fissure. N-S faults cross-cut all structures in the mine suggesting

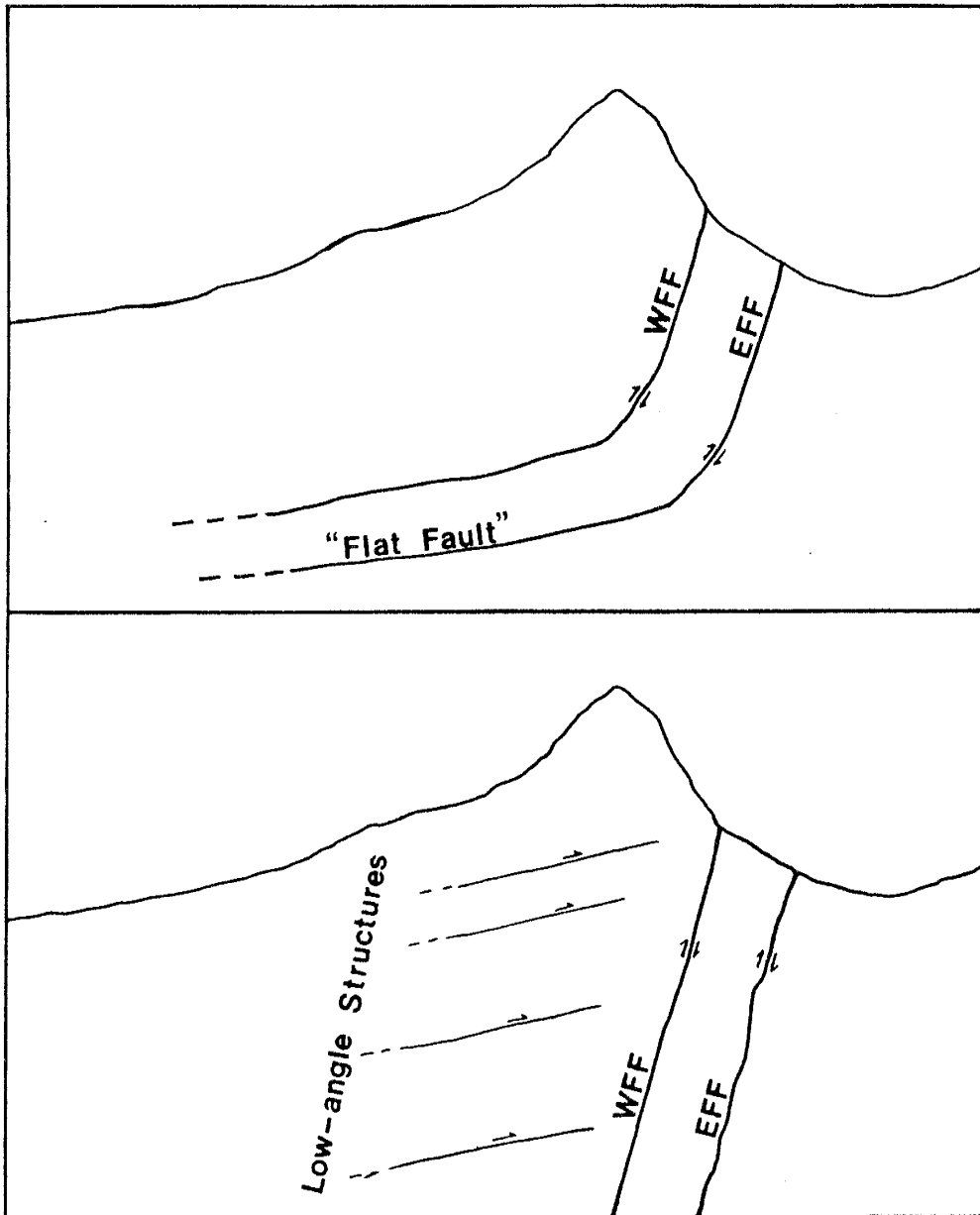


Figure 15-- Cross-section sketch of the Footwall Fissure and "Flat Fault" of Lovitt and Skerl (1958) (top) and the reinterpretation of the Footwall Fissure (bottom).



that they are among the youngest structures associated with deformation of the mine sediments.

Associated with the N-S structures are small-scale north and northeast trending structures. They are parallel to sub-parallel to the larger N-S faults, exhibit the same lateral offset and are interpreted to be the result of stress generated within the blocks between the major structures. As indicated by cross-cutting relationships, these structures are among the last generated during deformation of the host sediments.

As suggested by the orientation of bedding, sediments of the L-D mine probably represent one limb of a northwest-trending fold generated during continued wrench-fault activity. The orientation of the fold is consistent with other folds in the graben. Recent drilling in the same sediments north of the L-D mine encountered what is interpreted to be an anticline which has the same orientation as the folded mine sequence (Roberts, 1988).

In support of the folding hypothesis is the occurrence of bedding-plane slips which suggest flexural-slip folding. These structures offset veins, suggesting that folding is post-mineral. The joint pattern can also be interpreted as related to a folding event, and the fact that the joints cross-cut veins and are unmineralized indicate the folding event post-dates at least main stage mineralization. Folding apparently occurred after

mineralization, but prior to the development of N-S faults.

In contrast to veins in the Cannon mine, which are interpreted to be fold-related a-c extension joints (Ott, 1988), major veins in the L-D mine are arranged in an en echelon pattern and are vertically and laterally continuous, not indicative of fold related joints. The vein structures are interpreted instead as tension fractures within the Eagle Creek structure and their orientation is consistent with right-lateral wrenching. Cross-cutting relationships indicate that vein structures were the first structures to be generated during deformation of the mine sediments.

### Sediments

Sedimentary rocks are the most abundant lithologic types in the vicinity of the mine. As discussed in an earlier section, the number of distinct formations within the graben is controversial. Below are described two of the formations which occur within the graben, as well as the "mine sequence", which I believe to be a third sedimentary formation within the Chiwaukum graben.

#### Wenatchee Formation

The Wenatchee Formation was formally identified and described by Gresens and others (1981) and is the youngest formation in the area. Total thickness of the Wenatchee Formation is 253 meters. Zircon dates from

preserved tuff beds reveal an age of 34 ma. Previous workers (Russell, 1900; Smith and Calkins, 1904; Chappell, 1936; and Alexander, 1956) included the quartzose sandstones of the Wenatchee Fm. with the Swauk Fm. However, deposition of the Wenatchee Fm. was apparently not controlled by the Chiwaukum graben because outcrops are found east of the graben bounding Entiat fault. The type section occurs approximately 150 meters west of the mine (figure 16). Contact relationships with the mine sequence rocks are not exposed and have not been drilled. Gresens (1980, 1983), however, indicates the contact is unconformable.

The Wenatchee Formation is formally divided into two members, a sandstone and shale member overlain by a conglomerate member. Gresens and others (1981) further subdivided the sandstone and shale member into three distinct subunits: 1) shale-dominated fluvial beds, 2) sandstone-dominated fluvial beds, and 3) lacustrine shale and sandstone beds.

The shale-dominated subunit consists of grayish-blue tuffaceous shale and siltstone with interbeds of buff, fine to medium grained quartz sandstone. The sandstone-dominated subunit consists of cross-bedded, medium to coarse quartz sandstone. Lacustrine beds are composed of brown shales, siltstones and minor sandstones. The overlying conglomerate member is characterized by poorly sorted



Figure 16-- Photograph of the type section of the Wenatchee Formation in Squilchuck Canyon, taken from the L-D mine.

conglomerate and sandstone.

A petrographic study by Klisch (unpub. data) on a sample from the conglomerate member reveals a texturally immature rock that is poorly sorted, having angular to subrounded grains and a relatively high matrix content. Table 2 lists the composition and relative percentages of components in the sample. In addition, tuff clasts are noted in hand specimen. Textural immaturity and composition indicate a local source for the Wenatchee Formation, but one that is weathered deeply enough to remove mafic minerals. Gresens and others (1981) proposed that the Swakane Biotite Gneiss and reworked Chumstick sediments are the most likely sources. The large percentage of monocrystalline quartz, however, is more indicative of a reworked sedimentary source or a volcanic source.

#### Chumstick Formation

As early as the turn of the century, it was recognized that the thick sedimentary pile in central Washington could be subdivided into distinct units. Russell (1900) divided the "Swauk Formation" into the older "Wenache sandstone" and the younger "Camas sandstone". Smith and Calkins (1904), however, argued that differences throughout the region were due to facies changes in a large lake. Waters (1932) agreed with the interpretation of Smith and Calkins and grouped all sediments in the northern part

of the graben into the Swauk Fm., as did Chappell (1936) in the area around the town of Wenatchee. In 1956, Alexander

Table 2- Composition and relative percentages in a sample from the conglomerate member of the Wenatchee Formation. Percentages were determined by the Gazzi-Dickenson method. (from Klisch, unpub. data)

<u>COMPONENT</u>	<u>PERCENTAGE</u>
Monocrystalline quartz	41
Polycrystalline quartz	16
Potassium feldspar	1.75
Meta-sed lithics	2
Zeolites	9.25
Matrix	29
Miscellaneous	1
Total	100

undertook a detailed sedimentary study in the area and his results corroborated the earlier hypothesis of Russell. Gresens and others (1981) confirmed the existence of two separate formations and formally named the older of the two the Chumstick Formation after exposures along Chumstick Creek north of Leavenworth, Washington.

The Chumstick Formation as defined by Whetten (1976) and Gresens and others (1981) consists chiefly of fluvial sandstones, conglomerates and mudstones with an upper fine grained lacustrine unit known as the Nahahum Canyon member. This upper lacustrine unit occurs in the vicinity of the mine. Evans (1989) on the other hand has reinterpreted the Chumstick Formation as a humid-tropical alluvial-fan system and divided it into three depositional phases occurring in two sub-basins of the Chiwaukum graben, which he refers to as the Chumstick basin.

The three phases of deposition as interpreted by Evans are an early period of fluvial activity in the western sub-basin, followed by continued fluvial activity in the western sub-basin and combined fluvial-lacustrine deposition in the eastern sub-basin. The third and final depositional phase consisted of a continuous fluvial system across both sub-basins. Age dates from zircons in tuffs and detrital zircons from sandstones range from 49 to 42 ma (Whetten, 1976; Evans, 1988).

Four facies associations were recognized by Evans(1989) and include: 1) gravel-bedload stream deposits, 2) sand-bedload stream deposits, 3) mixed-bedload stream deposits, and 4) lacustrine deposits. Gravel-bedload facies consists of 40 to 90% pebble-cobble conglomerate with subordinate amounts of sandstone. Clasts in the conglomerates include primarily biotite gneiss, schist,

granite, granodiorite, felsic to intermediate volcanics, and vein quartz. Sand-bedload deposits consist of 40 to 90% sandstone, 10-30% shale, and up to 50% conglomerate. Mixed-load deposits are composed of 50-70% cross-bedded sandstone and 30 to 50% mudstone. The lacustrine facies is 50 to 60% planar-bedded sandstone and 40 to 50% mudstone.

The ore-hosting, Chumstick sediments in the Cannon mine are divided by Ott (1988) into four units based on the proportions of sand, silt and mud, bedding and structures. Unit 1 consists of evenly bedded medium grained sandstone and siltstone. Individual beds are about 50 cm thick and carbonaceous material is locally abundant. Unit 2 is made up of thinly bedded silty sandstone. Carbonaceous material and soft-sediment deformation are common. Unit 3 is composed of massive feldspathic sandstone that ranges from medium to very coarse grained and locally conglomeratic. Unit 4 consists of interbedded siltstone and carbonaceous claystone. The sediments are light-gray, poorly sorted, and grain shape ranges from angular to subangular. Composition includes quartz, K-spar, plagioclase, chlorite, muscovite, zircon, and epidote in a matrix of clays.

Understanding of the stratigraphy in the graben has been greatly advanced by the recognition of tuff beds in the Chumstick Formation. Tuff beds are preserved ash-fall and ash-flow tuffs, as well as water-laid tuffs of rhyolitic composition (76-79% SiO<sub>2</sub>). McClincy (1986) recognized



nineteen distinct tuff beds based primarily on REE chemistry. Tuffs have been recognized by Ott (1988) and Mehlhorn (personal comm., 1989) in the Cannon mine sediments and work is in progress to attempt to use the tuffs as marker horizons to decipher the stratigraphic position of mine sediments and in interpreting structures.

Chumstick Fm. rocks adjacent to the L-D mine have not been studied in detail. Mapping of limited outcrop and underground diamond drilling indicate the presence of a coarse cobble conglomerate (figure 17) on the east side of the mine sequence which is in fault contact with the silicified sediments. This conglomerate is composed chiefly of subrounded to well rounded porphyritic volcanics, plutonics, gneiss, and quartz vein clasts up to 15 cm in diameter. Minor sandstone and mudstone beds are also encountered. One drill hole went through 52 meters of conglomerate before being shut down, still in conglomerate. This unit is interpreted as a fan conglomerate adjacent to the Eagle Creek fault. Recent mapping (Klisch and Roberts, 1989) indicates that this boulder conglomerate is quite extensive and is present as far north as the Cannon mine, where it occurs along the western boundary of mineralization.

I interpret the sediments adjacent to the silicified mine sediments as belonging to the proximal, gravel bedload and sand-bedload facies of the Chumstick Formation which was deposited adjacent to the Eagle Creek



Figure 17-- Photograph of the boulder conglomerate on the east side of the L-D mine, taken from the 1250 level.

structure. Further to the east are cross-bedded sands and shales of the distal mixed-load facies (figure 18). The sedimentary package hosting mineralization in the Cannon mine is extremely complex due to deformation, but probably corresponds to the more distal, mixed-bedload and lacustrine facies of the alluvial-fan system. The coarse cobble conglomerate directly adjacent to the L-D mine is a fanglomerate deposited relatively close to a structural high.

#### Mine sequence

Sediments of the L-D mine are distinctly different from those that host mineralized veins in the Cannon mine. The L-D mine rocks are a monotonous sequence of interbedded sandstones, siltstones, shales, and conglomerates. Sandstones range from coarse to fine grained, are poorly sorted, and grains are angular to subrounded. Unaltered sandstones are medium gray when fresh and weather to a light gray or white (figure 19). The sandstones are not well indurated, therefore, they weather easily and form slopes and low areas throughout the district. Outcrop exposure of these sediments is extremely rare and mapping is frequently done based on the occurrence of cobble and pebble float from conglomeratic beds.

Medium and coarse sandstones of this sequence are massive, while fine grained sandstones are laminated or



Figure 18-- Photograph of thick, cross-bedded sandstones and shales of the mixed-load facies of the Chumstick Formation, 120 meters east of the L-D mine.



Figure 19-- Photograph of unaltered mine sequence sediments exposed in a cut 200 meters southwest of the L-D mine.

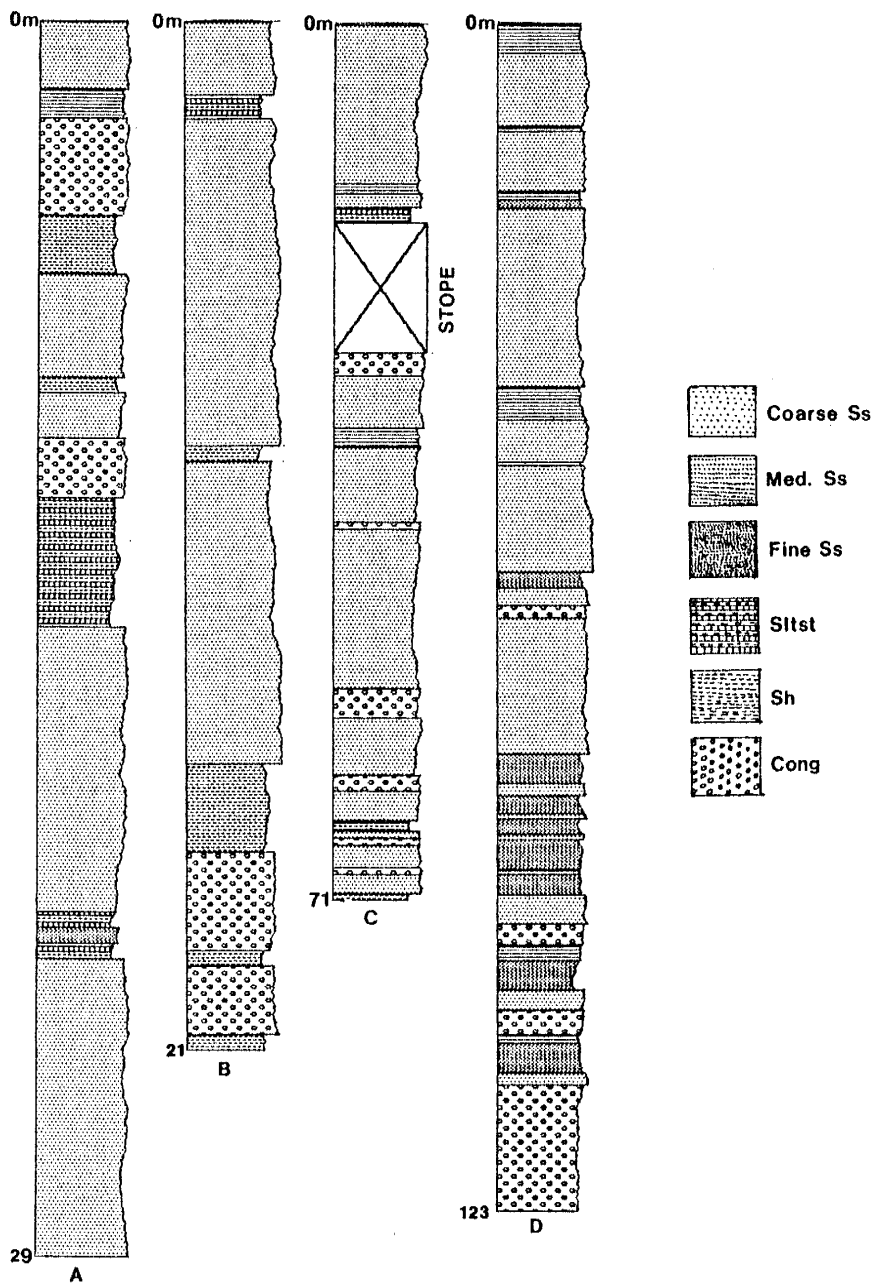


Figure 20-- Stratigraphic sections of the L-D mine sediments. The sections were measured from drifts and drill holes oriented perpendicular to bedding. Measured by T. Roberts, L. Ott, and M. Klisch. Note that stratigraphy does not correlate between drifts with only 50 feet of separation (2 and 2.5).  
 A. 0 drift; B. 2 drift; C. 2.5 drift; D. C88-7m.

rarely cross-bedded. Interbedded siltstones are usually black and finely laminated to rarely cross-bedded with mica and/or carbonaceous material defining the laminations. The shale units are black, carbonaceous and sheared to some degree. Recognizable plant material can be found on laminated surfaces in the siltstones and shales. Pebbly sandstones and conglomerates are quite common and occur as both thin intervals and massive, thick beds. Clasts are up to 10 centimeters in diameter and are exclusively quartz, coarse grained felsic plutonics, and biotite gneiss. Sandy siltstones are observed occasionally and are generally massive.

Graded sequences are frequently encountered and consist of conglomerate or pebbly sandstone which fines upward into fine grained sandstone or siltstone. Incomplete graded sequences are the general rule. Shaley beds do not occur in the graded sequences and are probably overbank muds. No coarsening upward sequences have been recognized. Individual beds range in thickness from a few centimeters up to 12 meters, but seldom exceed 6 meters.

Composition of the sediments classifies these rocks as feldspathic subquartzose sandstone (figure 21). Clastic grains include quartz, plagioclase feldspar, biotite, lithic fragments, potassium feldspar, chlorite, epidote, garnet and muscovite. By far the most abundant grains are quartz and plagioclase feldspar, occurring in

subequal amounts, and biotite. Table 3 shows the composition and average percentage based on several samples of unaltered sediments in the district.

Composition is quite uniform throughout the mine, and any variation is manifested by a slight increase in a particular component. For example, garnet usually is observed in only trace amounts, but in a sample taken from the 1550 level in Block Two garnet comprises 3 % of the sandstone.

Table 3-- Composition of sediments from the L-D mine.

<u>COMPOSITION</u>	<u>PERCENTAGE</u>
Quartz	36
Plagioclase	34
Biotite	9
Lithics	7
K-spar	tr.
Chlorite	1
Muscovite	1
Epidote	tr.
Garnet	tr.
Matrix	13



Sources of the sedimentary detritus can be derived from the composition of the rocks. In this case, there seems to have been a significant input from metamorphic and plutonic terrains. The biotite, gneiss pebbles, quartz vein material, and some of the quartz and plagioclase grains were undoubtedly derived from the Swakane biotite gneiss to the north and northeast. Plutonic pebbles, quartz, plagioclase and K-spar grains were probably weathered from the Mount Stewart batholith and felsic dikes and small intrusions within the Swakane terrane.

Diagenesis of the sediments is similar to that undergone by the Chumstick Formation (Evans, 1988; Taylor and others, 1988). Plagioclase feldspar is partially altered to laumontite. Calcite and zeolites occur as fracture filling and calcite is common as a cement.

Early workers grouped the sediments of the L-D mine with the Swauk Formation (Russell, 1900; Smith and Calkins, 1904; Chappell, 1936; Alexander, 1956). More recently these sediments have been grouped with the Chumstick Formation (Tabor and others, 1982; Margolis, 1987; Evans, 1988). Gresens (1982a, 1983), however, correctly pointed out that the narrow belt of sediments hosting some of the mineralization in the district are distinctly different from the Chumstick sediments prevalent in the graben. Gresens considered these sediments part of the Swauk Formation on the basis of field and laboratory

criteria (Table 4). Margolis (1987) considered the "Swauk" rocks of Gresens to be propylitically altered Chumstick sediments, a result of a broad district scale alteration associated with precious metal mineralization. Petrography

Table 4-- Criteria for distinguishing Swauk Fm. from Chumstick Fm.. (from Gresens, 1983).

Wenatchee 7 1/2-minute quadrangle			
	Swauk(?)	Chumstick	
Field criteria	Bedding	Generally evenly bedded. Arkose typically in 2- to 6-ft beds; shale/siltstone typically in 1/2- to 1 ft beds. Poorly sorted coarse conglomerate is in 1- to 4-foot lensoidal interbeds. Some arkose is graded, with siltstone tops having small-scale crossbeds; in a few graded beds there is a conglomeratic base	Sandstone is in massive beds 20 to 40 ft thick, and which may reach thicknesses of about 100 ft. Large-scale fluvial cross-bedding is common, and other features such as cut-and-fill structure and rip-rap clasts of shale are occasionally seen. More evenly bedded lacustrine facies are mostly shale and siltstone, but are locally incised and filled with channel sandstone
	Color	Light to dark gray on fresh exposures. Weathers to tan or brown. Isolated weathered outcrops of arkose are difficult to distinguish from Chumstick arkose	Generally lighter colored than Swauk(?). Has tan to light gray color even on fresh rock
	Lithification	Very well lithified in fresh exposures, to the extent that hammer blows bounce off the rock as they would a crystalline rock. In conglomerates, fractures cut across both clasts and matrix due to firm cementation of the clasts	Less well lithified than Swauk(?) to the extent that even fresh exposures of arkose are slightly friable. Fractures in conglomerates are around, rather than through, the clasts
	Veining	Fractures filled with coarse calcite are common in the belt of Swauk(?) rocks. Veins several cm in width are typical	Minor calcite veins are thin and infrequent
	Source, including clast lithologies	Arkose derived from crystalline terrane. Conglomerate clasts are mainly plutonic and gneissic rocks of granodioritic composition. Minor amounts of other metamorphic rocks. No clasts of volcanic origin have been noted. Some very large clasts (0.5 m in diameter) are present	Bulk of arkose is similar to Swauk(?) arkose, although locally becomes a more quartzose sandstone. Clast types found in Swauk(?) are all present in Chumstick conglomerate, but abundant volcanic clasts also present, making up 90 percent of total clasts in some rocks. A variety of felsic volcanic rocks are represented, including some distinctive porphyries. Large clasts of vein quartz occur in some conglomerates
	Structural and stratigraphic relations	There is always a structural discordance between rocks from the belt of Swauk(?) and the nearest Chumstick outcrops, although the contact is nowhere exposed	
	Tectonic history	Local evidence of multiple deformation (refolded folds). High degree of fracturing and veining	Apart from later minor thrust faulting of Oligocene age, deformation is a single folding event with gentle, open folds
Laboratory criteria	Thin section	Biotite is completely chloritized. No cross-hatched twins of microcline	Biotite is fresh or only partly chloritized. Cross-hatched twinning of microcline usually present
	Staining of rock slabs	Potassium feldspar not detected in specimens from the belt of Swauk(?)	Potassium feldspar noted in all specimens of Chumstick sandstone

and mapping does indicate a broad area of propylitic alteration, but the controversy involves much more than the just the occurrence of chlorite.

Evans (1988) proposed that Phase 1 deposition in the Chumstick basin occurred simultaneously with that of Swauk deposition and in fact formed a continuous depositional system with the Swauk Formation prior to activity along the Leavenworth fault zone. The east boundary of Phase 1 deposition was the Eagle Creek fault zone.

Comparing the sediments in the L-D mine to those of the Swauk Pass facies in the eastern portion of the Swauk basin reveals striking similarities. The sandstone facies of Swauk Pass forms the lower portion of the Swauk formation in the region (Taylor and others, 1988). Swauk Pass sands are typically massive to cross bedded and grade upward into laminated mudstone and fine sandstone and are interpreted to have been deposited in a low-gradient, meandering river system (Taylor and others, 1985). A QFL diagram (figure 21) reveals the compositional overlap between the mine sequence sediments and the Swauk Pass facies of the Swauk Formation. Paleocurrent directions indicate a northeasterly source of detritus. Provenance studies from composition of the sediments indicate the most likely sources are the Mount Stewart batholith and the Swakane biotite gneiss. This would imply that the Swauk basin of Tabor and others (1982)

was not bound to the east by the Leavenworth fault, but did indeed extend as far as the Eagle Creek fault zone and possibly the Entiat fault zone, an idea proposed by Gresens (1982). The older age of the sediments is supported by the extrusive andesite sequence of Saddle Rock which is approximately 50 ma (Ott, 1988); by the lack of porphyritic felsic volcanic clasts, such as those commonly observed in the Chumstick Formation; and by the occurrence of intrusive gabbro, which has been dated by a single whole rock K-Ar date at 48.3 ma (Gresens, 1983). Felsic volcanism in the area ranges in age from 47-40 ma (Margolis, 1987). Age dates from the Silver Pass volcanic member of the Swauk Formation in the Swauk basin range from 54-50 ma (Tabor and others, 1984).

#### Assessment of stratigraphic relationships

Basically, the stratigraphic confusion is brought about by the nomenclature as applied to the division of stratigraphic units. Evans appears to be correct in his assessment of a continuous depositional system that included both the Swauk and the future Chumstick basin beginning at about 52 ma; however, separation of the two basins, and hence the two depositional systems, did not occur until the Leavenworth fault zone was activated. Therefore division of the systems into two distinct sedimentary formations should not be done until they are physically divided by uplift

along the Leavenworth fault zone forming two separate basins. To avoid confusion, sediments deposited prior to activity along the Leavenworth fault should be classified as Swauk Formation. This includes those sediments that underlie the 51 ma volcanics, i.e. the sediments that are exposed in the southern part of the Eagle Creek structure and are host to mineralization of the L-D mine. Figure 22 is a revised stratigraphy based on this study. I conclude, therefore, that the mine sequence sediments are equivalent to the Swauk Formation.

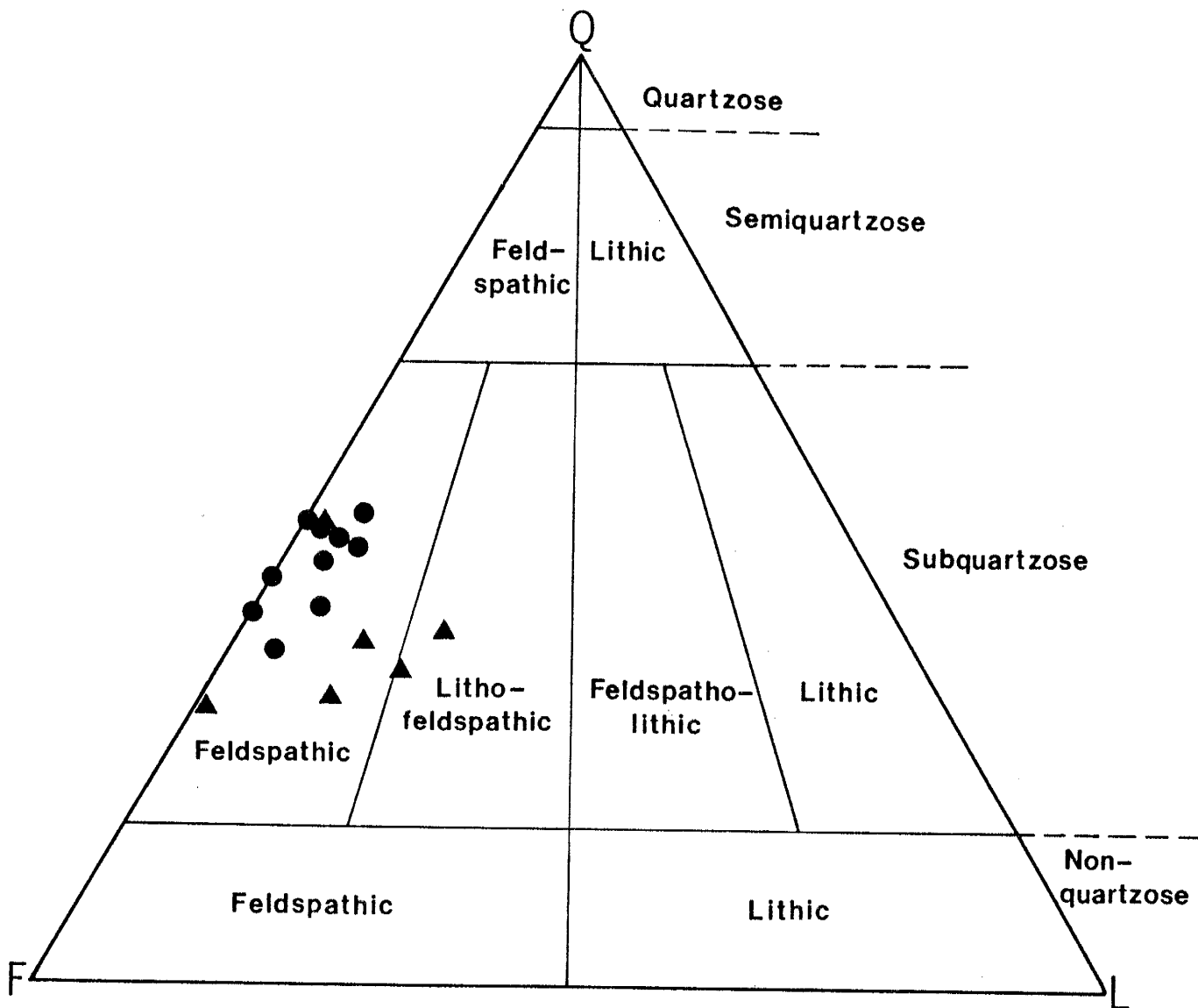


Figure 21-- QFL diagram of mine sequence sandstones in comparison with sandstones from the Swauk Formation. Circles=mine sequence, Triangles=Swauk Formation. (data of Swauk Formation from Frizzell, 1979).

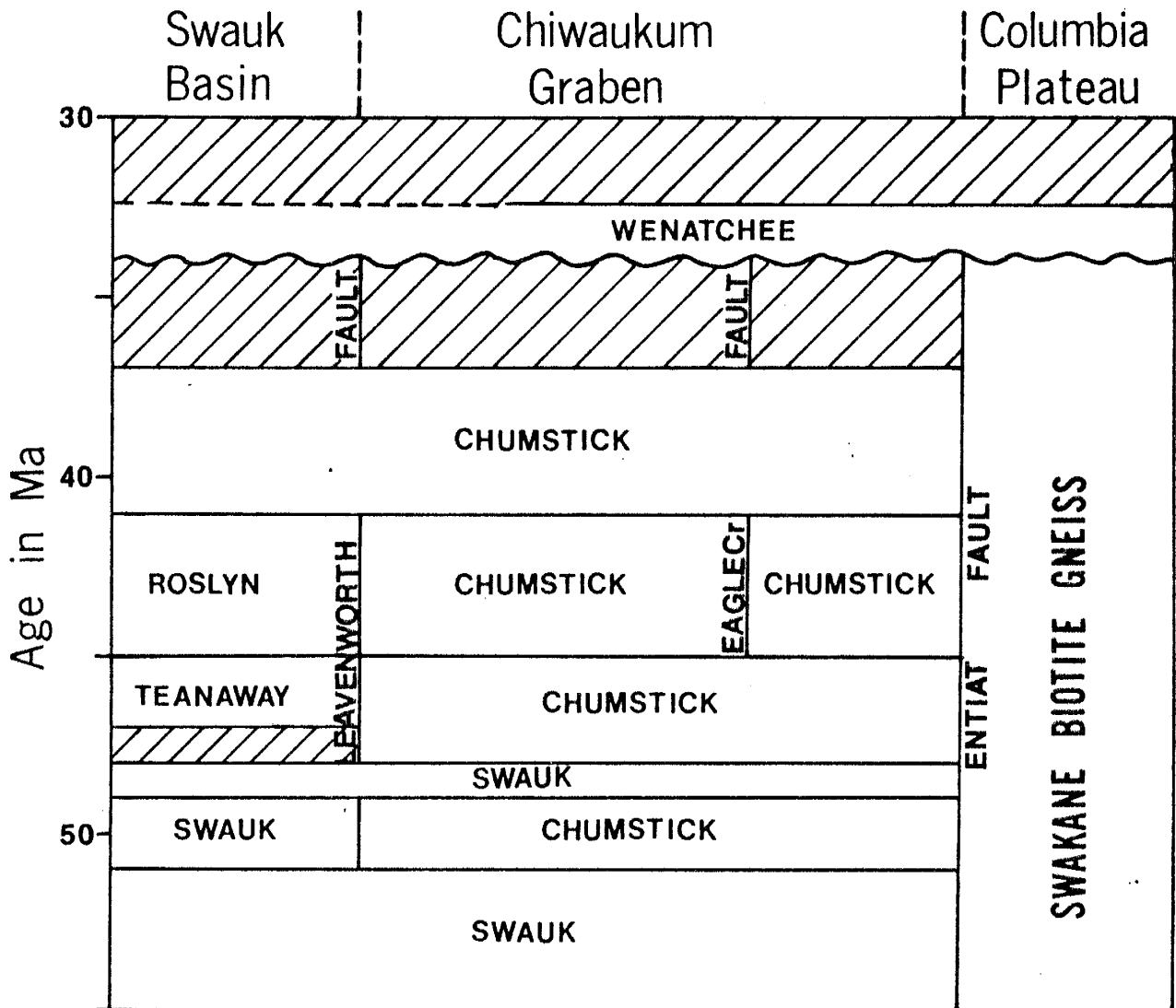


Figure 22-- Revised schematic stratigraphy of the Chiwaukum graben and adjacent Swauk basin. This is a more simplified stratigraphy than that proposed by Evans and Johnson (1989).

## Igneous rocks

Although not particularly common in the Wenatchee District, a few surface exposures of igneous rocks can be found. The only igneous rock that is exposed in mine workings is a rhyodacite on the 1100 level. This occurrence is east of the Footwall fissure and not currently accessible. Within a kilometer of the mine, however, are basalts, rhyodacites, and andesites. Just to the east of C-reef a sequence of andesitic volcanics crops out. The rhyodacite of Rooster Comb crops out west of Block Three. Basalts, andesites, dacites, and rhyodacites are encountered in many drill holes around the mine. All igneous rocks were originally mapped as intrusions (Chappell, 1936; Coombs, 1952; Gresens, 1983; Ott, 1988). There is a close temporal and spatial relationship between volcanic activity and the mineralizing event.

### Andesite

Outcropping just to the northwest of Block 3 is an ash-flow tuff of andesitic composition (figure 23). The andesite is fairly resistant to erosion and forms the linear row of spires at the top of the ridge visible in the photo. The silicified ridge of C-reef lies only 75 meters to the east. Flow-banding is well developed in the flow and the tuff is moderately welded. The rocks of this type have been previously mapped as dacite (Gresens, 1983; Ott, 1988);





Figure 23-- Photograph of the andesitic unit adjacent to C-reef. Taken from the top of Block 3.

however, petrographic work indicates that these flows are actually andesite. The andesite unit is not completely exposed, but drilling throughout the district reveals that it is composed of flows, breccias, ash-flows, and volcanoclastic sediments and is quite variable in thickness. Andesitic volcanics are also encountered in a drill hole west of the L-D mine.

The andesite ash-flows are crystal-rich and consist of large euhedral zoned plagioclase, smaller lath-shaped plagioclase, euhedral hornblende, rare biotite, and accessory magnetite in a brown glassy groundmass. No quartz or K-spar were observed in the sample. Andesitic flows occur as two compositional types, both are porphyritic, but one contains hornblende and plagioclase phenocrysts and the other only plagioclase phenocrysts. Flows with well developed flow-banding and breccias are observed. Flow-banded andesite is comprised of plagioclase phenocrysts that range in size from 1 to 5 mm. Where present, hornblende phenocrysts range from 1 to 2 mm. The groundmass is a mixture of plagioclase, glass, and minor pyroxene. Breccias are composed of altered porphyritic andesite fragments in a dark gray to black siliceous matrix. The clasts are angular and consist of plagioclase phenocrysts in a olive green aphanitic groundmass. The fragments are clay altered and quite soft.

Andesite adjacent to the Cannon mine is altered,

with intensity increasing toward the orebody. Plagioclase is altered to clays, sericite and calcite. Carbonate also replaces hornblende and fills vugs and fractures. Silicification is dominant nearest to the orebody (Ott, 1988; Klisch, 1989). The andesite near C-reef is not as intimately associated with the mineralized sediments and is not altered. Figure 24 is a photomicrograph of unaltered andesite tuff from Old Butte, 2 kilometers north of the L-D mine.

A detailed section of the Saddle Rock andesite was put together by Ott (1988) from exploration core drilling, and it shows that the volcanic-sediment contacts are parallel to bedding and may be depositional. In addition, the unit contains matrix and clast supported breccias, flow banded andesite, interbedded sediments, and individual units that vary in composition. Further detailed mapping and core drilling (Klisch and Roberts, 1989) supports an extrusive interpretation for the andesitic volcanic sequence.

The precise age of this volcanic package has been the subject of some dispute. Seven age dates have been performed on the andesite (Ott, 1988). Five of the dates are K-Ar dates on plagioclase and average 37.5 ma, a sixth is a K-Ar date on hornblende at 73.6 ma, and a seventh is a whole rock K-Ar date of 50.9 ma. The hornblende age is highly unlikely because it places the volcanics in the Cretaceous period which is very inconsistent with other ages

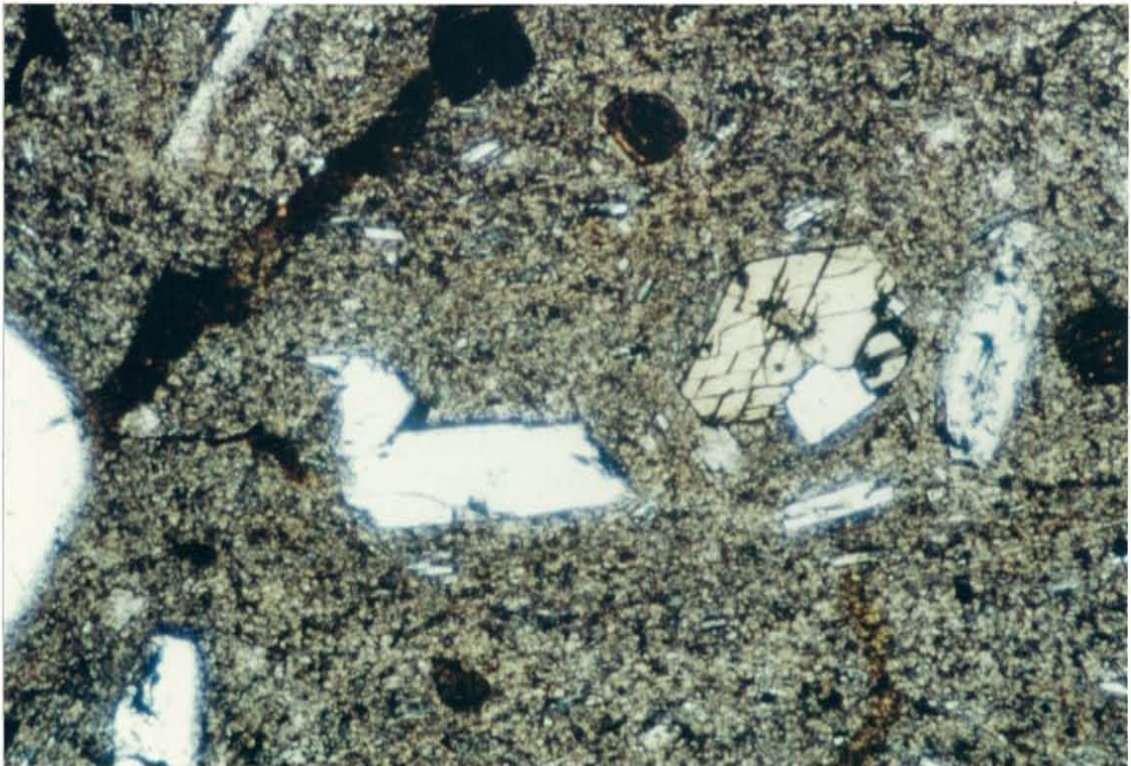


Figure 24-- Photomicrograph of an unaltered andesite ash-flow tuff at Old Butte. Sample OB-1. Hornblende grain is 15 microns across.

and events in this region. Mineralization in the Cannon mine has been established from vein adularia by K-Ar to be 44 ma. (Asamera Minerals, unpub. data) and since the andesite adjacent to the Cannon mine is altered, the five plagioclase dates are suspect. The whole rock date was performed on a sample of unaltered andesite, collected north of the Cannon mine and appears to be the most reasonable (Ott, personal comm.) given the minimum age constraint of mineralization and other ages in the region. This age places the volcanics in the same time frame as the Silver Pass volcanic member of the Swauk Formation in the Swauk basin. This unit is also andesitic in composition.

#### Rhyodacite

Only two surface occurrences of rhyodacite are found in the Wenatchee district: 1) Wenatchee Dome, east of the Cannon mine and 2) Rooster Comb, 213 meters northeast of Block 3 (figure 25). Diamond drilling shows that Rooster Comb and Wenatchee Dome are separated by a N-S fault, but they may be part of the same hypabyssal intrusive complex.

The rhyodacite of both Wenatchee Dome and Rooster Comb is light gray to white and consists of plagioclase, quartz and biotite phenocrysts in an aphanitic to glassy groundmass. Hornblende and zircon are minor constituents. The groundmass contains abundant spherulites and a few plagioclase microlites. Strongly developed flow-banding is



Figure 25-- Photograph of the rhyodacite of Rooster Comb  
taken from the top of Block 3.

defined by alternating layers of glassy and aphanitic material. Bordering the rhyodacite is perlite. The boundary between the two is generally gradational with layers of rhyodacite followed by mixed perlite and rhyodacite layers and finally, perlite layers. The perlite is > 90-95% glass with characteristic onion-skin cracks. The remainder of the perlite consists of phenocrysts of quartz, plagioclase and biotite with minor sanidine, orthopyroxene and zircon. Both the rhyodacite and perlite are unaltered except for minor devitrification along cracks and fractures.

The rhyodacite of Rooster Comb was interpreted by Margolis (1988) to be a locally thickened portion of the Compton Tuff, which is an important unit under Wenatchee Heights. Flow-banding orientations measured all over the outcrop clearly indicate that Rooster Comb is an intrusion. Moreover, there is a rind of perlite exposed in a few places around the outcrop of rhyodacite, similar to the perlitic border of Wenatchee Dome.

Wenatchee Dome and Rooster Comb are both unaltered and K-Ar age dates on biotite average 43 ma (Gresens, 1983), indicating that the intrusions may be post-mineral. This conclusion is also supported by the lack of alteration. The intrusions were implaced along the Eagle Creek fault zone (Evans, 1988) and may represent late felsic domes associated with the waning stages of volcanic activity.

Situated just east of the FWF is another occurrence of rhyodacite. This unit is not exposed on the surface and the mine level on which it was encountered is unfortunately not accessible. Drilling did not intercept much of this unit because holes were shut down upon entering it. From sketchy descriptions, it appears to be a greenish rhyodacite flow. The unit is brecciated and may be altered or severely weathered. Relationship to other rhyodacite units in the area cannot be determined. It may be part of the felsic volcanic sequence under Wenatchee Heights or part of the intrusion of Rooster Comb.

#### Other Felsic Volcanics

Rhyodacite has been encountered in other drill holes south of the L-D mine. Three holes in particular pass through a sequence of sediments, faults and rhyodacite volcanics. Correlation with Rooster Comb and occurrences adjacent to the L-D mine are difficult, but they are no doubt related.

#### Basalt

Basalt occurs in limited outcrop 60 meters south of Rooster Comb and in the subsurface based on drill hole information. The basalt exhibits spheroidal weathering and has broken down into a generally magnetic, green to red soil. Outcrops of basalt near mineralized areas are shot



through with calcite veinlets and possess a calcareous matrix. Basalts far from silicification have experienced diagenesis and propylitization (figure 26). Basalts encountered in drill holes include porphyritic, aphanitic, amygdaloidal and brecciated varieties. Phenocrysts consist of plagioclase and olivine occurring both together and separately in different units. Amygdules are filled by calcite, zeolites and chalcedony, frequently in combinations, olivine is characteristically altered to iddingsite, and chloritic fractures are common. Contacts with the surrounding sediments are not exposed at the surface, so the nature of basalt emplacement is not everywhere clear. In the subsurface contact relationships between the sediments and basalt units are generally depositional, but a couple of the contacts are sheared. The shearing, however, may be due to bedding plane slip between units of different competence during folding. In addition, some basalt units are clearly discordant to bedding, so dikes do occur. For the vast majority of occurrences, however, the evidence for extrusive origin is overwhelming and can be summarized as follows: 1) depositional contacts with sediments, 2) red stained intervals which may indicate subaerial weathering, 3) amygdaloidal intervals that indicate tops of individual flows, and 4) interbedded sediments often containing basalt clasts.

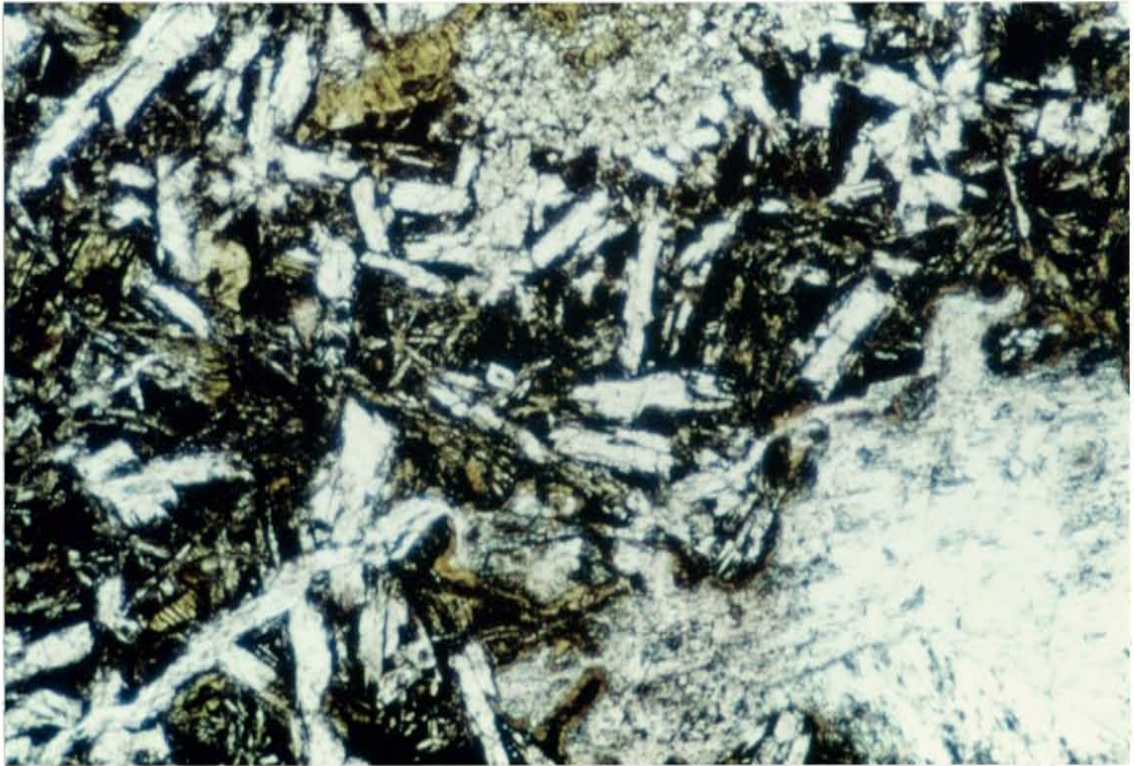


Figure 26-- Photomicrograph of propylitically altered basalt from sample SR-4a 646'. Calcite veinlet is 1 micron wide.

Several age dates determined for various basalts encountered in drill holes throughout the district, average 40 Ma (Ott, 1988; Asamera Minerals, unpub. data). The age of mineralization, once again, disputes the basalt ages which have undoubtedly been affected by alteration/diagenesis. Because the basalts are extrusive, and they are interbedded with sediments that underly 51 ma volcanics, then the basalts are about 54-51 ma.

### Geologic history

The history of the rocks in and around the L-D mine is tied closely to the structural evolution of the Chiwaukum graben. The Chiwaukum graben is a classic wrench-fault or pull-apart basin and displays the diagnostic characteristics: 1) great stratigraphic thickness relative to basin size, 2) high rates of sedimentation, 3) asymmetry of sediment thickness and facies patterns, 4) abrupt lateral and vertical facies changes and thickness variation, 5) textural cycles that reflect tectonic activity, and 6) well-defined geometrical relationships between bounding faults and sediments (Evans, 1988). The tectonic location of the wrench-fault basin within the Challis arc, its concurrent volcanic activity, elevated geothermal gradient and the controlling effect of the Eagle Creek structure made the area a prime location for the generation of a gold-

bearing hydrothermal system. Moreover, deformation of basin lithologies due to wrench-faulting generated an ideal structural setting for the transport and localization of those hydrothermal fluids.

The history of the district begins with deposition of the middle Swauk Formation, specifically the Swauk Pass facies, from 55-51 Ma. Periodic basalt flows were also deposited. The Swauk basin during this phase extended at least as far east as the Eagle Creek fault and possibly the Entiat fault. The sediments of the L-D mine are equivalent and were deposited during this time. Source region for the sedimentary detritus was confined to the Swakane Biotite gneiss and the Mount Stewart batholith resulting in a relatively homogenous arkosic sand.

Initiation of activity along the Leavenworth fault zone divided the Swauk basin into the Chiwaukum graben, or Chumstick basin, and the Swauk basin, creating two separate depositional systems from 51-49 Ma. Phase 1 of the Chumstick Formation began filling the newly formed Chiwaukum graben. In the Swauk basin the shale facies of Scotty Creek and Tronsen Ridge, the conglomerate of Tronsen Creek, and the breccia facies of Devils Gulch were being deposited (Evans and Johnson, 1989). By 49 Ma relief along the Leavenworth fault had been reduced and Phase 1 Chumstick streams flowed once again into the Swauk basin.

In conjunction with Silver Pass volcanism in the

Swauk basin, a period of volcanic activity at about 50 Ma resulted in deposition of a sequence of andesitic volcanics and volcanoclastic sediments conformably on the mine sequence. Continued deposition of arkose followed this period of volcanic activity, as indicated by the occurrence of sediments with abundant andesitic clasts, mixed with material from the plutonic and metamorphic terrains, overlying the volcanics. The existence of the Corbaley Canyon dikes (figure 4) and intrusive gabbros, both dated at 48 Ma., further indicate that igneous activity did indeed take place during this time (Gresens, 1982a, 1983).

Deformation of the Swauk Formation into NW trending folds was the result of renewed activity along the Leavenworth fault zone beginning at about 48 Ma (Evans and Johnson, 1989). This folding event did not carry over into the Chumstick basin. Uplift and erosion of the Swauk followed and volcanics of the Teanaway Formation were deposited unconformably on the Swauk from 47-45 Ma. At the same time, over in the Chumstick basin, the NORCO volcanic complex (Margolis, 1987) was being deposited in the southern part of the graben. Although the Teanaway and NORCO volcanics are the same age, the felsic NORCO does not correlate with the more basaltic Teanaway. Phase 1 Chumstick sediments continued to be deposited elsewhere in the graben along with ash-fall beds, thin ash-flows, and water-laid tuffs probably originating from the NORCO

volcanic field.

From 45-41 Ma dextral movement occurred simultaneously along the Leavenworth, Eagle Creek and Entiat faults resulting in the segmentation of the Chumstick basin into two sub-basins (Evans and Johnson, 1989). This period of activity initiated Phase 2 of the Chumstick Formation. The thick boulder to cobble conglomerates adjacent to the L-D and Cannon mines mark the initiation of tectonic activity and comprise the base of Phase 2 sediments. They were deposited in alluvial fans and are made up of felsic volcanic rocks shed from the NORCO volcanic complex, in addition to sedimentary clasts and clasts from the traditional Swakane and Mt Stuart terrains.

The Eagle Creek fault zone was an area of positive relief and the locus for extreme deformation. The mine sediments within the Eagle Creek structure were deformed for the first time in the 45-41 Ma episode. The en echelon vein structures formed early in this period of deformation and were later displaced by structures formed during subsequent phases. Synchronous with deformation was the mineralizing event at 44 Ma as indicated by K-Ar dates from adularia (Asamera Minerals, unpub. data). Mineralization occurred early in the deformational event, which is substantiated by structural interpretations. Volcanic activity in the NORCO field began to subside and culminated with emplacement of the rhyodacite flow-domes of the Wenatchee Dome and Rooster

Comb along the Eagle Creek structure.

By 41 Ma, relief along the faults was reduced and the Chumstick was once again reunited with the Swauk basin, now being filled by sediments of the Roslyn Formation. The third and final phase of Chumstick sediments were deposited.

Chumstick sedimentation ended with a period of deformation lasting from 37-34 Ma and characterized by dextral transpression which resulted in NW trending folds (Evans and Johnson, 1989). Sediments of the L-D mine were folded during this time as evidenced by post-mineral joints and bedding-plane slips. Continued deformation resulted in formation of a set of en echelon N-S faults that offset the folded rocks and the ore body. Erosion ensued, and finally the Wenatchee Formation was deposited unconformably on Chumstick sediments. Volcanism narrowed westward into the present Cascade arc and with it the deformational regime changed from extensional strike-slip to compressional. Northeast directed compression resulted in folding of the Wenatchee Formation into NW trending open folds, reverse faulting along the Footwall Fissure and dip-slip movement along north-south faults.

Basalts and mass wasting debris of the Columbia River Basalt group covered most of the area beginning at about 16 Ma. Extensive erosion and weathering has produced the topography and exposure that occurs in the district today.

## ALTERATION

Hydrothermal alteration of the host sediments is pervasive and controlled by permeability of the sediments and discontinuous, irregular fractures. Alteration is quite difficult to distinguish in the field due to its subtle nature. A combination of optical and X-ray diffraction techniques was necessary to discriminate these subtle zones of alteration. Alteration types include propylitization, sericitization, and silicification.

A major problem in deciphering this system was in differentiating between diagenesis and hydrothermal alteration, specifically, recognition of propylitic alteration. By nature sedimentary detritus can be subjected to alteration in several stages: 1) prior to weathering, 2) weathering, 3) diagenesis, and 4) a subsequent hydrothermal system. An analysis of diagenetic vs. hydrothermal alteration effects on the L-D mine sedimentary rocks follows.

### Types of alteration

#### Diagenesis

The process of diagenesis is simply a sub-metamorphic alteration of primary minerals by pore fluids during the temperature and pressure conditions experienced during burial. Most sediments experience some degree of



diagenesis at some point during their history. The sediments in the Chiwaukum graben are no exception.

Diagenetic products have been reported in the sediments throughout the graben (Gresens, 1983; Taylor and others, 1985; Evans, 1988) and include calcite cement and veinlets, and zeolitization of plagioclase. The zeolites laumontite and clinoptilolite have been identified. Based on the zeolite assemblage as well as discordant apatite and zircon fission track ages, and vitrinite reflectance data, Evans (1988) determined the thermal maturity of the Chumstick Formation to be in the range of 100 to 175 C, suggesting a maximum depth of burial of no more than 2.5 km.

In addition to calcite and zeolites, two other minerals occurring in the district are considered diagenetic products: pyrite and chlorite. Because pyrite is only observed in proximity to hydrothermally altered rocks, it is surmised to be a hydrothermal product. Chlorite occurrence is somewhat more problematic. Biotite is one of the first detrital minerals to be altered during burial and is commonly altered to chlorite in early diagenesis (Kisch, 1983). In thin-section chlorite is observed as individual grains and replacing biotite. Occasionally chlorite, fresh biotite and chloritized biotite are observed in the same sample along with zeolites and calcite, with or without pyrite. Some individual chlorite grains exhibit detrital textures.

...however, chlorite is

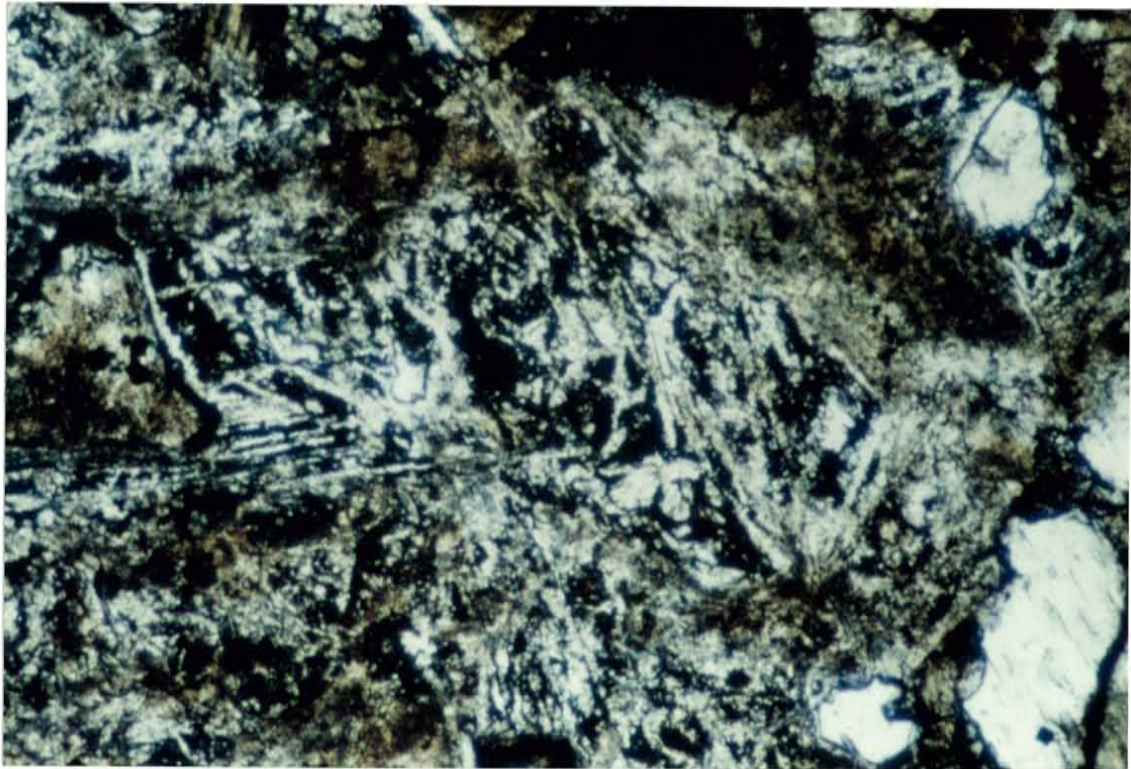


Figure 27-- Photomicrograph of diagenetically altered  
sediments from sample I88-2a 32'. Field of view is  
1000 microns.

In other areas of the graben, however, chlorite is not observed, even as a detrital component, nor is it observed in the Swauk basin. Although chlorite is most abundant in the Swauk Formation within the district, which would have undergone deeper burial than the Chumstick Formation, the strong spatial association of chlorite to mineralization leads to the conclusion that such chlorite is not of diagenetic origin.

Calcite and zeolites in the district occur as discrete veinlets and replacing plagioclase. This assemblage is interpreted as diagenetic, although the occurrence of veinlets is unique to the Wenatchee district, and may at least suggest a hydrothermal origin for the veinlets. It is also possible to speculate that diagenesis and hydrothermal alteration may overlap during the early stages, but no dating has been attempted to test this idea.

#### Propylitization

As with diagenesis, a similar dilemma exists in the determination of what mineral assemblage constitutes propylitic alteration. Typical propylitic assemblages observed from numerous districts include chlorite, epidote, albite, pyrite, carbonate, sericite, and zeolites (Meyer and Hemley, 1967). Of these phases, it is noted that zeolites and calcite in the sediments are of probable diagenetic origin, for they occur throughout the Chiwaukum graben, and

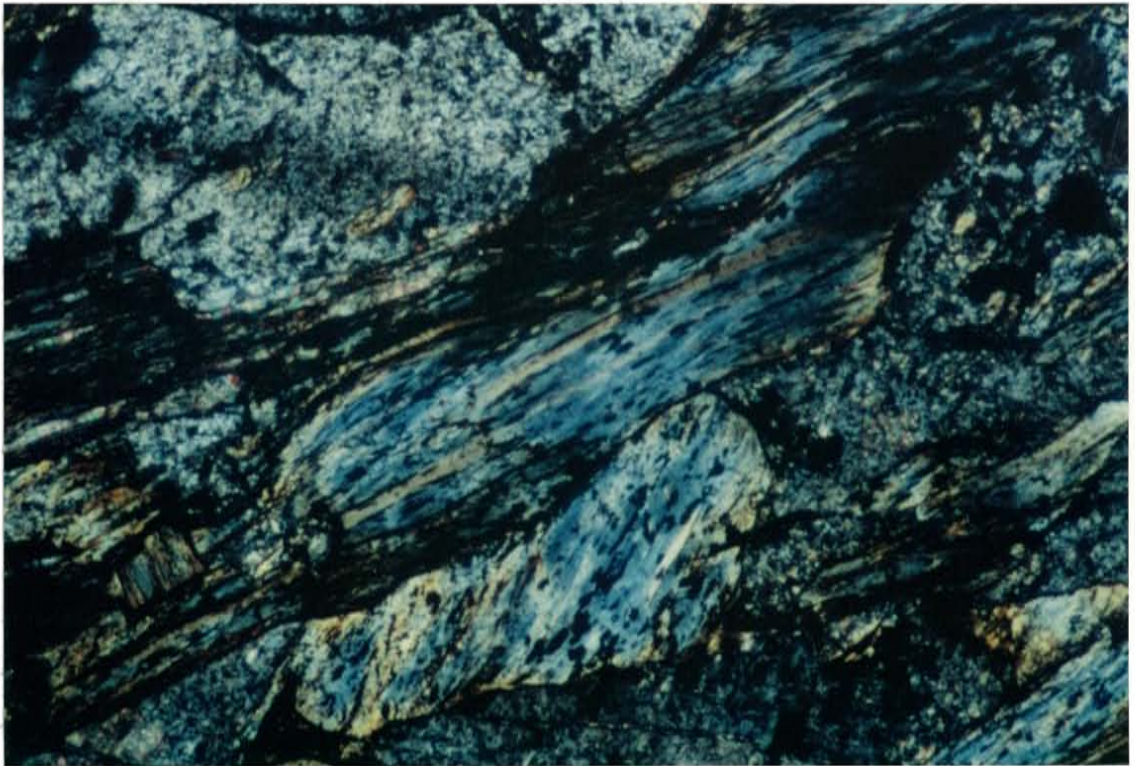


Figure 28-- Photomicrograph of chloritized biotite from the propylitic zone in sample C88-7m 380'. Field of view is 1000 microns.

the Swauk basin.

Ott (1988) did not define a zone of propylitic alteration associated with mineralization in the Cannon mine. He interpreted the presence of epidote, chlorite, and chloritized biotite in both altered and unaltered sediments to be of detrital origin. In contrast, Margolis (1987) recognized propylitic alteration associated with mineralization under Wenatchee Heights based on the presence of chlorite, brown biotite, carbonate, pink albite, and epidote. He further states that this same assemblage is also found at the L-D mine. This study does not support the observations of Margolis.

In samples from the L-D mine, chlorite, rare epidote, chloritized biotite, and plagioclase altered to illite are observed in drill core proximal to silicification. Pink albite was not observed. Brown biotite is an important detrital component throughout both the Chiwaukum graben and Swauk basin. Epidote does not exhibit any replacement characteristics, rather it occurs exclusively as individual grains and is most common in granitic lithic fragments. As such, epidote apparently is a product of alteration that occurred in the source region.

Nonetheless, it is important to ascertain what does characterize the outermost propylitic zone of hydrothermal alteration. Evidently, the assemblage pyrite, chlorite, and illite comprise L-D mine propylitic

alteration. Pyritization extends approximately 30 meters beyond the limit of silicification. Even in poorly indurated, friable rocks near mineralization, pyrite still persists. It occurs as tiny anhedral grains replacing biotite along cleavage planes, replacing chlorite; as narrow discontinuous veinlets, and as disseminated grains in matrix, probably replacing carbonaceous material. Chlorite-after-biotite is still recognizable in areas of weak silicification and extends outward beyond pyritization. All of the sediments and basalts in the district are affected by propylitization. Given the metamorphic source region, however, some of the chlorite may in fact be detrital. Although illite can be a diagenetic product it is here interpreted to be a hydrothermal product because it is not recognized in sediments outside of the district, and is spatially related to silicification. As suggested earlier, the veinlets of zeolites and calcite may also be part of the propylitic assemblage.



Figure 29-- Photomicrograph of pyrite replacing biotite in propylitized sediments from sample C88-7m 380'. Field of view is 700 microns.

## Silicification

Silicification is by far the most intense and pervasive hydrothermal alteration present in the system. Such alteration is important because it imparted substantial competence to otherwise poorly indurated and friable sediments. This competence helped to maintain dilutant openings during subsequent brittle deformation. Silicified sediments are quite resistant to erosion and are the only recognizable surface expression of mineralization, hence have been the primary exploration target throughout the history of the district.

Silicified sediments are characterized by: 1) quartz deposition in pore space, 2) replacement of matrix, 3) overgrowths on detrital grains, 4) veinlets, and 5) limited replacement of detrital grains. These textures are also encountered in silicified sediments of the Cannon mine (Ott, 1988). Quartz deposited in pore space is clear and consists of small anhedral grains arranged in mosaic aggregates. Replacement of sandstone matrix varies with proximity to veins and is characterized by a mixture of anhedral quartz and clays. Sediments directly adjacent to veins often have an interlocking igneous texture caused by complete replacement of matrix. Quartz overgrowths on detrital grains are not particularly common, but are observed on quartz and feldspar grains. This texture occurs chiefly in Block Two, associated with the intense stockwork



veining. Overgrowths are generally anhedral and form a thin (< 50 micron) coating. Veinlets are the most recognizable sign of silicification. Density of veining is directly proportional to intensity of fracturing and proximity to the major veins. Much of the veining, however, is not a product of the initial quartz flooding of the sediments as are the other textures. Veinlets associated with this event are composed of fine grained, anhedral mosaic quartz which is barren of sulfides. Recognition is based on the distinguishable "snaking" of the veinlets around detrital grains, indicating that the sediments were incompetent and very porous. These veinlets are commonly found along the outer fringes of silicification.

Replacement of detrital grains is similar to that of matrix replacement in that it is most common directly adjacent to major veins and in areas of strong stockwork veining.

Biotite is replaced along cleavage planes and to a lesser extent is plagioclase along cleavage and fractures.

Fractures in detrital quartz are healed by hydrothermal quartz, a feature recognized by contrasting extinction in polarized light.

Overall, Block Two experienced the most intense silicification, associated with dense stockwork and sheeted vein development. All of the above textures are frequently observed in the same sample. In Block One, intensity is more variable ranging from strong silicification directly

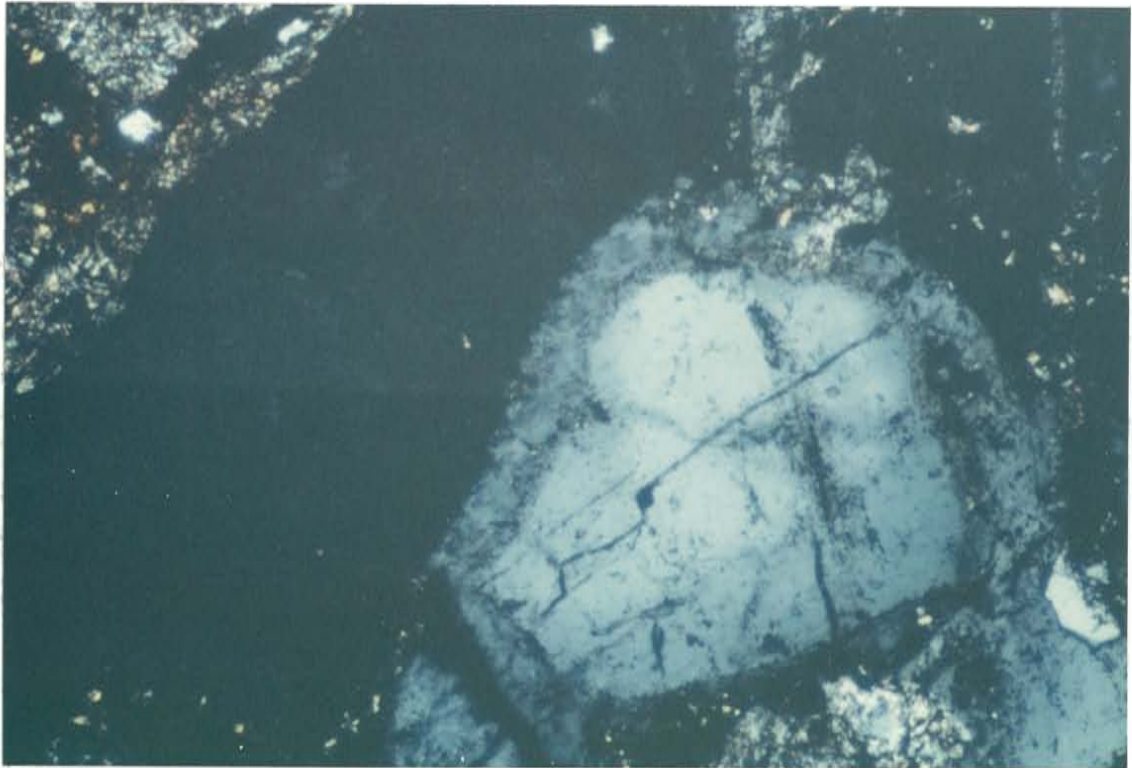


Figure 30-- Photomicrograph of hydrothermal quartz  
overgrowth on detrital quartz in sample C88-7n 16'.  
Field of view is 1000 microns.

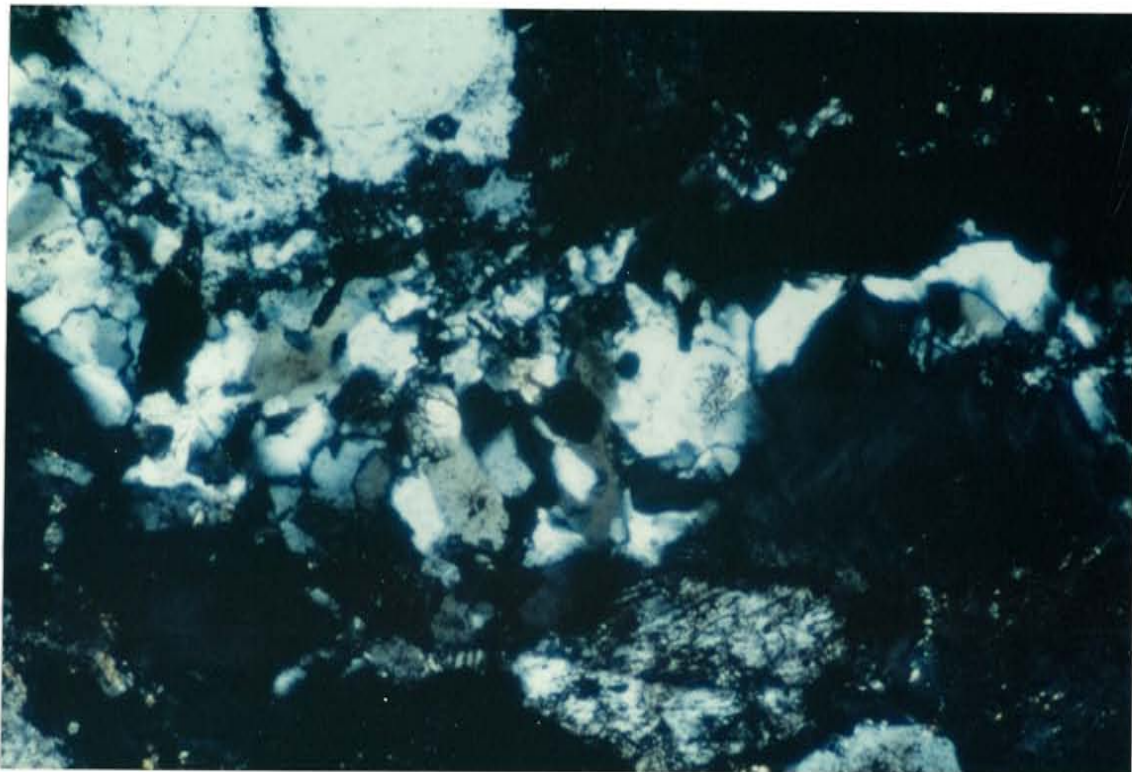


Figure 31-- Photomicrograph of early quartz veinlet. Note that the vein is going around detrital grains. Sample C88-9b 174'. Field of view is 1000 microns.

adjacent to the major veins, to moderate in the intervening wall rock. Weak silicification occurs along the outer edges of the entire system and in isolated areas between major veins. Based on a preliminary examination, the southern end of Block Three experienced a strong degree of silicification, similar to Block Two, but grades quickly from weakly to unsilicified and weathered sediments.

Stratigraphy imparts only local variations in intensity of silicification. In general, coarse sandstones have developed the greatest silicification, and shales the least. An exception is Block Two, where shales and mudstones are strongly silicified attesting to high fluid pressures.

Arsenopyrite is the only other sulfide encountered in the sedimentary wall rock besides pyrite and scant marcasite. Contact relationships between arsenopyrite and pyrite indicate that arsenopyrite is the later phase, as arsenic apparently accompanied the early silica-rich fluids. No precious metal phases were observed in silicified wall rock. Guilbert (1963) reported electrum in wall rock immediately adjacent to veins, but such occurrences were not observed in this study. Ott (1988) also reported gold and silver phases in sediments of the Cannon mine associated with strong silicification.

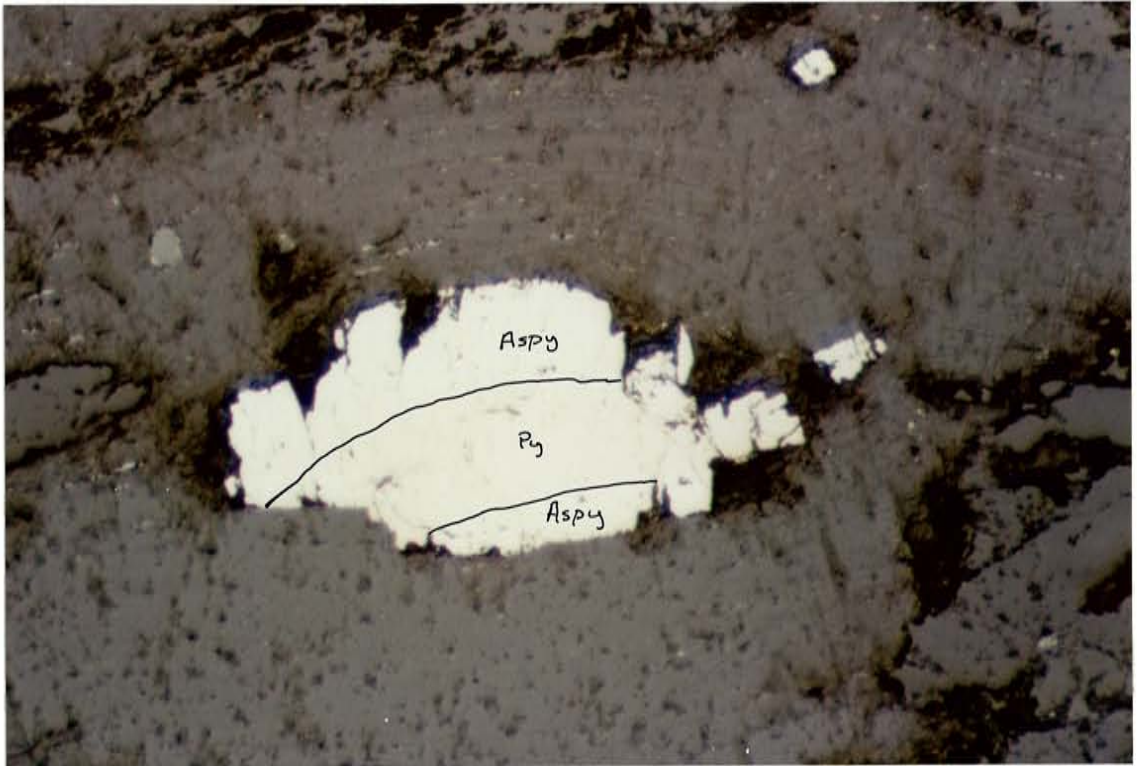


Figure 32-- Photomicrograph of arsenopyrite replacing pyrite in sample C87-2v 293'. Grain is 300 microns in length.

## Sericitization

The mineral assemblage representing this type of alteration includes illite, sericite and mixed layer illite-smectite. Clay alteration associated with weathering will be discussed in a later section. Sericitic alteration varies from strong to weak depending upon the degree of silicification, suggesting sericitization accompanied silicification. Two distinct zones are recognizable: 1) strong sericitic alteration comprising sericite, and illite; pyrite is present, chlorite is absent, and 2) weak sericitic alteration characterized by mixed layer illite-smectite, minor sericite, chloritized biotite, fresh biotite and pyrite.

Alteration of biotite, plagioclase and matrix characterize the zone of sericitic alteration. Potassium feldspar, as in all other alteration types, remained stable. Biotite is altered to sericite in areas of strong sericitization, but remains fresh or chloritized in weak sericitization. Chlorite is not present in areas of strong sericitic alteration, and it is possible that chlorite has been replaced by sericite. The zone of weak sericitization is recognized by the appearance of fresh biotite and chlorite.

Plagioclase on the other hand is altered to some degree in every type of alteration; in sediments unaffected by hydrothermal alteration, plagioclase is diagenetically

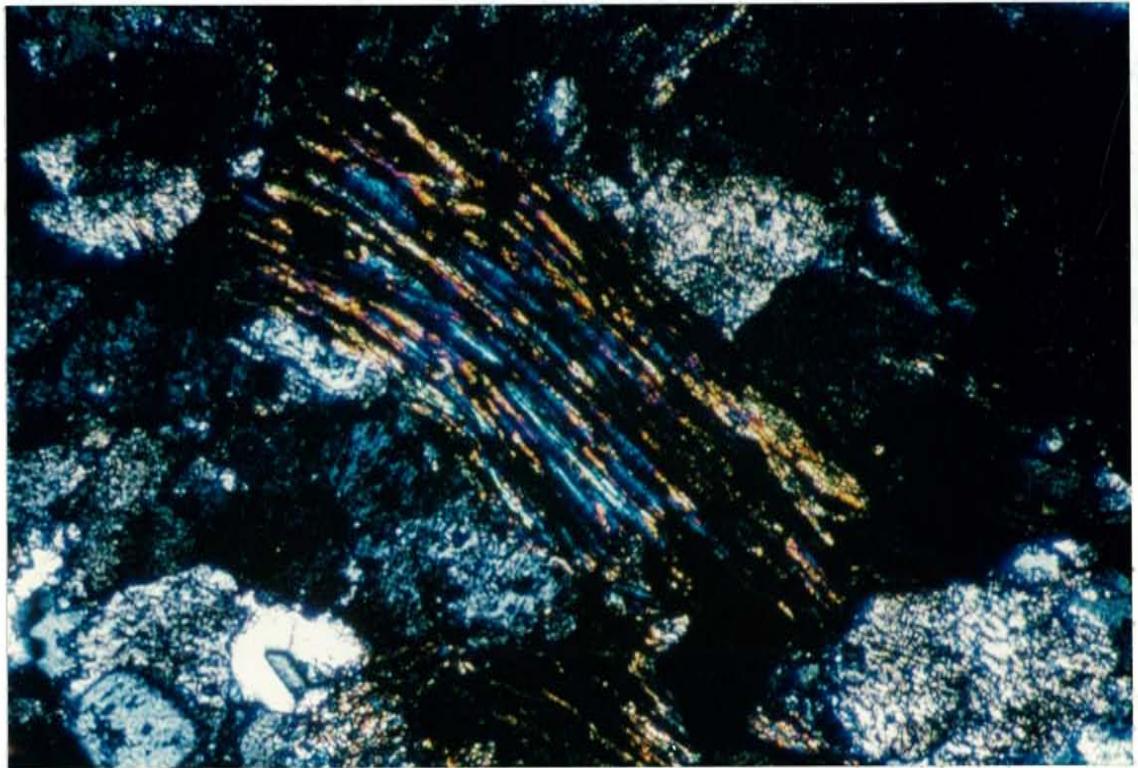


Figure 33-- Photomicrograph of sericitized biotite in sample C88-7n 101'. Field of view is 1000 microns.

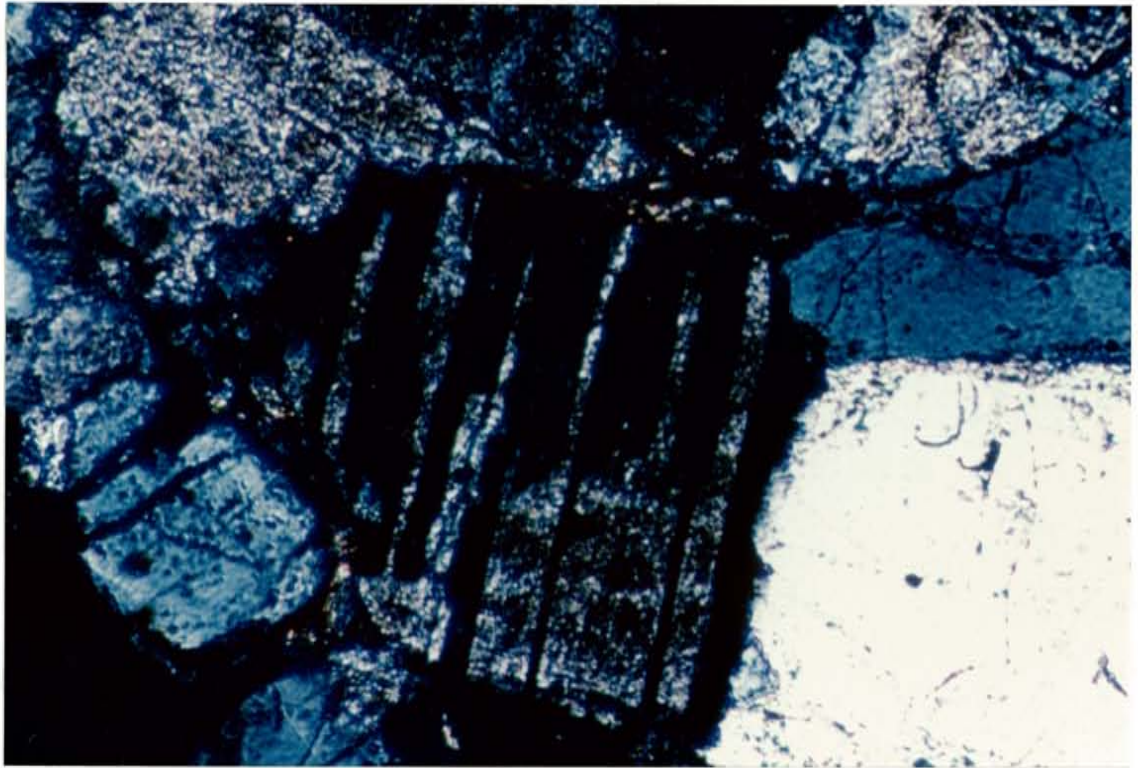


Figure 34-- Photomicrograph of weakly illitized plagioclase in sample C88-7m 256'. Field of view is 1000 microns.



altered to laumontite and/or calcite. In weakly sericitized sediments plagioclase displays a brown, cloudy appearance. In polarized light, twinning is apparently preserved, but grains are made up of a mixture of fine grained high and low birefringent material. X-ray analysis has identified this material as mixed layer illite-smectite. Strong sericitization is characterized by destruction of twinning and an abundance of highly birefringent material, identified as illite and occasionally sericite by x-ray and optical analysis. Alteration of matrix is easily recognized by an increase in the amount of highly birefringent material mixed in with hydrothermal quartz, probably illite or sericite. The alteration of plagioclase and biotite and the stability of potassium feldspar and muscovite indicates that potassium was an important component of the mineralizing fluids.

#### Argillization

Unlike Wenatchee Heights (Margolis, 1987) and the Cannon mine (Ott, 1988), there does not appear to be a distinct argillic halo around silicification at the L-D mine. Remnants of a possible clay cap is found in a road cut above Block Three, which is the highest point in the L-D system; however, the clays may also be due to weathering, since no sulfides are observed and jarositic and iron oxide staining is present. Given the extensive erosion of unsilicified rocks around the L-D mine, any hydrothermal clay cap would

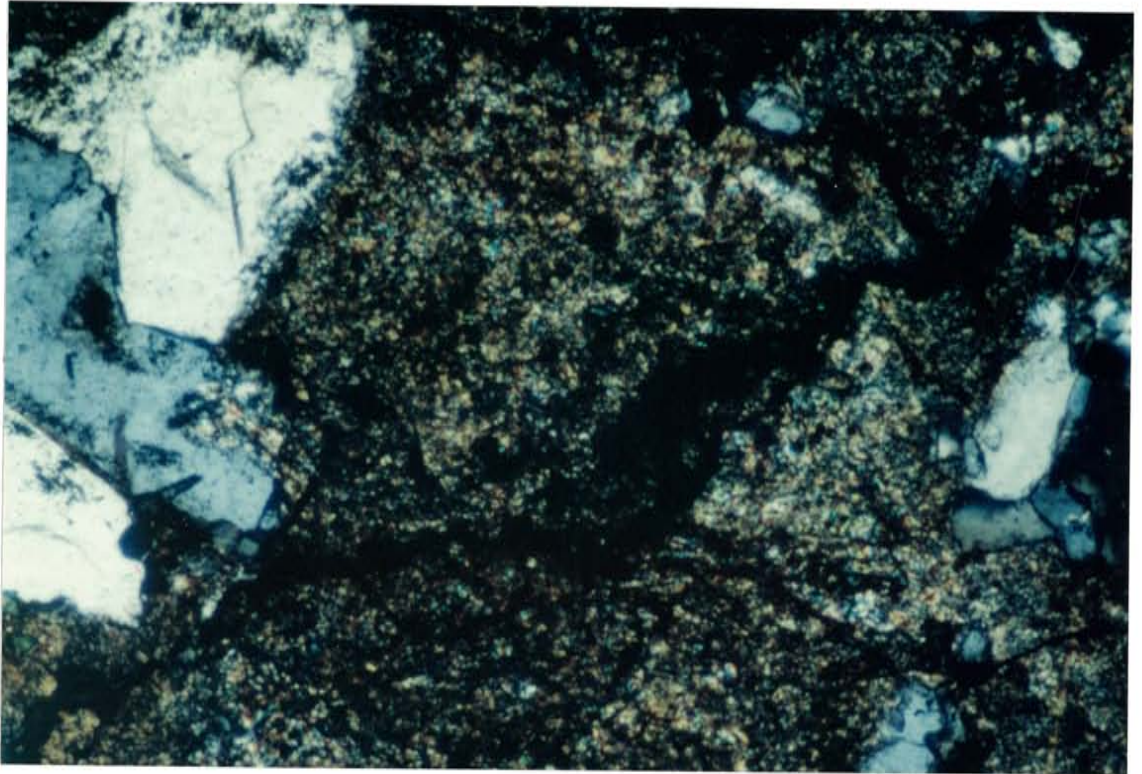


Figure 35-- Photomicrograph of strongly illitized and sericitized plagioclase in sample 28-10. Field of view is 1000 microns.

have been destroyed.

### Supergene Alteration

Oxidation due to the weathering of hypogene sulfides has had the most profound visual affect on the L-D mine host rocks. Iron oxide staining is one of the more recognizable attributes at both the outcrop and hand specimen scales. The assemblage jarosite, kaolinite, goethite and hematite indicate that the solutions were low pH. Copper sulfates commonly coat fractures and the walls in underground workings and gypsum is present in surface and underground exposures. Occasional tiny grains (< 15 microns) of native gold are associated with iron oxides.

Oxidation extends to just below the 1150 level in Block One. At about the 1150 level oxidation becomes more vein and fracture controlled before it ceases. In the upper levels, weathering was more pervasive and penetrated permeable sandstones as well as fractures and veins. This transition at the 1150 level is manifested by varying degrees of oxidation, from strong to weak in Blocks One and Three. In Block Two oxidation extends only as far as the 1500 level, probably due to the significantly reduced permeability by strong silicification. Iron oxide staining is found as fracture filling in wall rock, fractures crosscutting veins, and patches in the wall rock. In contrast to unoxidized wall rock, which is gray and contains

sulfides, wall rock associated with strong oxidation is white in appearance and barren of sulfides. Fracture controlled oxidation is accompanied by a selvedge of bleached rock, barren of sulfides (figure 36).

Typical alteration of wall rock in oxidized areas includes kaolinite after illite and sericite in plagioclase and biotite, jarosite after pyrite in biotite grains. Areas affected by strong oxidation are characterized by complete replacement, and destruction of phyllosilicate textures (figure 37). Goethite and hematite (figure 38) occur as fracture filling and in the matrix surrounding clastic grains. Jarosite occurs as fracture filling (figure 39), in matrix enclosing clastic grains, and rarely replacing pyrite. Pseudomorphs after pyrite are rarely observed, indicating some mobility of iron.

As mentioned briefly before, occasional tiny grains of native gold have been observed with goethite and hematite suggesting the possibility of supergene gold mobilization. To test this hypothesis assay results from intervals with less than 50 % oxidation were compared with assays from intervals with greater than or equal to 50 % oxidation. Percentage of oxidation is based on the amount of rock effected by oxidation as determined visually by the abundance of oxidized fractures, oxide staining, and white color of the rock.

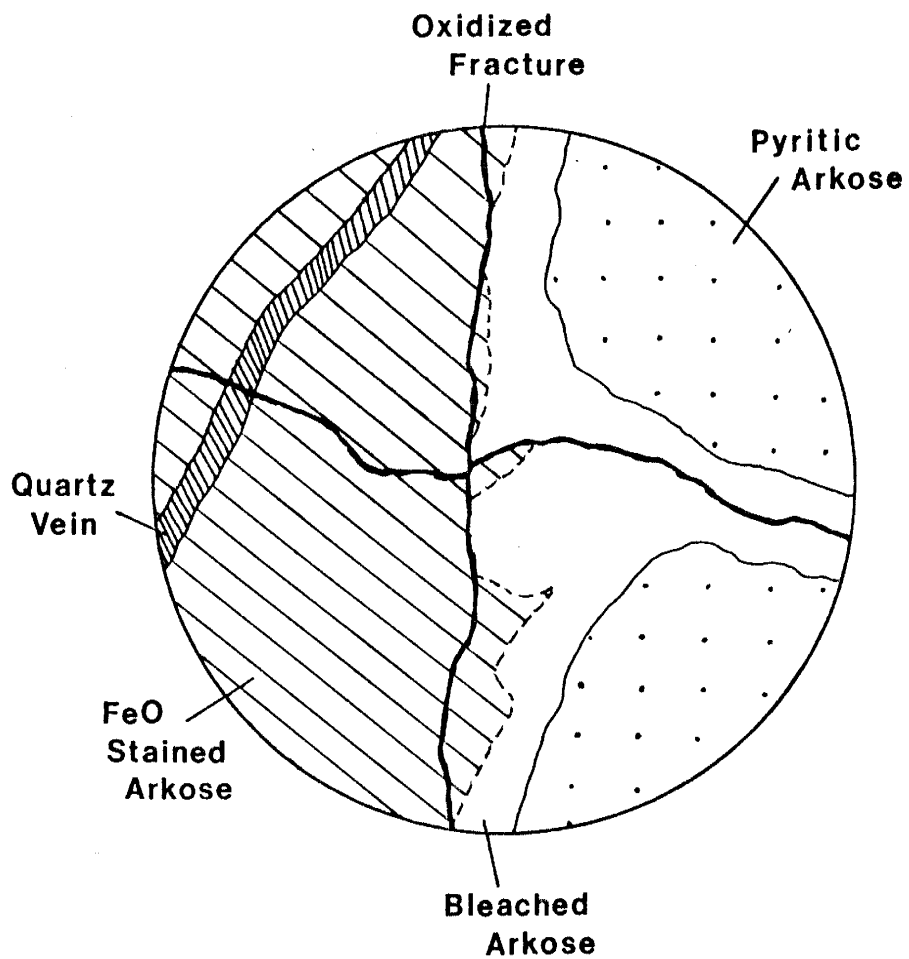


Figure 36-- Sketch of fracture controlled oxidation with thin selvedge of bleached wall rock from sample C87-2z 42'.

Figure 40 shows histogram plots of gold values in less than 50 % rock and more than 50 % rock. There does not appear to be any difference between the two, indicating that gold was not mobilized on a significant scale. Silver values were looked at next, since silver is generally more mobile in supergene solutions. Figure 41 shows histogram plots of silver values in intervals with less than 50 % and more than 50 % oxidation. In samples from areas with less than 50 % oxidation there is a higher frequency of low value samples and a lower overall average. Samples from intervals with greater than or equal to 50 % oxidation have a slightly lower average. It appears there was very little if any mobilization of silver. This is in agreement with production records of the L-D mine which reveal silver grades were two to three times higher than gold in oxidized ore (Lovitt and Skerl, 1958).

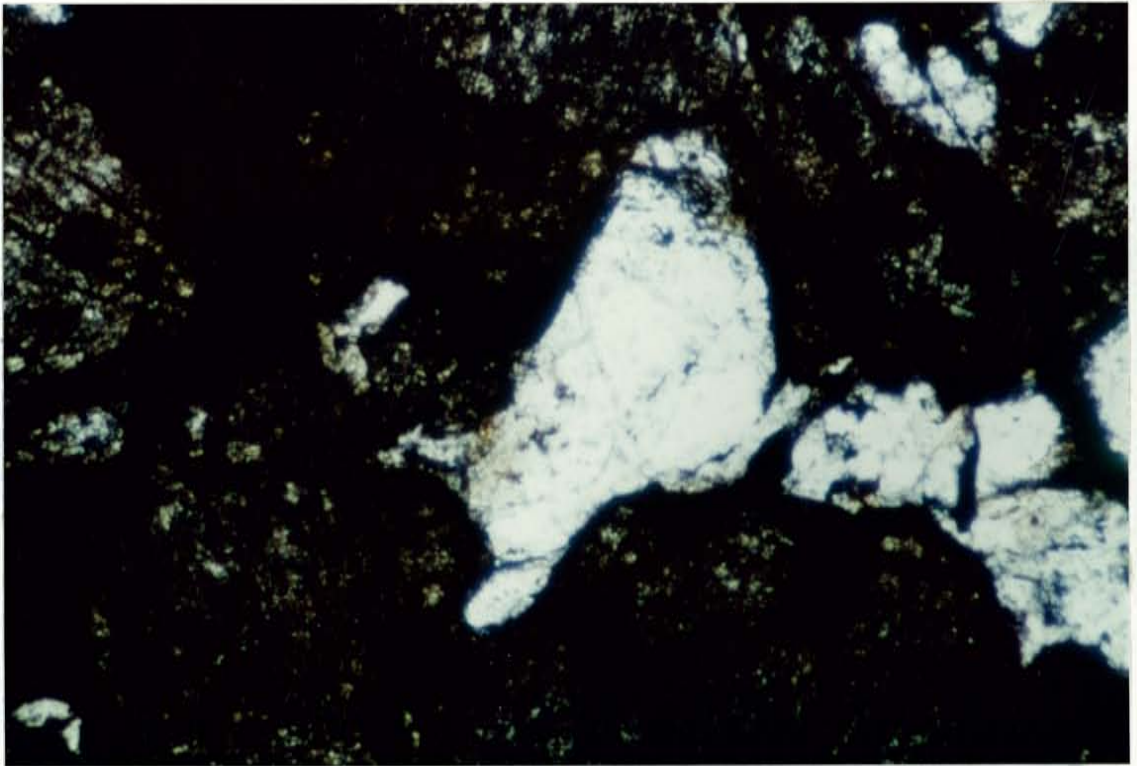


Figure 37-- Photomicrograph of strongly oxidized sediments.  
Note the absence of phyllosilicates which are normally 10 % of the wall rock. Sample C87-1q 83'.  
Field of view is 1000 microns.

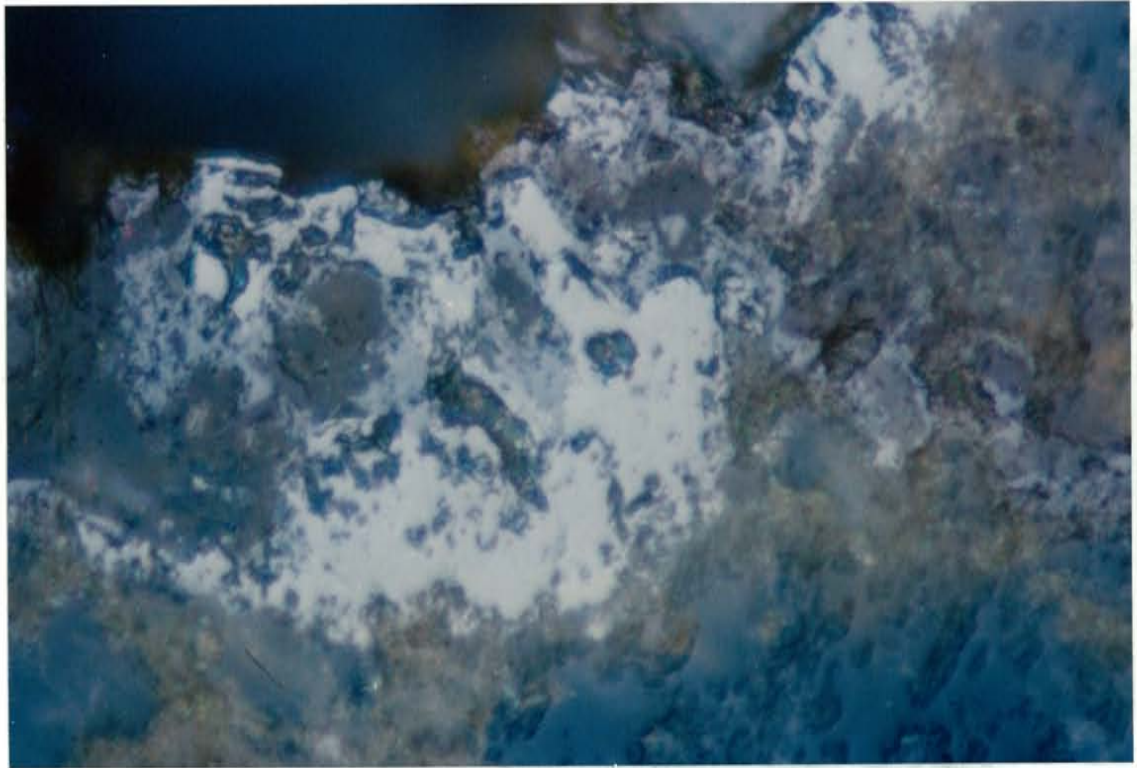


Figure 38-- Photomicrograph of goethite and hematite in matrix of oxidized wall rock from sample C88-7n 16'. Field of view is 250 microns.



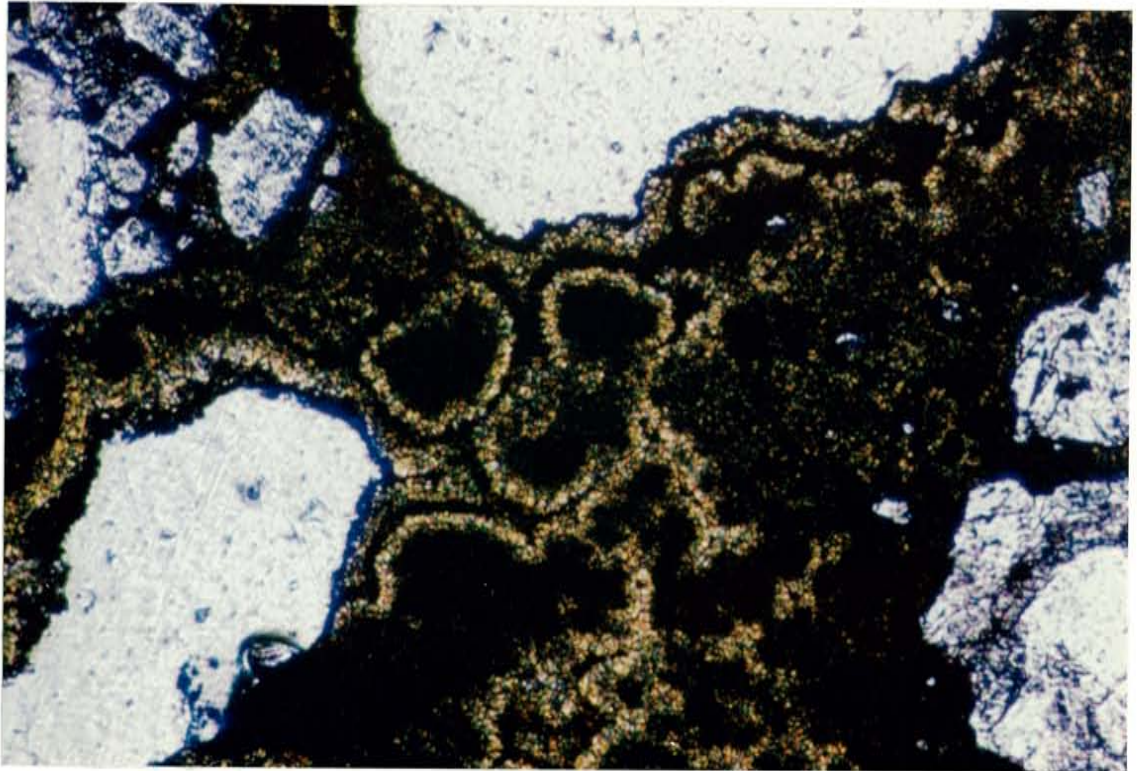


Figure 39-- Photomicrograph of jarosite in a fracture cross-cutting sediments from sample C88-7m 97'. Field of view is 1000 microns.

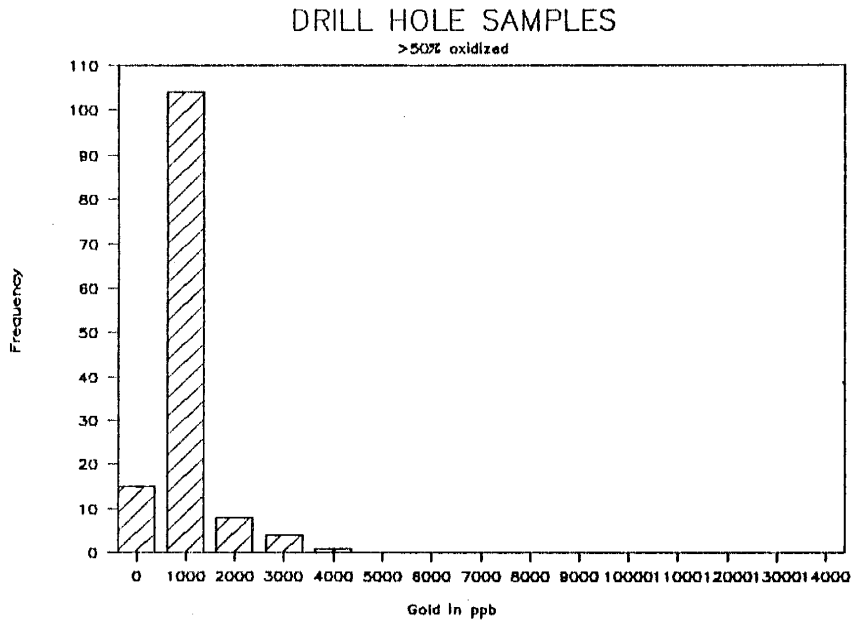
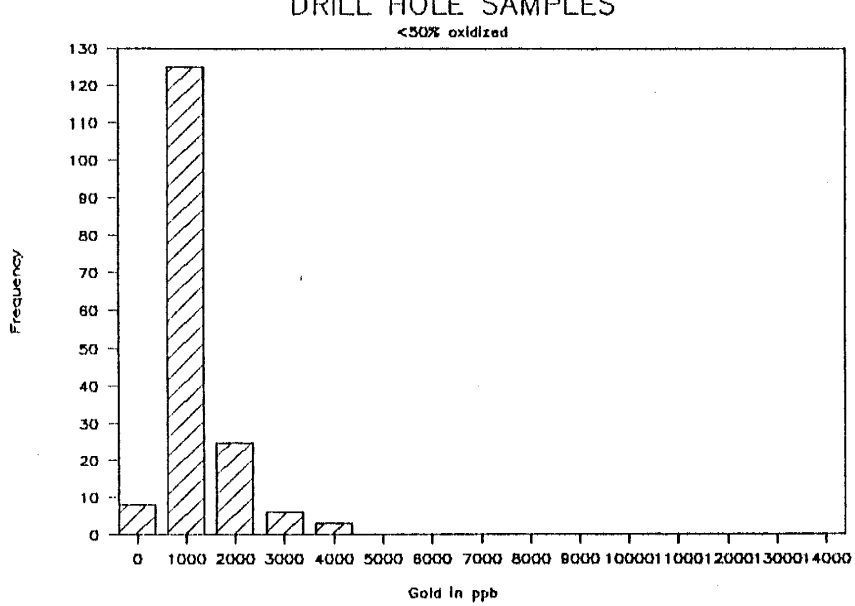
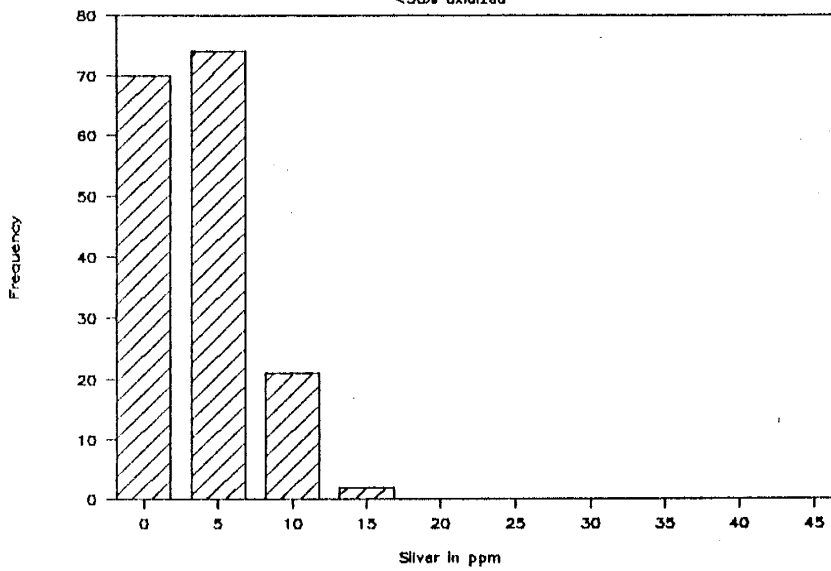


Figure 40-- Histogram plots of gold values in ppb for samples of intervals with less than 50 % oxidation (top) and greater than or equal to 50 % oxidation (bottom). n = 299.

### DRILL HOLE SAMPLES

<50% oxidized



### DRILL HOLE SAMPLES

>50% oxidized

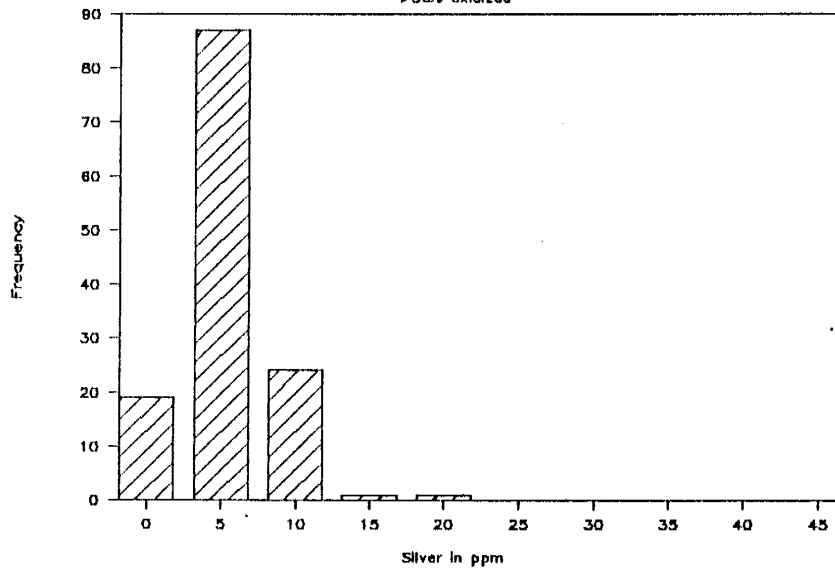


Figure 41-- Histogram plots of silver values in ppm for samples of intervals with less than 50 % oxidation (top) and greater than or equal to 50 % oxidation (bottom). n = 299.

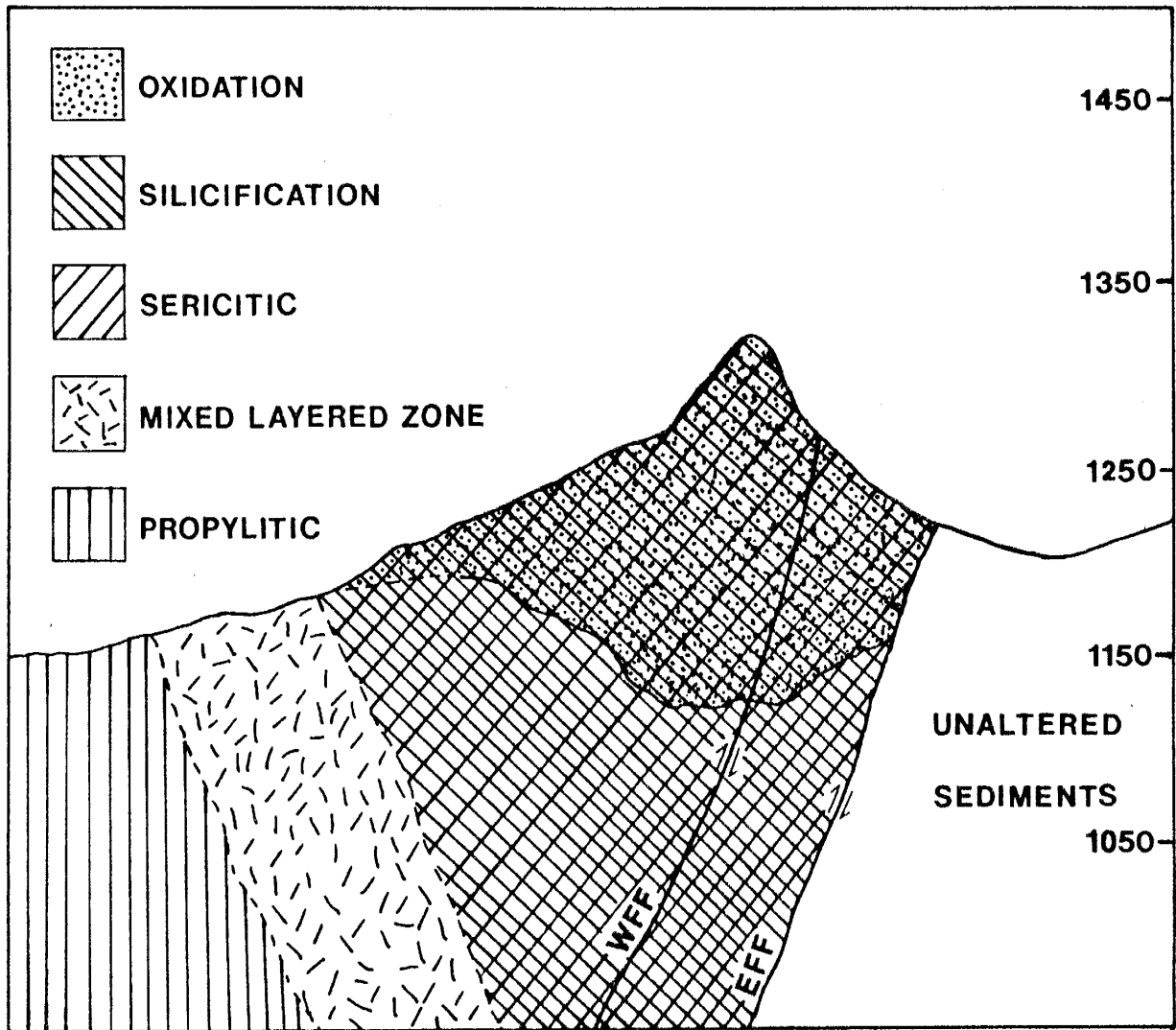


Figure 42-- Cross-sectional sketch of the distribution of alteration types in the L-D mine. Zones are defined by drill hole information.

## MINERALIZATION

The orebody of the L-D mine crops out for virtually its entire length, forming the erosionally resistant ridge present today (figure 43). It was this bold outcrop that first attracted prospectors in the late 19th century. At outcrop scale the pervasive silicification of the sediments and the heavy oxide staining caused by weathering are the most prominent features. Only upon closer examination does one notice the wide veins, stockworks and sheeted veins that carry precious metals.

This subtle nature of mineralization is prevalent in all aspects of the system, including alteration, mineralogy and geochemistry. Ore and gangue minerals are not abundant, nor are they coarse grained. Mineralization is generally difficult to distinguish at hand specimen scale. Exceptions are pyrite, which can often be seen in the wallrock, and quartz and calcite, which comprise the veins and impart significant competency to the sediments.

### Types of mineralization

#### Major Veins

Economic mineralization in the L-D mine is exclusively vein hosted, from the widest veins to the most minute veinlets. Block One is characterized by an en echelon set of laterally and vertically continuous veins up



Figure 43-- Photograph of the outcrop of the L-D mine  
looking northeast.

to 2 meters wide. These veins were wide enough and high grade enough to be mined as separate entities by the Lovitt Mining Co. Veins in Blocks Two and Three are generally less than half a meter wide, but are also fairly continuous over several hundred feet, both vertically and laterally.

Textures in the veins are indicative of open space filling. Crustiform banding, coxcomb quartz, brecciation, and calcite boxwork occur throughout the mine (figure 44). Crustiform banding is characterized by alternating generations of milky and clear quartz, or fine, medium, and coarse grained quartz. Brecciation is present in all of the major veins and occurred at least twice, once early and once during final stages of vein formation. Early brecciation consists of silicified wall rock fragments in a matrix of fine to medium grained quartz and is a product of the initial stages of structurally controlled mineralization, although it is not present in every vein. Late brecciation is composed of vein fragments in a powdery, siliceous matrix. In thin section the matrix is brown and may be a mixture of clays, quartz and rock flour. Calcite boxwork texture is also indicative of open space filling as well as being suggestive of boiling. The texture is a framework of calcite blades that closely resembles the boxwork found in gossan caps.

## Sheeted Veins

The narrower veins in Blocks Two and Three occur as parallel to subparallel closely spaced structures with orientations identical to the major veins in Block One. The density of these veins allowed them, as well as the intervening wall rock, to be mined en masse, producing large stopes. Figure 45 is a sketch of one such stope, the "49 stope" in Block Three. Vein formation of this type probably occurred in the upper portions of the system, where the fluid pressures caused greater fracturing of wall rock.

Vein textures are similar to those in Block One, but brecciation is not as common.

## Stockwork

Stockwork veining is present in all portions of the mine and comprises the narrow veinlets between the major veins in Block One and the sheeted veins in Blocks Two and Three. Dense stockwork is best developed in the areas of sheeted veins where fracturing was more intense. This stockwork veining makes up the present reserves in the L-D mine.

Individually, the small stockwork veinlets do not display all of the textures present in the wider veins. Late brecciation, for example, is not observed. Rather a single veinlet exhibits only one or two textures. This indicates that the stockwork was built up over time, with



each veinlet reflecting a single period of deposition in the major veins and occupying fractures developed in the wall rock during concurrent deformation along the larger structures.

### Breccias

Hydrothermal breccias in the L-D mine are scant and are volumetrically minor. They are generally in the form of clastic dikes discordant to bedding. Cross-cutting relationships indicate these features were developed early in the system, perhaps during silicification, before the sediments were competent.

These features are narrow and discontinuous and consist of detrital material with disseminated pyrite and arsenopyrite, cemented by quartz. Detrital material consists of rock fragments, individual detrital grains, and rock flour. There are no precious metals associated with these breccias.

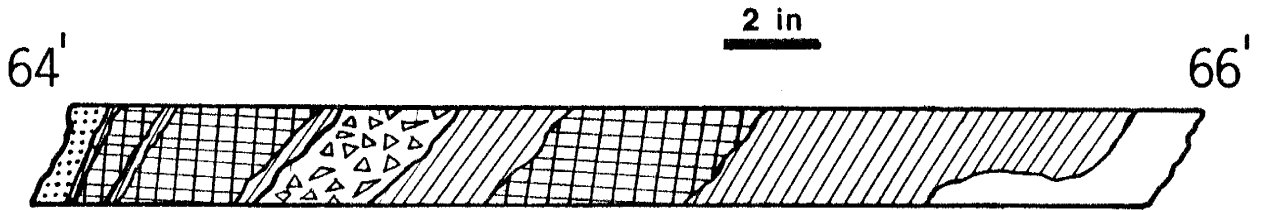
### Gangue mineralogy

As is characteristic of all mineralization in the Wenatchee district, the non-opaque gangue mineralogy is very simple, consisting only of quartz, calcite, and adularia.

### Quartz

Quartz is the most abundant mineral phase in the

C88-8H






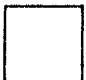
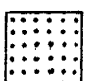
-  CRUSTIFORM BANDING
-  CALCITE BOXWORK
-  QUARTZ BRECCIA
-  GRANULAR QUARTZ
-  ARKOSE

Figure 44-- Sketch of typical vein in Block One. From drill hole C88-8h.

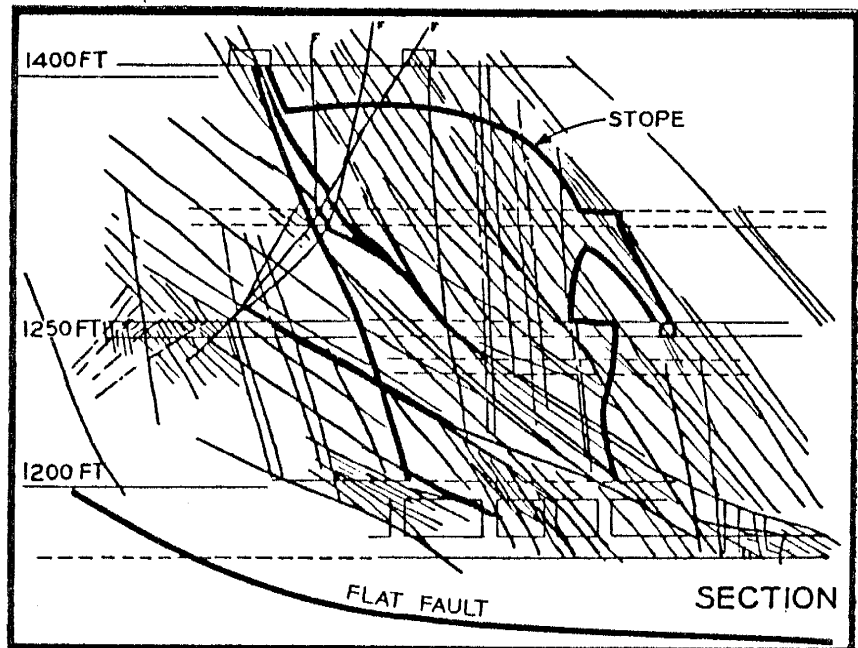
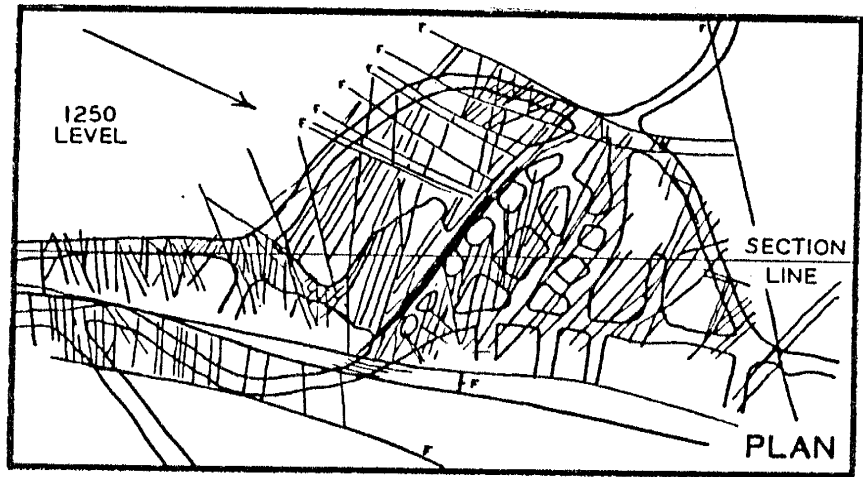


Figure 45-- Cross-section of 49 stope in Block Three.

Note the sheeted veins. (from Lovitt and Skerl, 1958)

L-D mine system. It is the only non-opaque hydrothermal gangue mineral found in both wall rock as an alteration phase, and in veins.

Quartz exhibits a wide variety of epithermal textures including, chalcedonic, plumose, coxcomb, drusy, pseudomorphs of bladed calcite, recrystallization textures, and mosaic aggregates of anhedral grains. Size ranges from microcrystalline up to a maximum of only 8 mm. Chalcedony (figure 46) is not an abundant phase and only occurs paragenetically late, in the northern end of Block One and in the upper levels of Block Two with no associated metallic minerals. Recrystallization of chalcedonic quartz (figure 47) is also limited to these two areas, so it would appear as though the limited extent of chalcedony is a primary feature. Pseudomorphs of bladed calcite (figure 48) occur extensively in Block One, but are rare in Blocks Two and Three. The other quartz varieties are equally distributed throughout the system. Some other textures observed in the L-D mine that are mere curiosities include "stratified" quartz (figure 49) and quartz spheres (figure 50). The stratified quartz consists of pockets of very fine grained quartz that exhibits micro-layering, often graded according to size, and occur associated with euhedral quartz. They are similar to a particular type of geode and may have formed from a trapped liquid. The quartz spheres were observed in a couple of narrow veins. These veins are

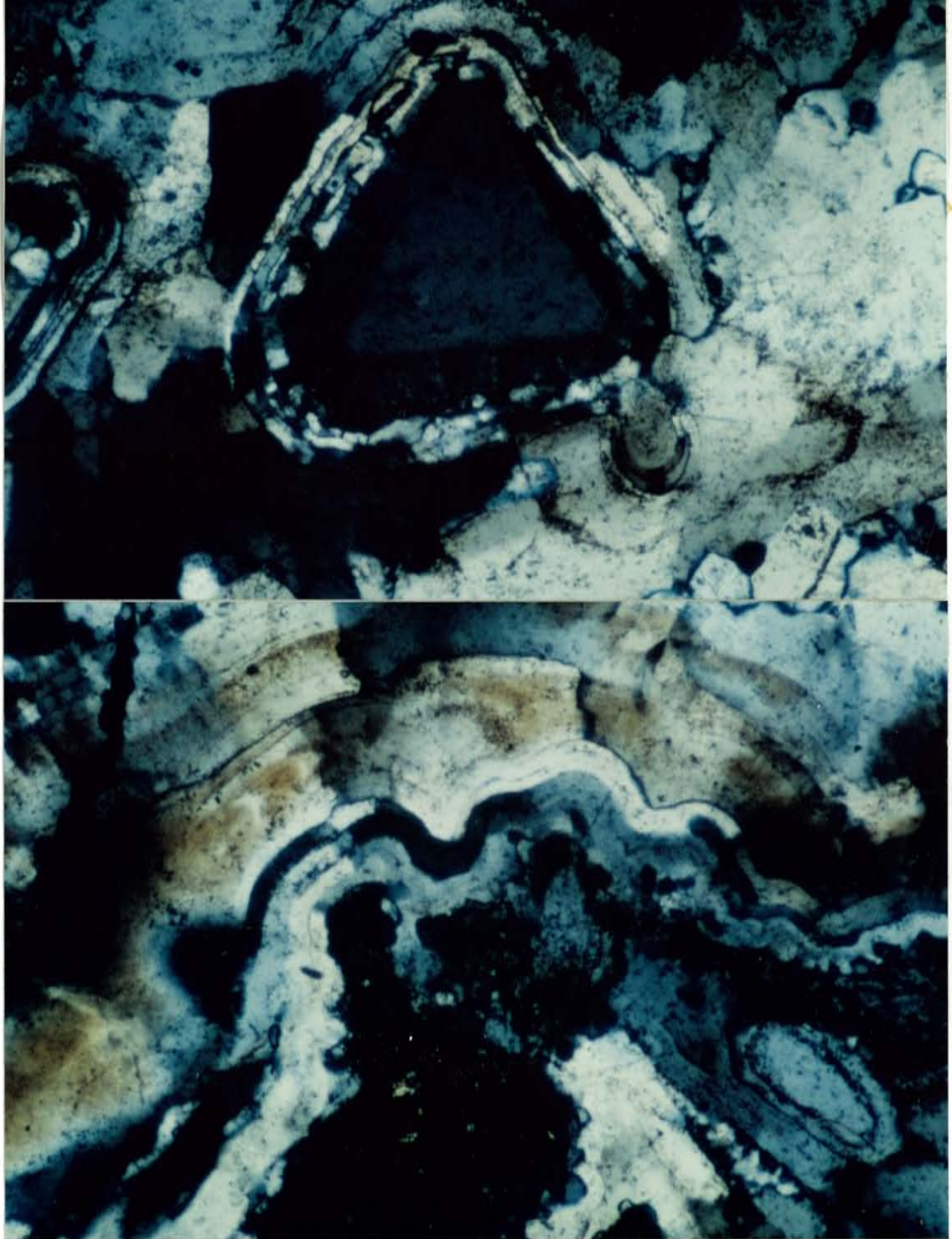


Figure 46-- Photomicrograph of chalcedonic quartz in sample 12-34 from Block One. Note that it is rimming earlier quartz (top) and a wall rock fragment (bottom). Field of view is 1000 microns.

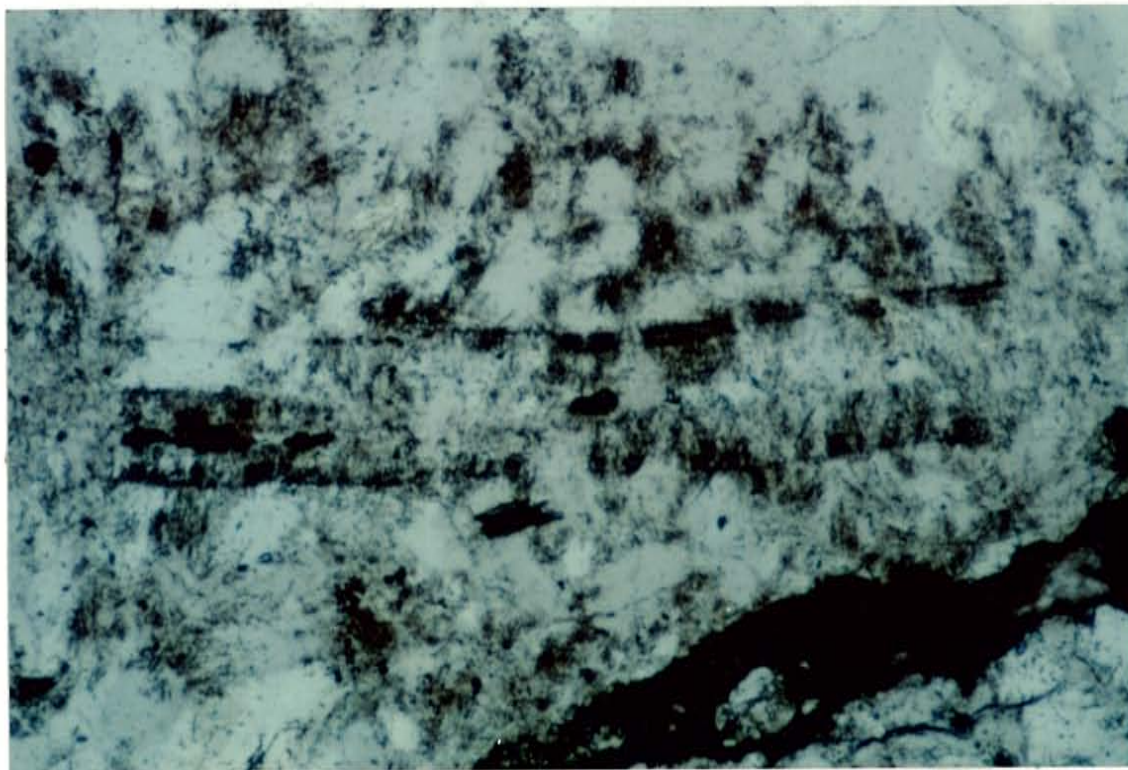


Figure 47-- Photomicrograph of recrystallized chalcedonic quartz in sample 13E-20. Note the continuous bands of fluid inclusions cutting across grain boundaries. Field of view is 1000 microns.

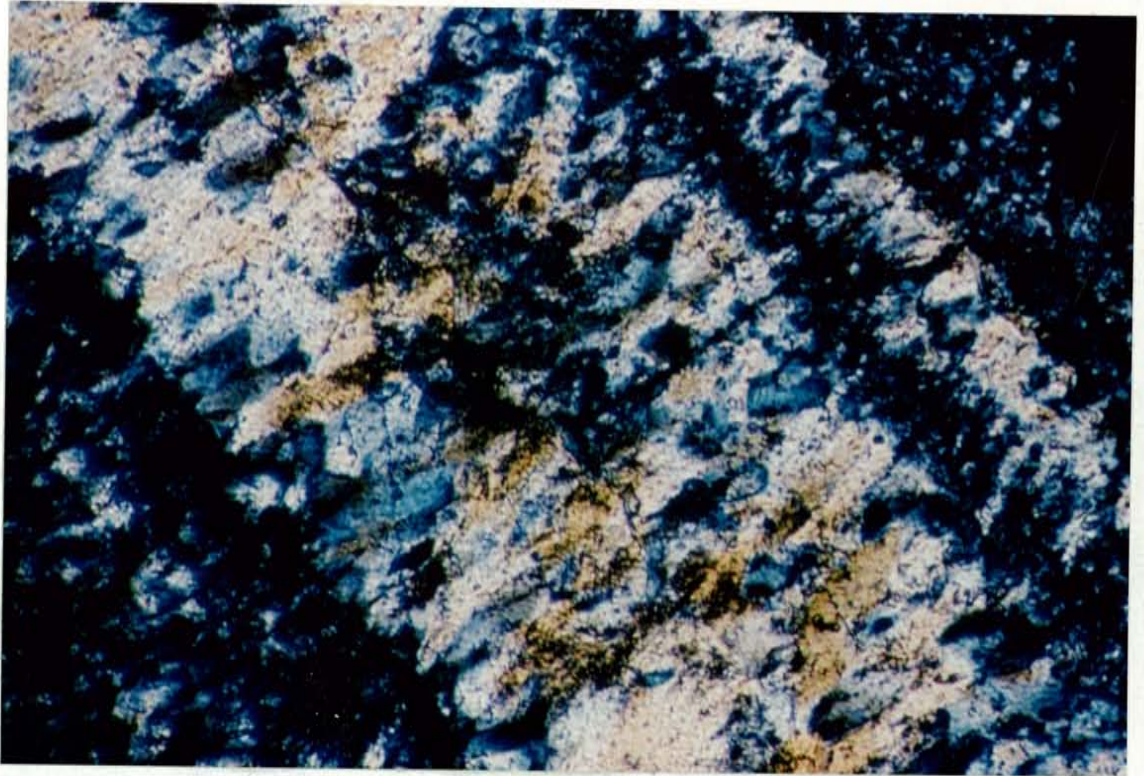


Figure 48-- Photomicrograph of quartz pseudomorphs after  
bladed calcite in sample C88-7k 34'. Field of view is  
1000 microns across.

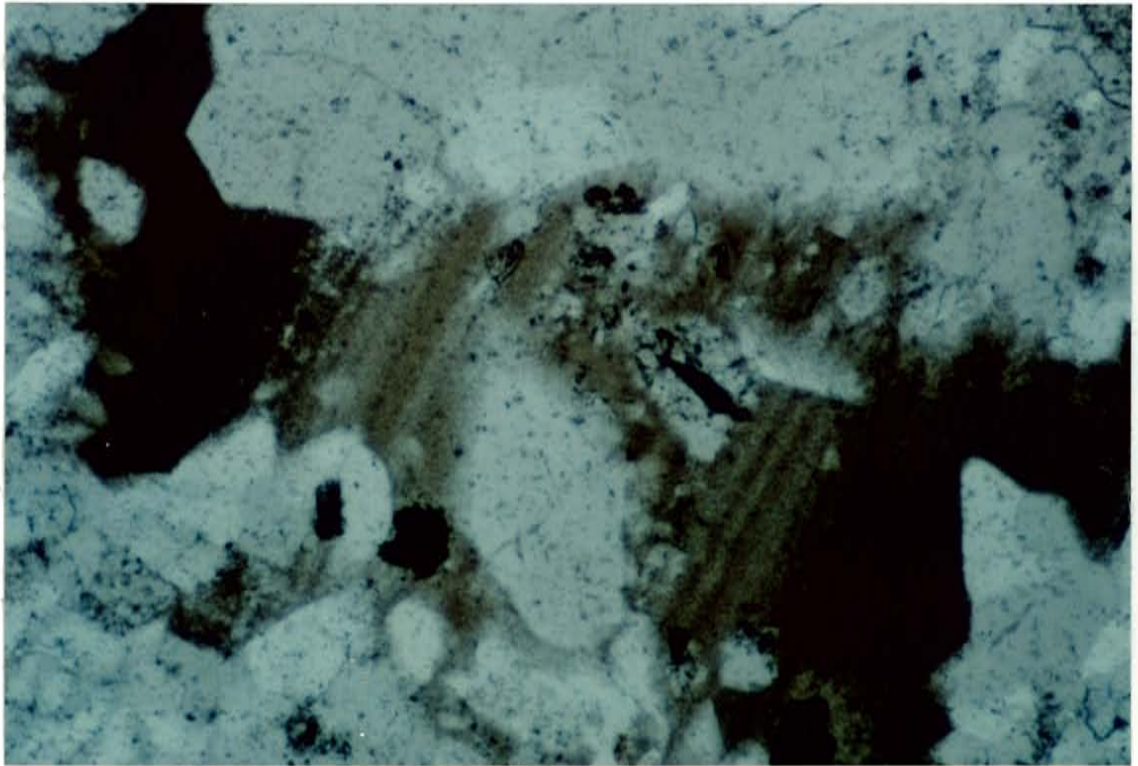


Figure 49-- Photomicrograph of "stratified" quartz in  
sample 19-52. Field of view is 1000 microns.



characterized by a dense array of 2-3 micrometer spheres  
and a zone of concentric quartz with a radiating  
ring of concentric quartz. Some of these structures in  
contact.

On the basis of petrographic relationships and  
compositions, it is clear that quartz was deposited  
throughout the history of the mineralizing system. It is

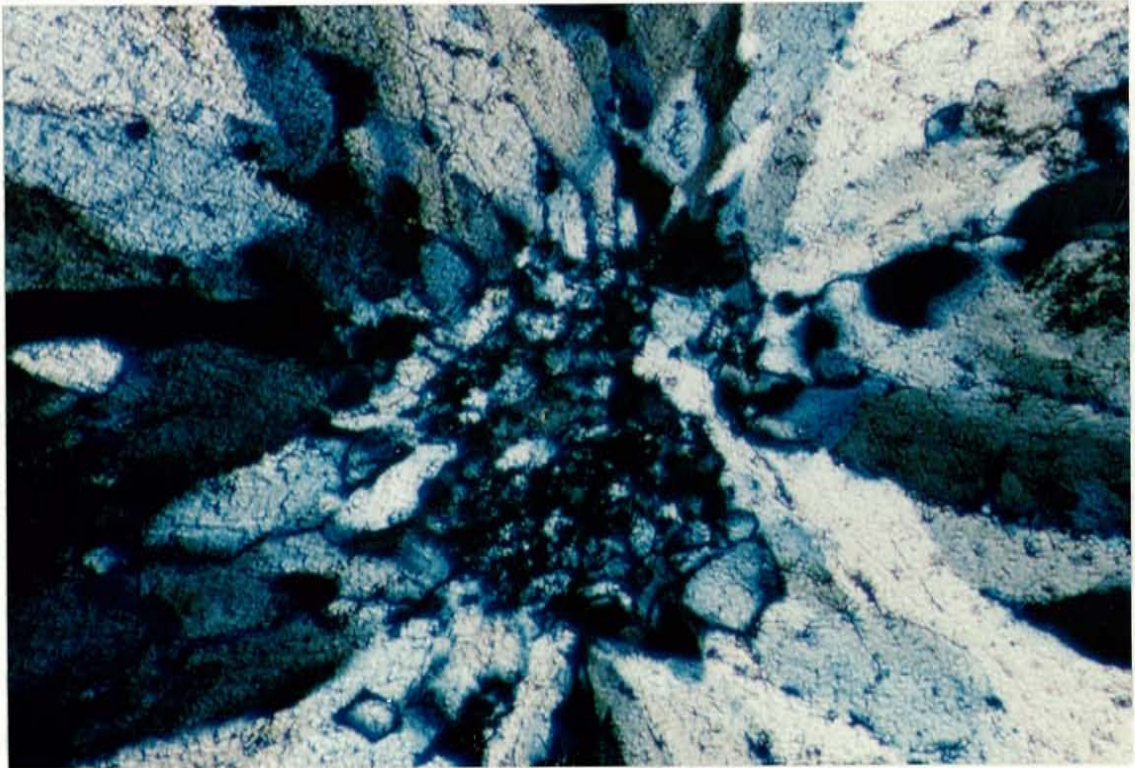


Figure 50-- Photomicrograph of quartz spheres in sample  
10-9. Field of view is 1000 microns.

characterized by a dense packing of 3 mm diameter spheres consisting of a core of anhedral quartz with a radiating rind of coxcomb quartz. Neither of these two textures is common.

On the basis of cross-cutting relationships and associations, it is clear that quartz was deposited throughout the history of the mineralizing system. It is associated with all metallic and non-metallic minerals. Including the initial silica flooding of the sediments, there are at least five periods of quartz deposition.

#### Calcite

Calcite is secondary to quartz in abundance and in its spatial distribution throughout the system. Calcite is quite rare in Block One, where it has been replaced by quartz, yet is quite abundant in Block Two where it is a major component of virtually every vein. Similarly in Block three, it is a volumetrically important phase. In contrast to quartz, however, hydrothermal calcite occurs exclusively in veins. As mentioned previously, the only other occurrence is of diagenetic origin.

Calcite exhibits only two textural varieties, bladed and blocky. Bladed calcite (figure 51) is by far the most abundant and was deposited throughout the L-D mine system; importantly, in Block One, it was subsequently pseudomorphed by quartz. Calcite blades are typically

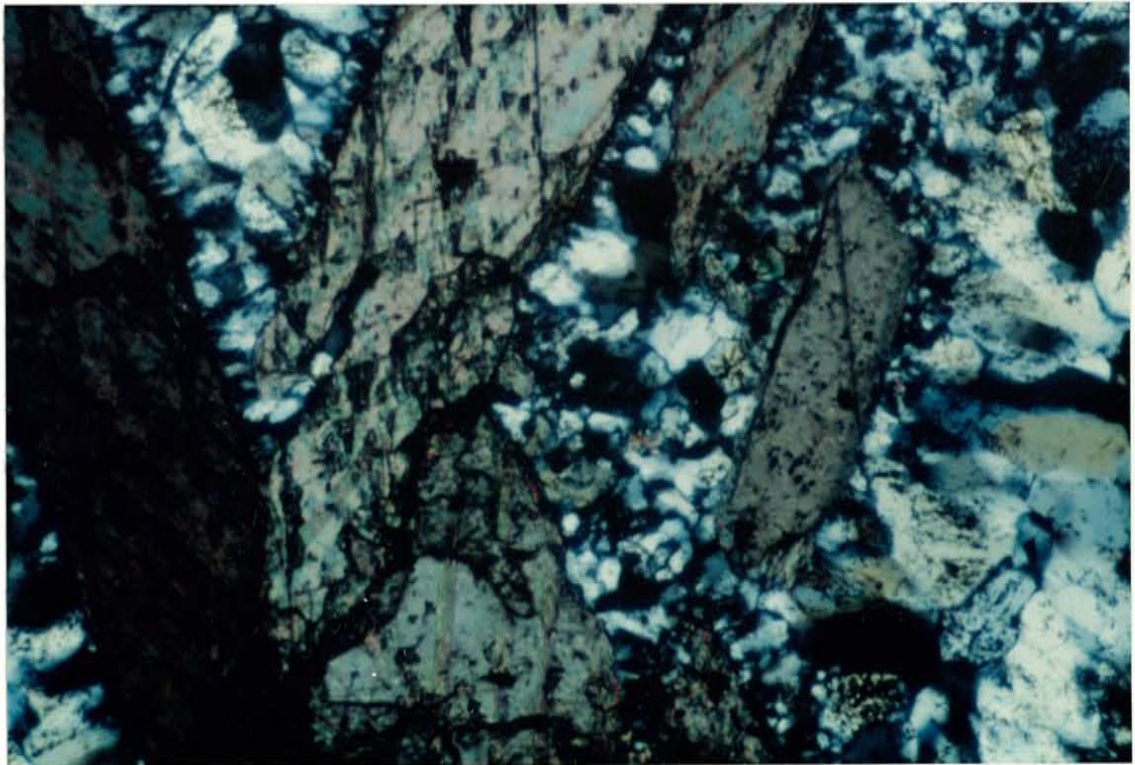


Figure 51-- Photomicrograph of bladed calcite in sample 22-101. Note the boxwork texture and drusy quartz. Field of view is 1000 microns.

arranged in a boxwork pattern with drusy quartz deposited on the blades, forming a rind of crystals projecting into the voids. Bladed calcite forms the largest single crystals, reaching a maximum of 5 cm in length. Blocky calcite is most common in the upper portions of the system in Block Two, where it occurs as late stage vug filling (figure 52). Portions of veins containing carbonate are characteristically poor in metallic phases and precious metal phases are not observed at all. Generally, the rare sulfide that is observed is arsenopyrite.

Based on paragenetic relationships, calcite has been deposited over a large portion of the life of the hydrothermal system. In terms of the five periods of quartz deposition, calcite is associated with the middle periods. The exception is the upper portions of the system where it occurs as the last stage of mineralization. Basically, the medial stages of mineralization are characterized by veins with alternating periods of quartz and quartz + calcite.

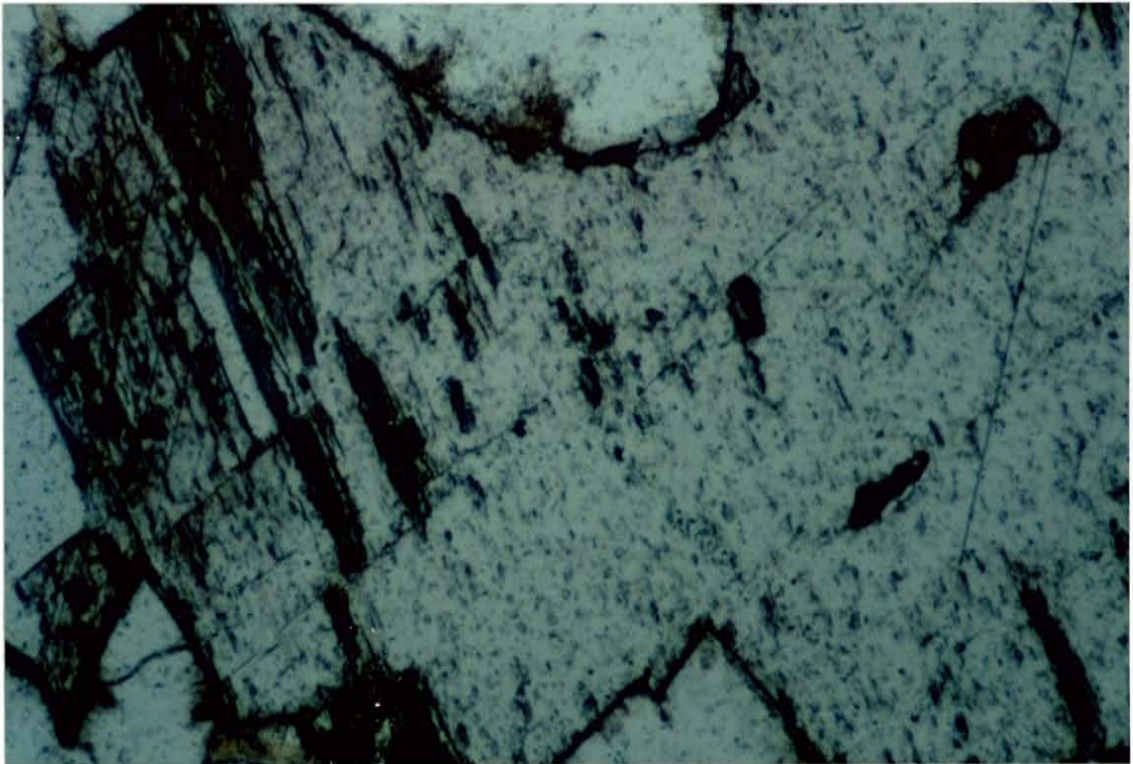


Figure 52-- Photomicrograph of blocky calcite filling a vug in quartz in sample 19-52. Field of view is 1000 microns.

## Adularia

Adularia is the least abundant gangue mineral in the L-D system and is confined exclusively to veins.

Spatially, adularia is most common in Block One veins, rare in Block Two, and not observed in Block Three.

Texturally, adularia occurs as euhedral grains (figure 53). The adularia is uncharacteristically coarse grained in this system, compared to other epithermal systems and the Cannon mine (Ott, 1988). The largest adularia grain was 9 mm across and they are commonly several hundred microns across, Block Two adularia is finer grained. Adularia is associated with coarse grained quartz in veins that contain no precious metals and are rare in sulfides. Chalcopyrite is the only sulfide observed in adularia bearing veins.

Unlike quartz and calcite, adularia was deposited over a limited time during the early part of the medial stages of mineralization.

## Metallic mineralogy

Simplicity is strictly confined to the non-opaque gangue mineralogy. In contrast, the metallic mineral phases include pyrite, arsenopyrite, chalcopyrite, electrum, native gold, marcasite, acanthite, proustite, pearceite, naumannite, native silver, aguilarite, sphalerite, and

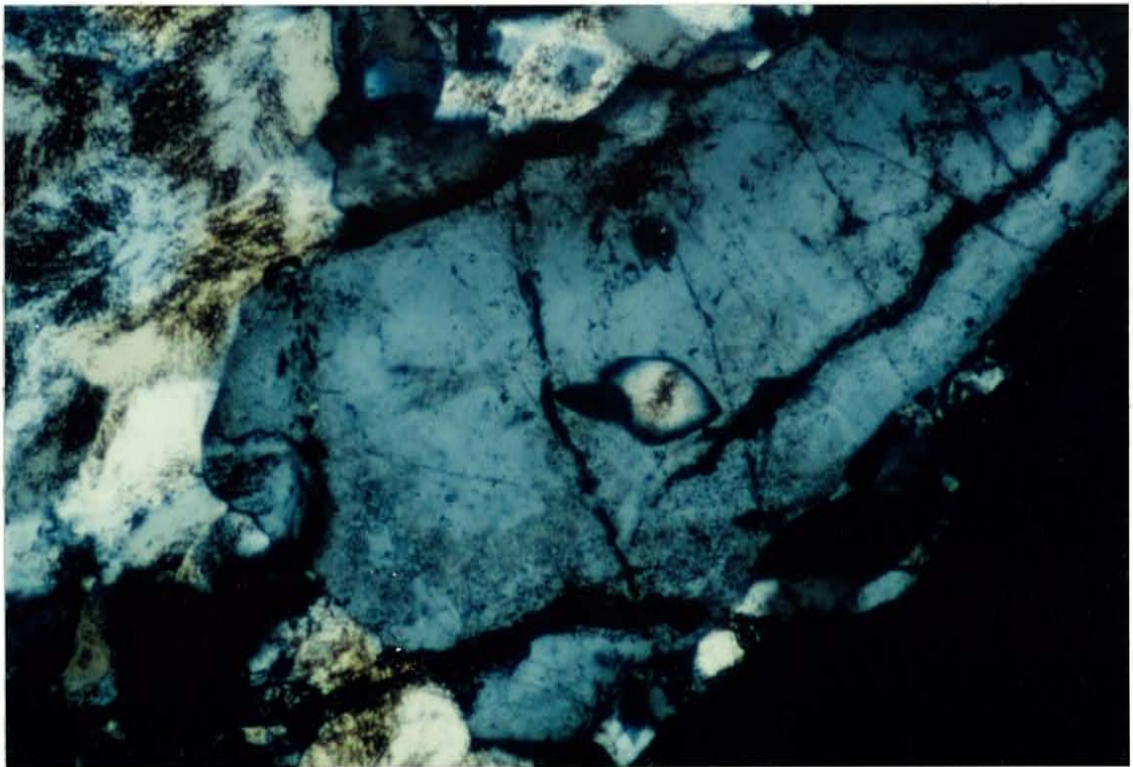


Figure 53-- Photomicrograph of euhedral adularia in sample 13B-1. Grain is 53 microns across long dimension.

pyrostitpnite, in order of decreasing abundance.

## Pyrite

Similar to most epithermal systems, pyrite is the most common metallic phase in the L-D system. Like quartz, it is present as an alteration phase in the wall rock as well as in veins. It is most important and most visible, however, in wall rock. Pyrite is equally distributed both laterally and vertically throughout the system.

In wall rock pyrite occurs most commonly replacing biotite along cleavage planes (figure 29). It also occurs as disseminated grains in the sedimentary matrix, possibly replacing carbonaceous material, and as tiny discontinuous veinlets (figure 54). The pyrite observed in the wall rock is almost always anhedral. Abundance in altered rock is as high as 3 % by volume, but averages about 2 %. Pyrite is also fine-grained ranging from 1 micron up to rare millimeter size cubes. In veins, pyrite is ubiquitous, but seldom exceeds 1 % by volume of vein material. Pyrite in veins is subhedral to euhedral and seldom exceeds 400 microns. Microprobe work shows that at least some of the pyrite in veins is arsenian (Modreski, written communication).

Pyrite is almost exclusively associated with fine to medium grained quartz, rare in portions containing calcite, and is not observed in adularia bearing veins. It



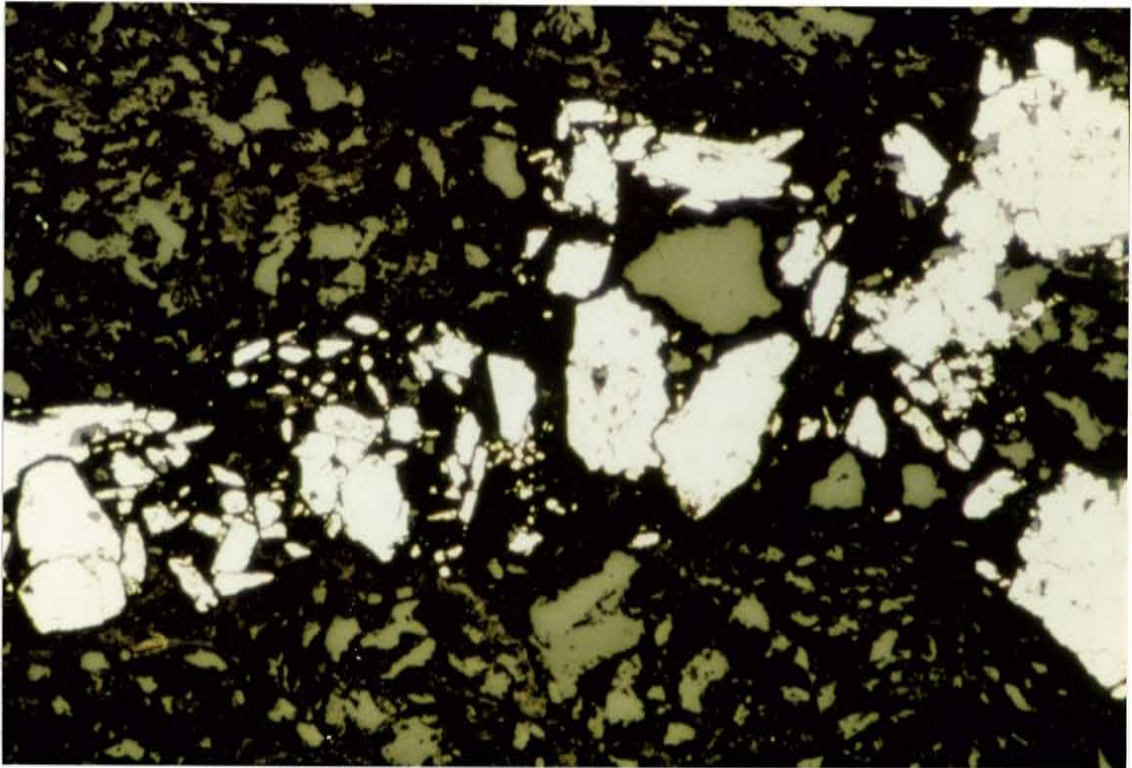


Figure 54-- Photomicrograph of discontinuous veinlet  
composed exclusively of pyrite from sample C87-2x  
115'. Field of view is 1000 microns.

is associated with every metallic phase and was deposited sporadically throughout the history of the system.

### Arsenopyrite

Arsenopyrite is the second most abundant metallic phase in the mine. Like pyrite, it occurs in wall rock accompanying alteration and is an important vein constituent. It is found throughout the entire system with no obvious lateral or vertical variation. Arsenopyrite was not identified in the L-D mine prior to this study.

In the wall rock, arsenopyrite occurs chiefly as a replacement of pyrite in both biotite grains (figure 32) and the matrix. Its abundance in the wall rock is less than that of pyrite, generally comprising no more than 2 % by volume. It occurs as anhedral to euhedral grains, with euhedral most common in veins. Arsenopyrite is also fine-grained reaching a maximum of only 500 microns. It is the only sulfide phase associated with bladed calcite, albeit in minor amounts. In addition, it is found with late vug filling calcite.

Paragenetic relationships with precious metal phases are rarely observed, but when the two occur together arsenopyrite is always earlier. Relationships with chalcopyrite in the same vein are similar, chalcopyrite is the later phase. Based on other criteria, however, it is apparent that arsenopyrite was deposited throughout the

history of the system.

### Chalcopyrite

Chalcopyrite is a common phase and although it occurs in all portions of the mine, it is most abundant in Block One.

Individual chalcopyrite grains occur exclusively as anhedral grains disseminated throughout fine to medium grained quartz, and is the only sulfide associated with adularia. In Block One, grains are less than 500 microns, which is in contrast to Blocks Two and three, where it is less than 300 microns.

Similar to the precious metals, chalcopyrite was deposited relatively early in the system. When associated with pyrite and arsenopyrite in the same generation of quartz, however, chalcopyrite is paragenetically last.

### Electrum

Electrum is the dominant precious metal phase in the system. It is most commonly observed in Block Two and Block Three veins. Grains occur as rounded anhedral grains and exhibit no contact relationships to other minerals in Block One, but is often observed rimming pyrite grains in Block Two. A silver-rich variety also occurs. Figures 55 and 56 are histogram plots of electrum grain sizes. In the major veins electrum is always observed in fine to medium

grained quartz adjacent to the wall of the vein. In all samples studied, electrum was deposited early in the system, but paragenetically later than pyrite.

#### Native gold

Native gold is not an abundant constituent of the veins sampled in this study, and was observed only in Block One veins. Although reported by Guilbert (1963), in this study no gold was observed in wall rock. Texturally, gold occurs as highly irregular grains (figure 57). Figure 58 is a histogram plot of gold grain sizes in two samples from Block One. Native gold is observed in the period of quartz deposition nearest to the wall of the vein, in early wall rock vein breccia, or more rarely with iron oxides. It is possible that some of the native gold is of supergene origin. Native gold was not noted in contact relationships with other metallic minerals.

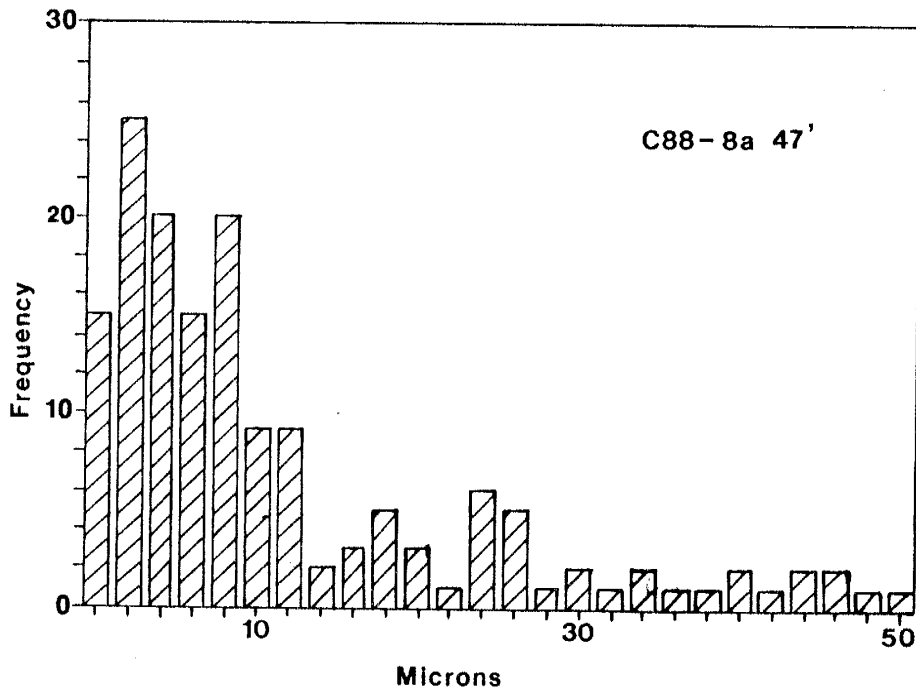
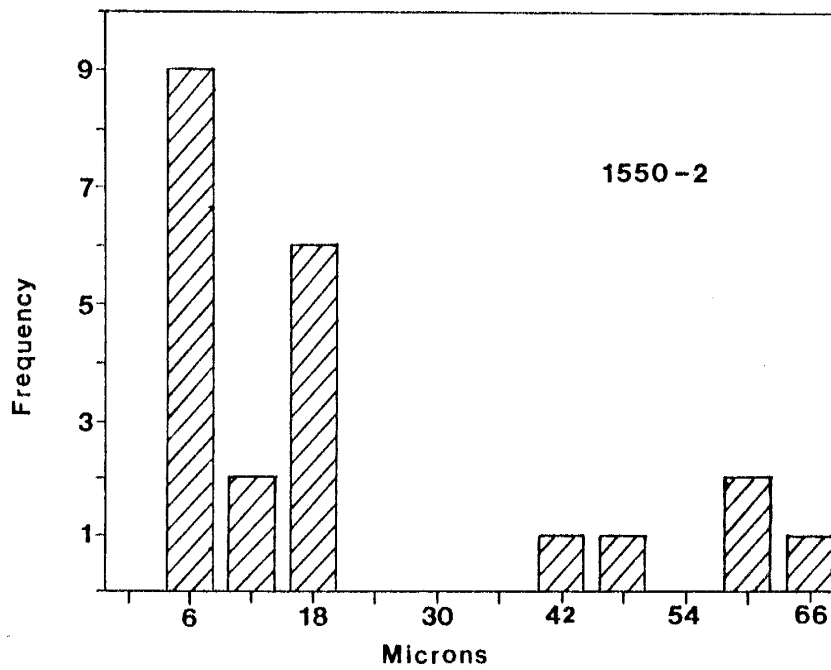


Figure 55-- Histogram plots of electron grain sizes in samples C88-8A 47' and 1550-2 from Blocks One and Two respectively.

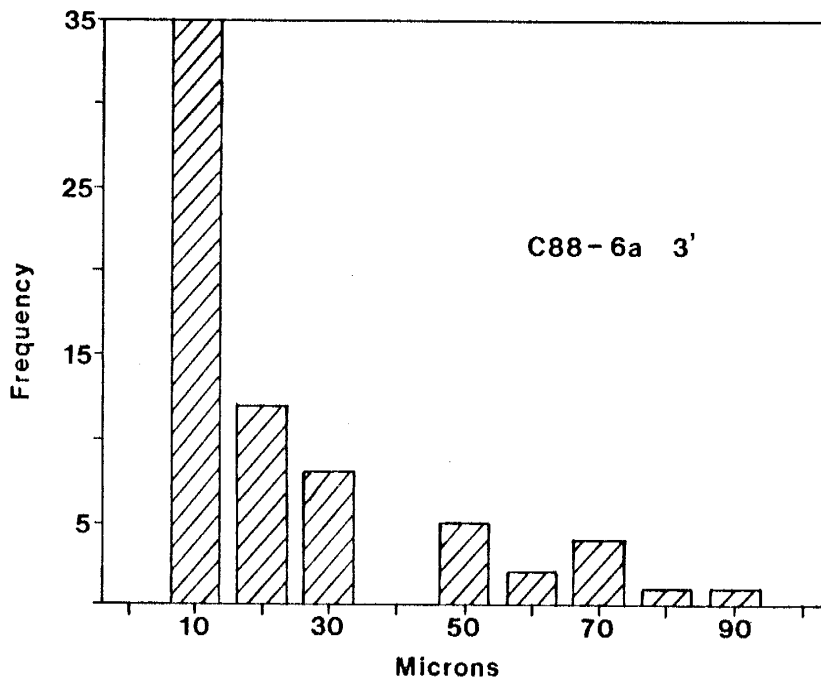
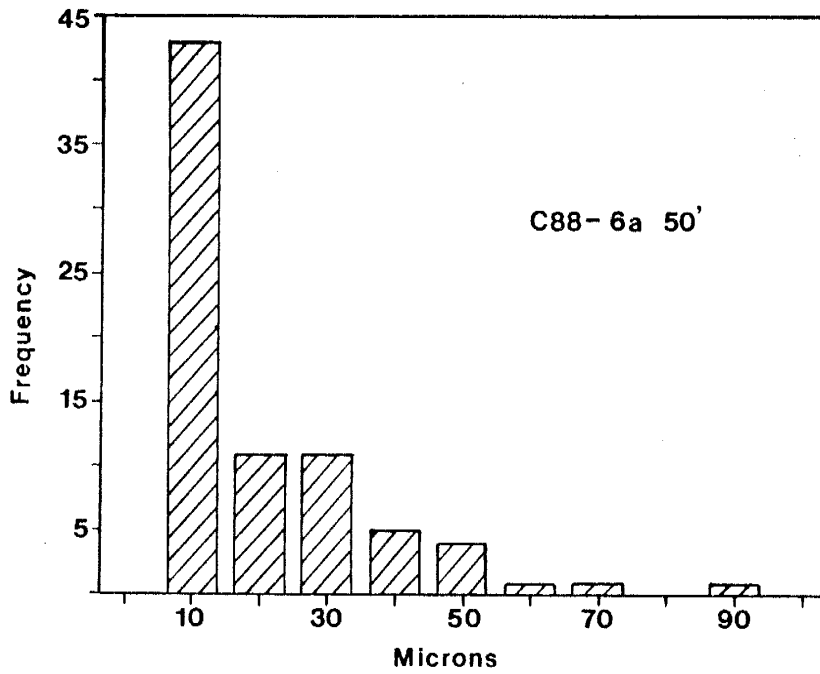


Figure 56-- Histogram plots of electrum grain sizes in samples C88-6A 3' and C88-6A 50' from Block Two.

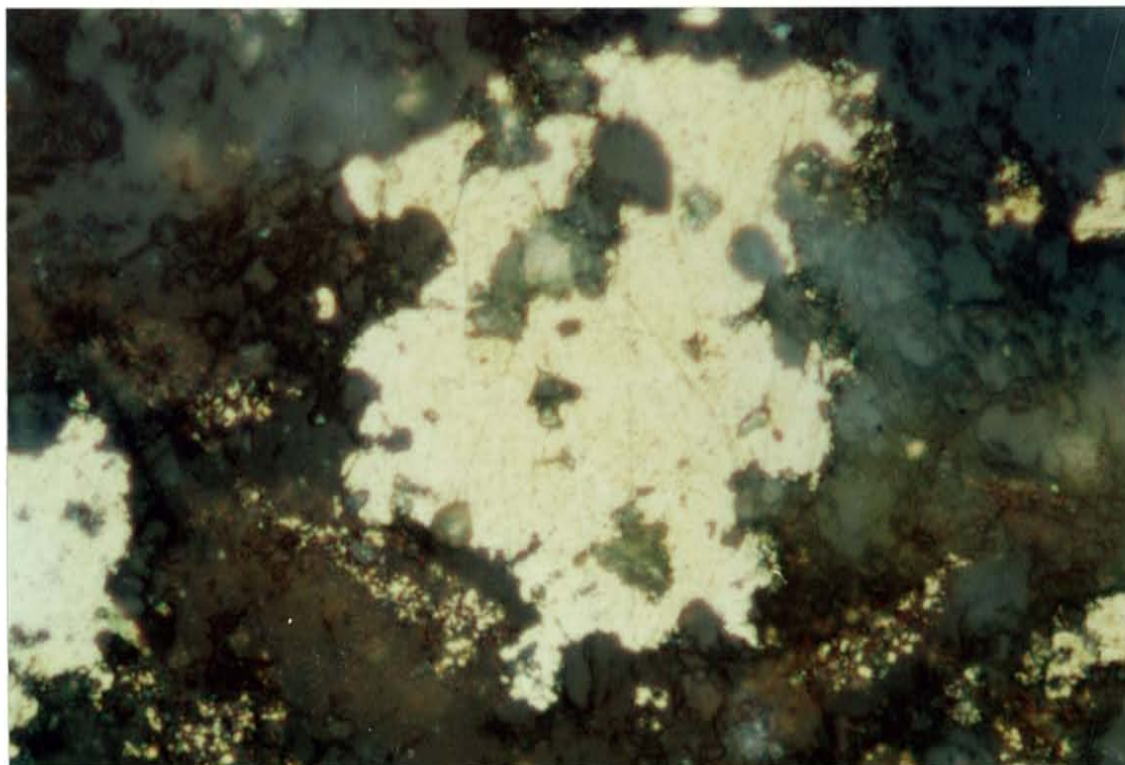


Figure 57-- Photomicrograph of large native gold grains in a sample of the 2.5 vein from the 1250 level of Block One. Grain is 90 microns across.

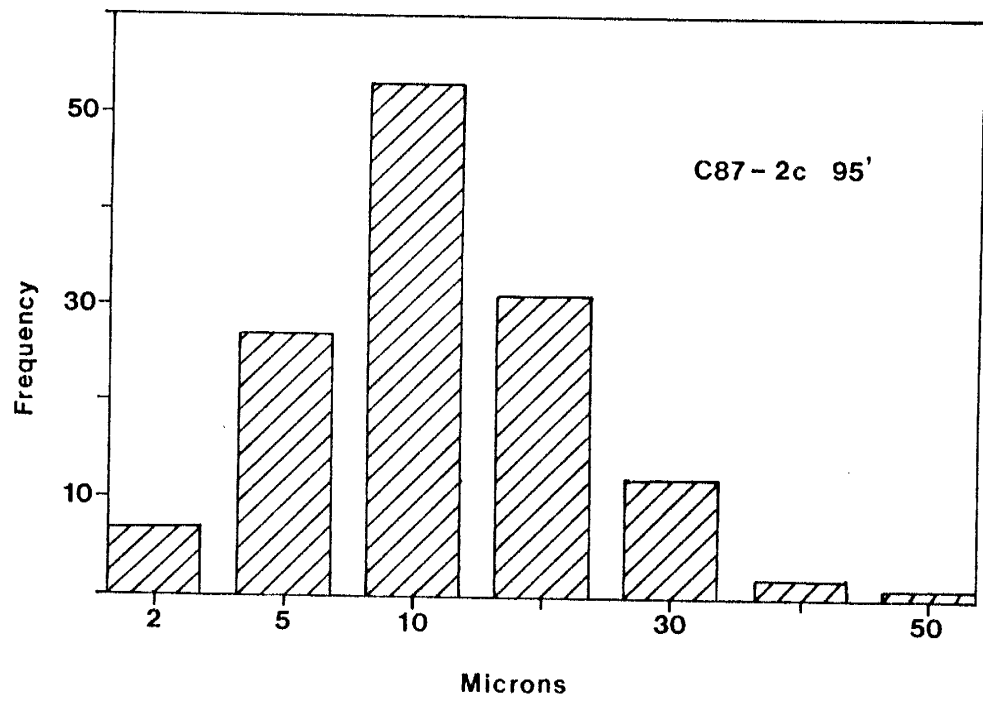
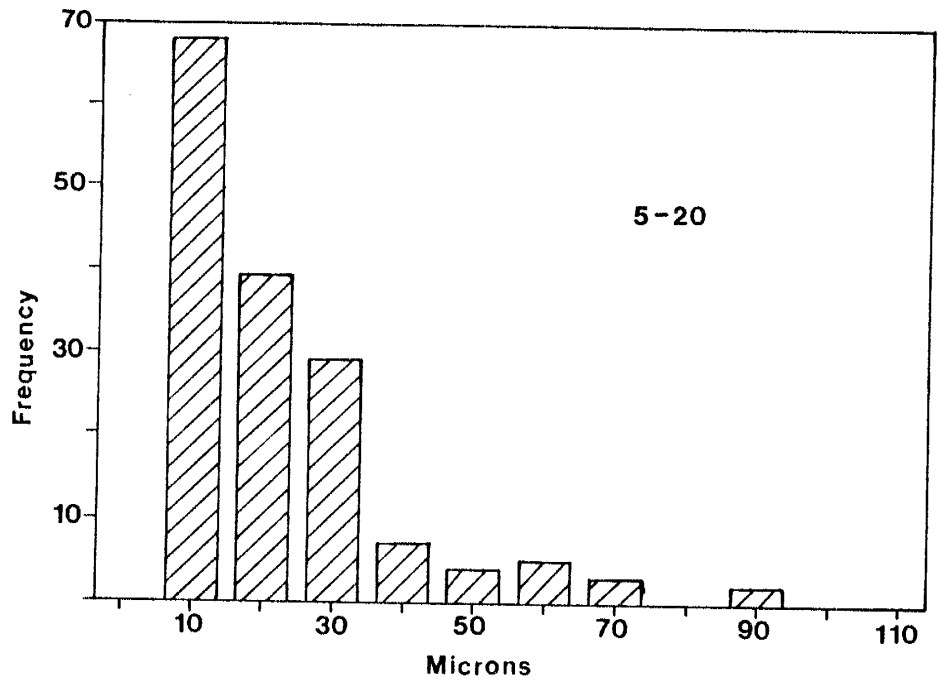


Figure 58-- Histogram plots of gold grain size from samples 5-20 and C87-2C 95' from Block One.



## Marcasite

Marcasite is observed exclusively in the wall rock, often associated with arsenopyrite, but paragenetically earlier (figure 59). Gilbert (1963) reported that marcasite was a very important gangue mineral occurring in the wall rock, veins and in vugs in late quartz.

## Acanthite

Acanthite is the most abundant silver phase other than electrum. It is observed throughout the system, but is not common, and until this study was not identified in the L-D mine. Acanthite grains are irregular and are as large as 100 microns in diameter. Acanthite is always paragenetically late and is observed in the matrix of brecciated portions of quartz veins, where it partially wraps around vein fragments (figure 60). This is in contrast to other precious metal phases which were deposited prior to brecciation.

## Sulfosalts

Sulfosalts identified in the L-D mine include proustite, pearceite and possibly pyrostilpnite. They are extremely rare and were found in only two samples, both from Block One. This is undoubtedly the reason they were never previously identified. Grains are subhedral and seldom exceed 150 microns in diameter. Pearceite was observed only

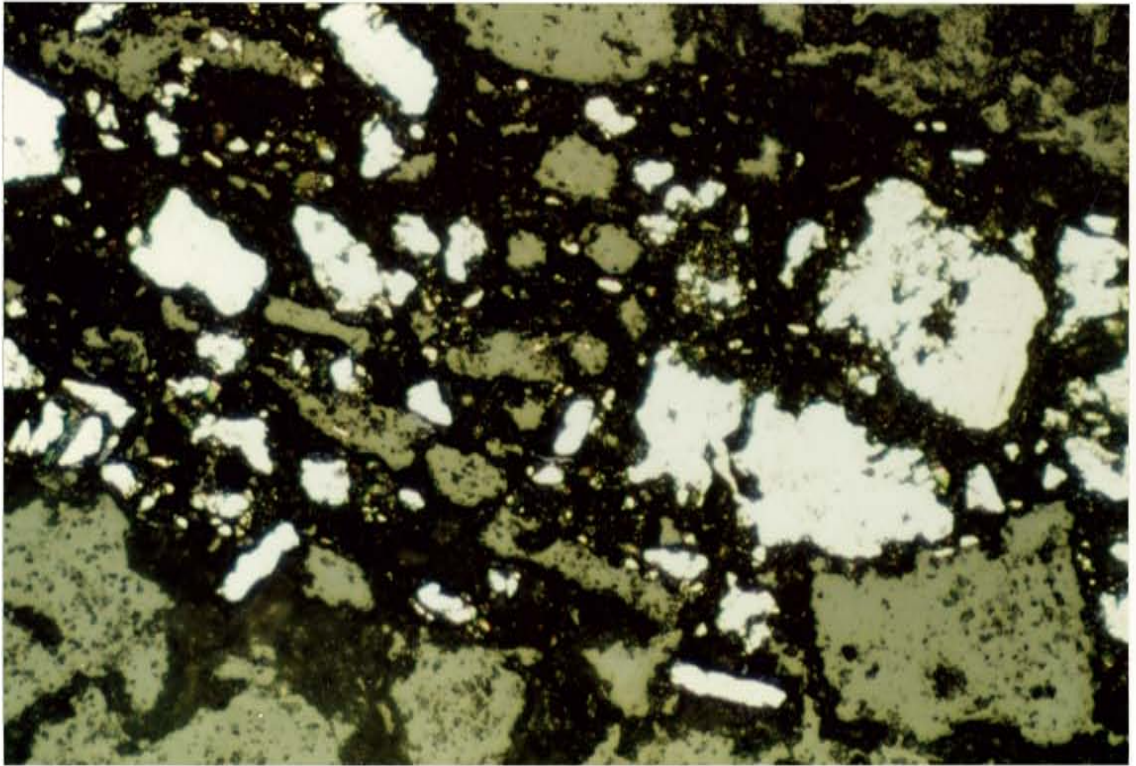


Figure 59-- Photomicrograph of marcasite occupying a fracture in arkosic wall rock from sample C87-1j 178'. Field of view is 700 microns.

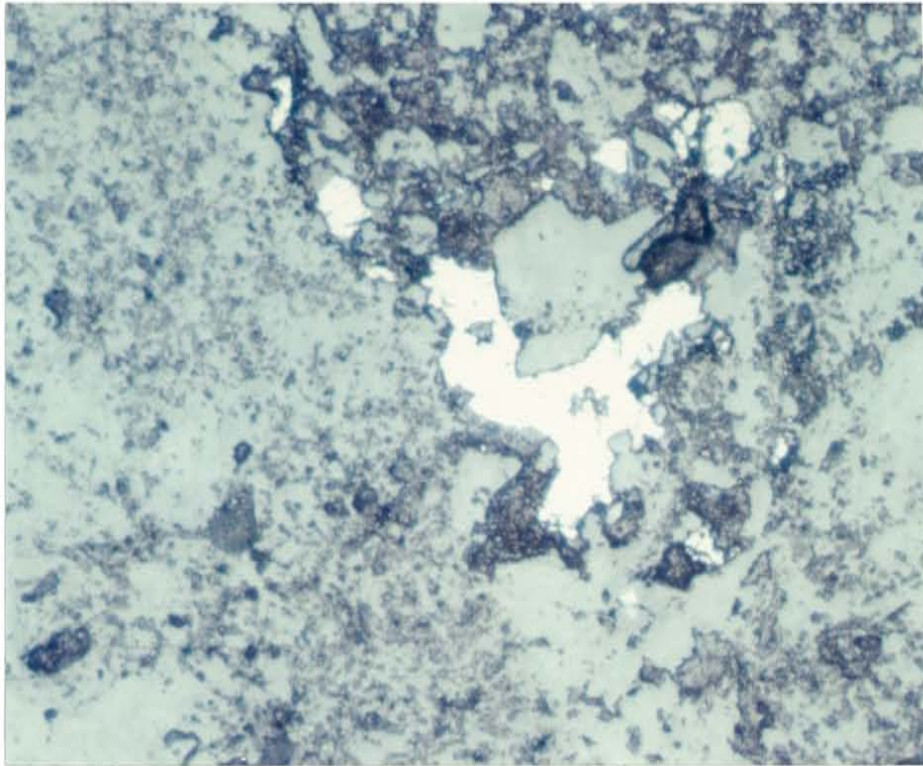


Figure 60-- Photomicrograph of an acanthite grain from sample C87-4m 33'. Note how the grain is partially wrapped around the vein fragment. Grain is 170 microns across.

in sample C87-4m, from the north end of Block One, and is closely associated with proustite (figure 61). The characteristic deep red internal reflections are diminished in all examples of this mineral indicating that it contains copper. Since chalcopyrite is present in the same vein and is paragenetically earlier, copper was certainly available. The other sulfosalt also occurs only in sample C87-4m. This mineral exhibits distinct yellow internal reflections and is closely associated with the other sulfosalts, so it is tentatively identified as pyrostilpnite. Virtually every sulfosalt grain is either in contact with or enclosing Ag-poor electrum.

The sulfosalts are not volumetrically important precious metal phases. Paragenetically, they occur in early stages of quartz, but are later than native gold and electrum. Contact relationships with electrum suggest the sulfosalts formed by sulfur and arsenic bearing fluids scavenging silver from electrum.

#### Native silver

Native silver is extremely rare and was observed in only one sample from the north end of Block One. It is closely associated with proustite, possibly as a replacement of the earlier sulfosalt. Microprobe work contracted by Asamera identified native silver occurring as fracture-filling material.

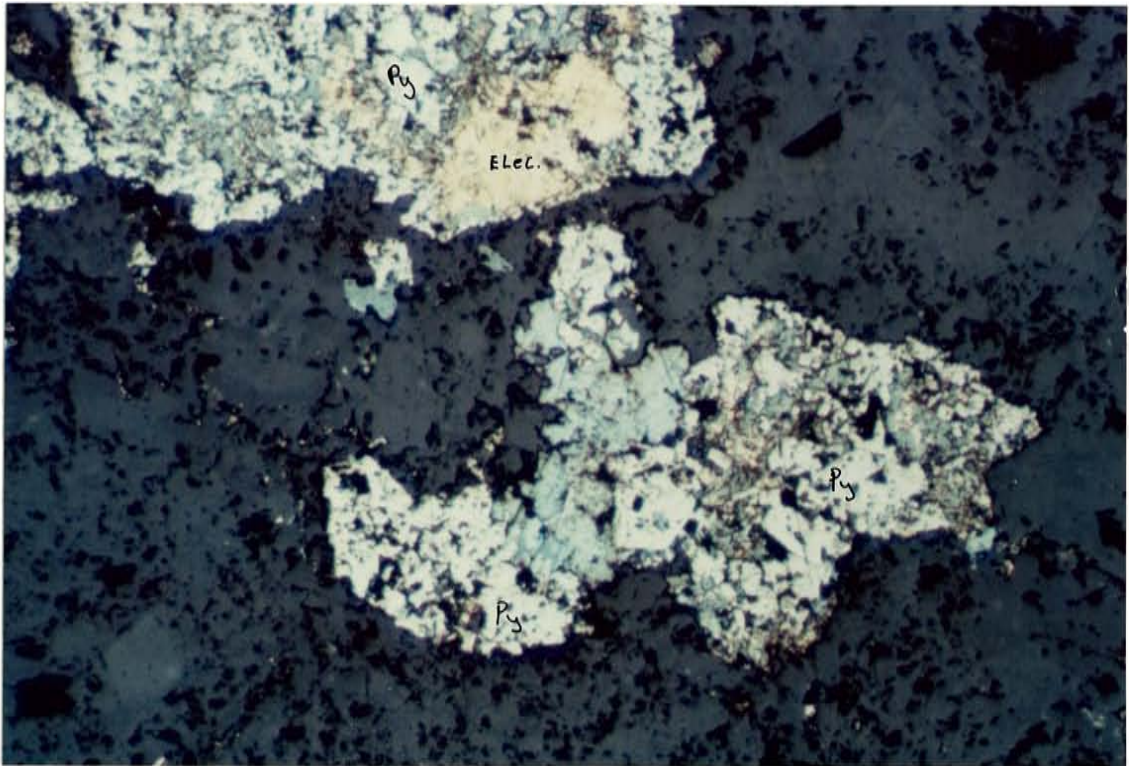


Figure 61-- Photomicrograph of pearcrite and proustite in sample C87-4m 33'. Field of view is 800 microns.

## Naumannite/Aguilarite

Naumannite is reported by Guilbert (1963) to be an important mineral in the L-D mine. Microprobe work contracted by Asamera confirmed the existence of naumannite in three samples. In two of the samples, naumannite, aguilarite and native silver occur as fracture filling in a quartz vein. As naumannite is the low temperature (< 133 C) orthorhombic polymorph of  $\text{Ag}_2\text{Se}$ , this together with the association of native silver suggests a low temperature hydrothermal assemblage. The third sample also shows naumannite and aguilarite paragenetically late with respect to other precious metal phases and probably also represents late stage, low temperature hypogene mineralization. Naumannite and aguilarite are volumetrically minor precious metal phases.

## Sphalerite

Sphalerite was identified by Guilbert (1963) as a rare accessory phase. Microprobe work by Asamera Minerals also confirmed the existence of the mineral. The petrography in this study revealed no sphalerite. As such, it is ascertained that sphalerite is a very minor phase.

Table 5-- List of the minerals and their idealized compositions, found in the L-D mine during the course of this study.

<u>MINERAL</u>	<u>COMPOSITION</u>
Quartz	$\text{SiO}_2$
Calcite	$\text{CaCO}_3$
Adularia	$\text{KAlSi}_3\text{O}_8$
Sericite	$\text{KAl}_2(\text{Si}_3\text{Al})\text{O}_{10}(\text{OH})_2$
Illite	$\text{KAl}_4(\text{Si}_7\text{Al})\text{O}_{20}(\text{OH})_4$
Chlorite	$(\text{Mg,Al,Fe})_{12}(\text{Si,Al})_8\text{O}_{22}(\text{OH})_{16}$
Kaolinite	$\text{Al}_2\text{Si}_2\text{O}_5(\text{OH})_4$
Jarosite	$\text{KFe}_3(\text{SO}_4)_2(\text{OH})_6$
Goethite	$\text{FeO}(\text{OH})$
Hematite	$\text{Fe}_2\text{O}_3$
Pyrite	$\text{FeS}_2$
As-pyrite	$(\text{Fe,As})\text{S}_2$
Marcasite	$\text{FeS}_2$
Arsenopyrite	$\text{FeAsS}$
Chalcopyrite	$\text{CuFeS}_2$
Electrum	$\text{AuAg}$
Native Gold	$\text{Au}$
Acanthite	$\text{Ag}_2\text{S}$
Proustite	$\text{Ag}_3\text{AsS}_3$
Pearceite	$\text{Ag}_{16}\text{As}_2\text{S}_{11}$
Pyrostilpnite	$\text{Ag}_3\text{SbS}_3$
Naumannite	$\text{Ag}_2\text{Se}$
Aguilarite	$\text{Ag}_4\text{SeS}$
Native Silver	$\text{Ag}$

## Paragenesis

Mineralogic associations and textures observed within a spatial context are a reflection of the variety of geologic, hydrologic and geochemical factors that change through time. Moreover, these factors vary not only with time, but in space as well. To break down and isolate each mineral phase and place it in a specific temporal relationship is difficult.

Prior to the main mineralizing event, hydrothermal fluids flooded permeable L-D mine sediments and altered the more reactive detrital grains, such as plagioclase and biotite; suggesting that early in the hydrothermal system permeability was an important control on mineralization. Paragenetically, this means propylitic alteration with chlorite and pyrite developed initially, followed by silicification with sericitization (K<sup>+</sup> metasomatism), arsenopyrite and minor pyrite. This produced a well sealed wall rock and, together with subsequent brittle deformation and continued hydrothermal activity, permitted development of main stage of mineralization. In contrast to early alteration, main stage mineralization was structurally controlled.

Mineralization occurred simultaneously with structural deformation along the Eagle Creek wrench-fault, generating the essential plumbing system and sites for mineral deposition during main stage mineralization.



Abundant cross-cutting veins attest to the synchronous activity of deformation and mineralization. It is clear from the textures observed in the major veins in Block One that the system was silica or, in part, carbonate-rich, producing alternating quartz-rich and calcite-rich bands. This alternating period of quartz, with associated pyrite and arsenopyrite, and calcite dominated the history of the system.

Based on mineral paragenesis, it is apparent the chemistry of the fluids, early in the system, were appropriate for the transport of precious and base metals, particularly gold and copper. Adularia was also deposited early. Silver was transported and deposited over a chronologically and volumetrically greater part of the L-D mine hydrothermal system.

Three changes can be deduced from this information. First, potassium was an important early constituent, because it comprises an important part of early alteration assemblages as well as hydrothermal K-spar development in the veins. Secondly, the fluids changed from gold dominant to silver dominant, reflecting either the diminished capacity to transport gold or perhaps depletion of gold in the source. Finally, the fluids became copper poor, reflecting a diminished capacity to transport copper. Iron and arsenic activity remained relatively uniform. Arsenic, sulfur and minor antimony content in L-D mine

fluids is reflected by replacement of early native metals by sulfosalts. Later stages of mineralization are characterized by silica, carbonate, no boiling, low sulfur, and are comparatively silver-rich as indicated by the assemblage acanthite, naumannite, aguilarite, and native silver. Figure 62 is a diagrammatic representation of the relative timing of mineral deposition.

Finally, uplift and erosion exposed the altered rocks to surficial weathering that produced an acid stable assemblage of kaolinite, jarosite, goethite, and hematite.

#### Fluid inclusions

During the course of petrographic studies some notes were made on the occurrence and types of fluid inclusions present in the L-D system. The only fluid inclusion work in the district was performed by Klisch (1989) on the Cannon mine. He identified three types of fluid inclusions in quartz: 1) two phase liquid-rich, 2) two phase vapor-rich, and 3) three phase with daughter mineral. Calcite contained only two phase inclusions. Homogenization temperatures in main stage quartz averaged 285 C with an average salinity of 8 wt % NaCl. Coexistence of vapor-rich and liquid-rich inclusions and variable salinity are cited as evidence for boiling.

Primary fluid inclusions in quartz from the L-D

MINERAL	ALTERATION	MINERALIZATION	WEATHERING
<b>Gangue</b> QUARTZ CALCITE ADULARIA CHLORITE ILLITE KAOLINITE JAROSITE HEMATITE GOETHITE SERICITE	<hr/> <hr/> <hr/> <hr/> <hr/> <hr/> <hr/> <hr/> <hr/>	<hr/> <hr/> <hr/> <hr/> <hr/> <hr/> <hr/> <hr/> <hr/>	<hr/> <hr/> <hr/> <hr/> <hr/> <hr/> <hr/> <hr/> <hr/>
<b>Metallic</b> PYRITE ARSENOPYRITE CHALCOPYRITE ELECTRUM SULFOSALTS ACANTHITE NATIVE Au NATIVE Ag NAUMANNITE AGUILARITE	<hr/> <hr/> <hr/> <hr/> <hr/> <hr/> <hr/> <hr/> <hr/>	<hr/> <hr/> <hr/> <hr/> <hr/> <hr/> <hr/> <hr/> <hr/>	<hr/> <hr/> <hr/> <hr/> <hr/> <hr/> <hr/> <hr/> <hr/>

Figure 62-- Diagram showing the paragenetic sequence of hydrothermal minerals in the L-D mine.

mine are abundant, but extremely small, usually less than 2 microns. These are mostly two phase, liquid-rich inclusions and occur in a variety of patterns (figure 63) and are found in only the early and middle stages of quartz deposition. The largest primary inclusions found in quartz were less than 10 microns across and were two phase, liquid-rich (degree of fill  $> 0.9$ ). These inclusions were in late stage quartz which was probably deposited at temperatures less than 200 c as suggested by the large degree of fill and the lack of associated sulfides. Secondary inclusions in quartz (figure 63) are single phase, liquid inclusions which are suggestive of low temperatures.

The best-developed inclusions, in terms of variety, abundance, and size, occur in calcite blades. Secondary inclusions in calcite are single phase, liquid and two phase, liquid-rich. Primary and pseudosecondary inclusions include: 1) two phase vapor-rich, 2) two phase liquid-rich, and 3) single phase vapor inclusions. Often a single blade of calcite will contain every type of inclusion (figure 64). The coexistence of liquid and vapor dominated inclusions, plus the bladed nature of the calcite is evidence for boiling.

Fluid inclusions were not observed in adularia, late blocky calcite, or early quartz.

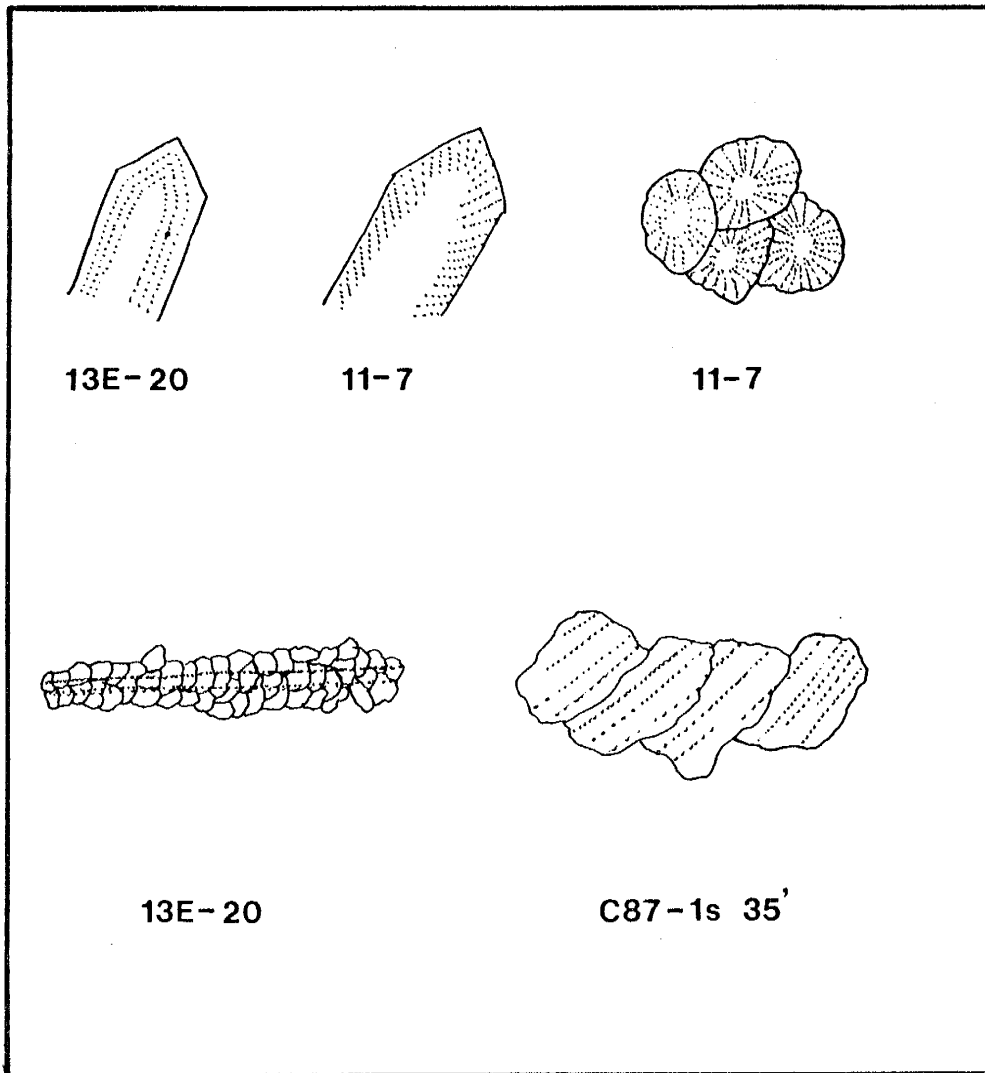


Figure 63-- Sketches of fluid inclusion textures in quartz.  
 The top three sketches are typical primary inclusions  
 and the bottom two sketches are typical secondary  
 inclusions.

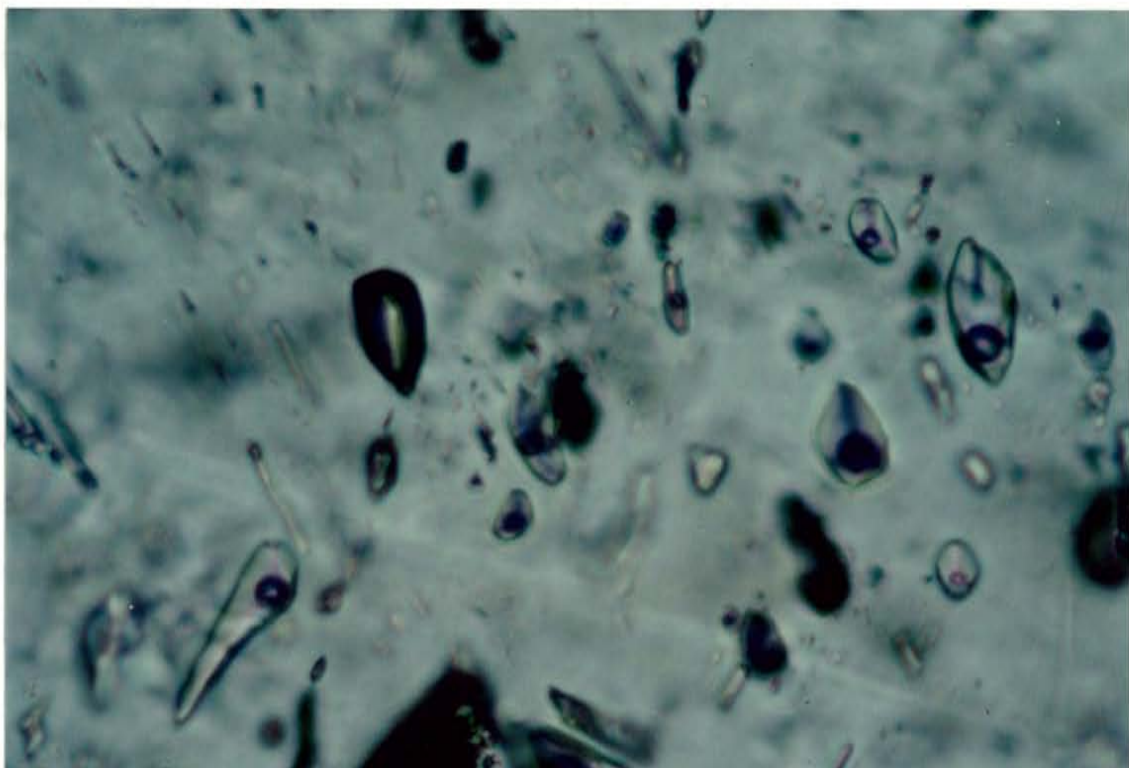


Figure 64-- Photomicrograph of fluid inclusions in a calcite blade from sample 22-101 in Block Two. Note the coexistence of vapor and liquid-rich inclusions. Large vapor inclusion is 20 microns in length.

## TRACE-ELEMENT GEOCHEMISTRY

The trace-element composition of a mineral deposit presents partial evidence of the characteristics of a hydrothermal fluid. Together with other aspects of mineralization, it provides insight into the nature of the entire hydrothermal system and the position of mineralization within that system. Mineral and alteration assemblages observed in the L-D mine are characteristic of dilute, neutral to weakly acidic, epithermal hydrothermal fluids. The trace-element make-up and low abundances also reflect these characteristics.

The data used in this section was collected by United Mining Corporation and Asamera Minerals during exploration and evaluation of the area. This study is a compilation and interpretation of that data. Analyses included the elements Au, Ag, Sb, Hg, Se, Cu, and Zn. Asamera Minerals samples are a composite of both veins and altered wall rock, so results provide an "average" over the duration of the hydrothermal system. Samples taken by United Mining consist of vein samples and wall rock samples, but the two are considered together. Data and figures are in Appendix II.

Data on precious metals is the most numerous. Analyses for precious metals was done from diamond drill holes and underground channel samples. A comparison of the results from the two methods and between the two companies

reveals some interesting results (figures II-1 to II-8). First, drill hole samples from Block One indicate a range of gold values from 0-3429 ppb and an average of only 510 ppb; silver values are in the range 0-15 ppm with an average of 2.5 ppm. Second, channel samples from Blocks 1 and 2 range from 0-14400 ppb for gold with an average of 1446 ppb and from 0-34 ppm for silver with an average of 4 ppm. Third, drill hole samples from Block 2 range from 0-24686 ppb and average 2544 ppb for gold and range from 0-32 ppm and average 7 ppm for silver. Fourth, United Mining Corporation's channel sampling program in Block 1 shows a range of gold values from 70-15325 ppb and an average of 2173 ppb, while silver ranges from 0.2-39 ppm and averages 6 ppm. Drill hole sampling shows substantially lower precious metal concentration than the channel samples. The reason why drill hole samples in Block One are uncharacteristically low is because the drill holes chosen for this study were those that cut across the entire spectrum of altered and unaltered rocks, so the drill holes are representative of the styles and distribution of mineralization, but not representative of the average grade of precious metals remaining in the ore body. This conclusion is supported by unpublished reserve estimates that indicate gold and silver grades in Block One are roughly similar to Block Two. The difference in channel sample results is due primarily to the fact that the UMC



data is biased with respect to vein samples. The average concentration of gold in the system is 2300 ppb and 6.5 ppm for silver, which translates to a silver to gold ratio of 3:1. Crustal Ag:Au is 17:1 (Levinson, 1974), which makes the L-D mine a gold-rich system.

In the Cannon mine (Ott, 1988), the silver to gold ratio is 4:1 and the overall precious metal content is similar with an average concentration of about 2109 ppb and 8 ppm for Au and Ag, respectively. There is no quantitative data published on the Wenatchee Heights mineralization, but Margolis (1987) indicated that the mineralization was zoned from Au-rich near the top to Ag-rich at depth.

United Mining Corporation, during their exploration program, analysed for As, Sb, and Hg, and included the elements Se, Cu and Zn on the basis of Guilbert's (1963) petrography. Arsenic values range from 9 to 290 ppm and average 114 ppm (figure II-9). Arsenic is present as arsenopyrite and as sulfosalts. Antimony concentration is quite low, ranging from 2-56 ppm with an average of only 8 ppm (figure II-10). This does not seem to support the occurrence of stibnite which Guilbert (1963) reported as quite common. It does, however, support the uncommon occurrence of sulfosalts revealed in this study. Mercury values range from 30-288 ppb and average 82 ppb (figure II-11). Primary mercury phases are not recognized in the L-D mine. Selenium concentration ranges from <5-28

ppm with an average of 4 ppm (figure II-12). Se is present as naumannite, aguilarite and possibly in acanthite, but the low concentration does not support the abundance of naumannite as reported by Guilbert (1963). As indicated by the mineral assemblage, base metals are quite low in this system. Copper ranges from 3-108 ppm and averages only 22 ppm (figure II-13), below the average crustal abundance of 68 ppm (Greenwood and Earnshaw, 1984). The mine average, however, is based on samples collected from a part of the mine effected by oxidation, so some of the data is not representative of hypogene conditions. Copper is present as chalcopyrite and possibly in sulfosalts, so is more abundant in veins. Taking these factors into consideration copper is, thus, only a minor component of this system. Zinc ranges from 1-99 ppm and averages 17 ppm (figure II-14), also below the average crustal abundance of 76 ppm (Greenwood and Earnshaw, 1984). The low values can be explained by the rarity of sphalerite and the effects of oxidation.

In the Cannon mine, arsenic averages 145 ppm and is higher in the veins than in the wall rock (Ott, 1988). The Wenatchee Heights mineralization is quite high in arsenic and although Margolis (1987) did not publish any exact figures, it is apparent from his graphical plots that the average is near 1000 ppm. Hg, Sb, and Cu average 617 ppb, 9 ppm, and 17 ppm, respectively in composite samples

from the Cannon mine. As, Sb and Cu values are remarkably similar to the L-D mine. Se concentration in the Cannon mine (0.7 ppm) is significantly lower than the L-D mine. Only Hg is reported from Wenatchee Heights and it averages 1000 ppb in altered arkose (Margolis, 1987). Telluride minerals are common in the Wenatchee Heights mineralization (Asamera Minerals, unpub. data), so Te is probably an important trace-element. Table 6 shows the range of trace-element composition for a variety of epithermal systems in comparison to the L-D mine.

In order to investigate possible correlations between elements, geochemical data for two elements were plotted on linear graphs. The results support much of the petrographic observations in this study.

The widely scattered data points on the Ag vs. Au plots (figures II-15 to II-17) is a function of the sampling bias mentioned previously, i.e. geochem sampling is a composite of all stages of mineralization. On the basis of mineralogic relationships, however, the data can be interpreted as a mixture of two characteristics: 1) gold and silver correlate in the early stages of vein mineralization where electrum is the primary phase, and 2) gold and silver do not correlate in the later stages of vein mineralization where acanthite is the primary precious metal phase, with subsidiary naumannite, aguilarite and native Ag.

Correlations between gold and other elements such

Table 6--Summary of trace-element variations in several epithermal systems from around the globe in comparison to the L-D mine. All values in ppm.

DEPOSIT	As	Sb	Hg	Cu	Zn
<sup>1</sup> Carlin	50->10,000	5-450	0.2-453	7-200	10-850
<sup>1</sup> Cortez	<500-500	<100-150	0.02-2.7	NA	NA
<sup>1</sup> Getchell	2800-128,000	NA	46-642	NA	NA
<sup>1</sup> Gold Acres	<200->10,000	<100-500	<0.1->10	<5-5000	<200->10 <sup>4</sup>
<sup>1</sup> Taylor	<150-15,000	200-20,000	3.2-380	10-2000	<150-700
<sup>2</sup> Rodalquilar	0-30,000	0-6000	NA	0-900	0-350
<sup>3</sup> El Indio	17,000*	1300	30	37,000	NA
<sup>4</sup> Ohakuri	0-800	0-250	0-5	NA	NA
<sup>5</sup> Round Mt.	1-10,000	0.5-3900	NA	5-2000	5-3500
<sup>6</sup> Bodie	3-800	1-100	0.01-20	2-1000	11-120
<sup>7</sup> Hasbrouck Mt.	2-550	1-280	0.02-7	NA	NA
L-D	9-290	2-56	0.035-0.3	3-108	1-99

<sup>1</sup> Bagby and Berger, 1985

<sup>2</sup> Sanger-von Oepen and others, 1989

<sup>3</sup> Siddeley and Araneda, 1986

<sup>4</sup> Henneberger, 1986

<sup>5</sup> Tingley and Berger, 1985

<sup>6</sup> Silberman and Berger, 1985

<sup>7</sup> Berger and Silberman, 1985

as As, Sb, Hg, Se, and Cu yielded similar results. Overall, arsenic would not be expected to correlate well with gold (figure II-18) because most of the As occurs as arsenopyrite in wall rock. This conclusion is confirmed by a lower average As value in vein samples (Schmidt, 1983). One would not expect to see a correlation between gold and antimony even though sulfosalts formed by partial replacement of electrum (figure II-19). The apparent lack of a correlation is because overall, sulfosalts are rare and chiefly arsenic-bearing phases. Too little is known about the occurrence of mercury to explain the plot in figure II-20, but it appears that Hg does not correlate well with Au. Although selenium data is not abundant, figure II-21 does suggest two data trends. The first trend is flat, indicating no increase in Se with increasing Au, and this is varified by the lack of selenide phases occuring with gold. The other trend is vertical indicating increasing Se with no increase in Au and is perhaps a reflection of the late hydrothermal nature of the silver selenides. The copper vs. gold diagram (figure II-22) also suggests two trends. Medial stages of mineralization are represented by the vertical trend when chalcopyrite was deposited, but no precious metals. The horizontal trend reflects early copper poor, precious metal-rich mineralization. Zinc data also defines two trends (figure II-23), but these can only be speculated about because no zinc phase was identified in this study.

Sphalerite was identified by Guilbert (1963) to be in close association with gold, which may explain the slope in some of the data.

The vertical and lateral distribution of trace-elements in the L-D system is poorly understood due to the limited data and the inability to identify the precise locations of much of the UMC data. However, the lateral distribution of trace-element data throughout the district show a general trend of decreasing concentration in the district from south to north, away from the suspected volcanic center (figure 65). Data from Wenatchee Heights is still being gathered and much of it is unpublished, but it appears to be characterized by higher abundances of As, Sb, Hg, Te, and base metals. In contrast, the L-D and Cannon mines contain significantly lower As, Sb, Hg, base metals, higher Se, and no Te. Further to the north, in the F and G-reef areas, trace-element concentration is even lower (Schmidt, 1983).

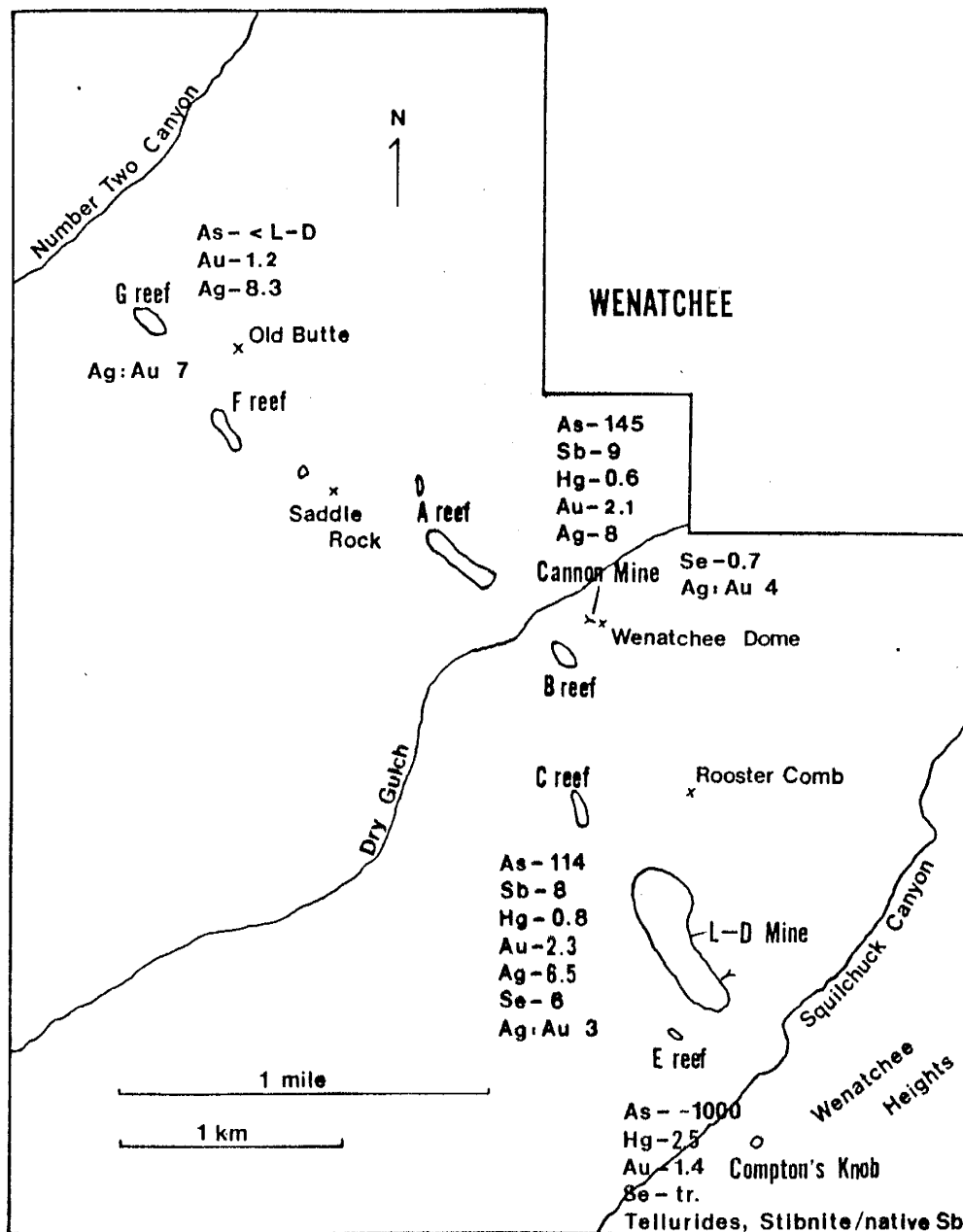


Figure 65-- Sketch map of the Wenatchee district showing the general distribution of trace-element concentration.

Data from Schmidt, 1983; Margolis, 1987; Ott, 1988; and Asamera Minerals, unpub. data.

## DISCUSSION

Mineralization within the L-D mine owes its existence to several geologic processes operating simultaneously. The result was an environment suitable for concentrating precious metals. Essential elements for any hydrothermal system include a plumbing system by which fluids can travel, fluids capable of transporting metals, a source of heat to drive the system, a source of the metals, a mechanism to deposit the metals, and a trap to hold the metals. Geologic events in the Chiwaukum graben satisfied all of the above criteria.

### Setting

Eocene and Oligocene events in the Pacific Northwest were dominated by oblique subduction between the North American and Kula plates that provided the driving force behind regional wrench-faulting and non-marine basin formation (Wells and others, 1984; Johnson, 1984). Johnson (1985) and Evans (1988) have demonstrated that the Chiwaukum graben is one such example. The graben bounding Leavenworth and Entiat faults and the internal Eagle Creek fault are the primary agents of deformation in the region, and particularly the Eagle Creek fault in the Wenatchee district. Important, is the intense local structural deformation that accompanies wrench-faulting. The primary



components of wrench-faulting are: 1) en echelon folds, 2) conjugate strike-slip faults, 3) the main wrench-fault, and 4) normal faults or tension joints oriented perpendicular to fold axes (Wilcox and others, 1973). All of these elements are present in the Wenatchee district, and are the product of dextral movement along the Eagle Creek fault.

There seems to have been a progression in the evolution of the Eagle Creek wrench-fault from the initial development of tensional fractures (vein hosting structures), to folding (bedding orientation, bedding-plane slips, joints) and finally conjugate strike-slip faulting (N-S faults) as revealed by mapping. This sequence is apparently typical in the evolution of a wrench-fault (Wilcox and others, 1973). On the basis of age dates and textural evidence (open-space filling, multiple periods of mineral deposition, brecciation) mineralization is interpreted to have occurred simultaneously with initial tensional fracturing and was subsequently deformed by the later events. It is these tensional structures and the synchronous activity of deformation and mineralization that provided the plumbing system and traps for mineralizing fluids.

#### Hostrock characteristics

Permeable sediments are locally important, especially during early stages of alteration, and allowed

propylitizing and silica bearing fluids to flood the matrix. This was an important event in that it significantly increased the competency of the sediments, which allowed for continued brittle deformation and the ability to maintain tensional openings for further, vein-hosted mineralization.

Deposition from an epithermal system, however, requires heated waters (100-300 c) circulating in a near surface (0-1+ km) environment. In order to achieve this condition the geothermal gradient must be elevated significantly over the norm. Volcanic/plutonic activity in a subsiding intra-arc basin is an ideal environment. This subduction environment and the calc-alkalic magmatism produced therein, are important in the generation of epithermal precious metal deposits world-wide (Silberman and others, 1976; Sillitoe, 1977; Mitchell and Garson, 1981). Calc-alkalic volcanic rocks and their hypabyssal equivalents are abundant in the Wenatchee district and age dates reveal a close temporal relationship to mineralization. It could be argued that the plutonic equivalents are also present at depth and are the dominant source of heat for the convective system.

The close association in time and space of mineralization with caldera volcanism can be demonstrated in many epithermal districts in the western U.S. (Albers and Kleinhampl, 1970; Lipman and others, 1976; Mckee, 1979; Rytuba, 1981; Heald and others, 1987). Whether or not the

Wenatchee district is associated with caldera-type activity remains to be demonstrated, nevertheless, the thick pile of rhyolitic volcanics, debris flows, and lacustrine units (Margolis, 1987) confined to a limited area are evidence of centrally located magmatic activity, suggestive of a caldera environment. In any case, a suspected volcanic center under Wenatchee Heights likely provided the heat source for mineralization.

### Alteration

Hydrothermal alteration in the L-D mine consists of pervasive silicification and sericitic alteration in areas of intense veining, which grades outward to weak sericitic and propylitic/diagenetic affects. Alteration is potassium metasomatic as indicated by alteration of biotite and plagioclase and the stability of potassium feldspar and muscovite. This assemblage is characteristic of neutral to weakly acidic conditions (figure 66) (White and Hedenquist, 1990). The dominant reaction in determining the chemistry of early hydrothermal fluids is the conversion of detrital plagioclase to clays. This situation is similar to that proposed by Giggenbach (1981) for a New Zealand system in which primary plagioclase is converted to clays and calcite by CO<sub>2</sub>. Calcite is recognized only in the propylitic/diagenetic alteration assemblage in the L-D system. Laumontite, another calcium phase, comprises part

of the propylitic/diagenetic zone. The only definite hydrothermal phase that may be calcium-bearing, is montmorillonite in the mixed layer zone. It is possible that zeolite and calcite veinlets observed in propylitically altered areas are hydrothermal in origin and thus may account for the calcium. An alternative explanation is that the calcium migrated into vein structures due to a chemical-potential gradient, and was deposited as vein calcite. Reactions with plagioclase is not a factor, however, in subsequent vein controlled mineralization because of the diminished permeability caused by silicification and the efficiency of earlier alteration.

#### Mineralization

Vein mineralogy consists chiefly of quartz, calcite, pyrite, arsenopyrite, chalcopyrite, electrum, and sulfosalts. This simple assemblage is the product of low Cl-, low total sulfur, low fO<sub>2</sub>, dilute, possibly high CO<sub>2</sub> solutions. Low chloride content is deduced from the lack of base metal sulfides. Sulfur activity is moderate as indicated by the assemblage pyrite and arsenopyrite (figure 67). Upper limit for oxygen fugacity is constrained by the occurrence of chalcopyrite instead of bornite in the hypogene sulfide assemblage; and the lower limit is constrained by the occurrence of pyrite instead of pyrrhotite. The dilute nature of the fluids is postulated

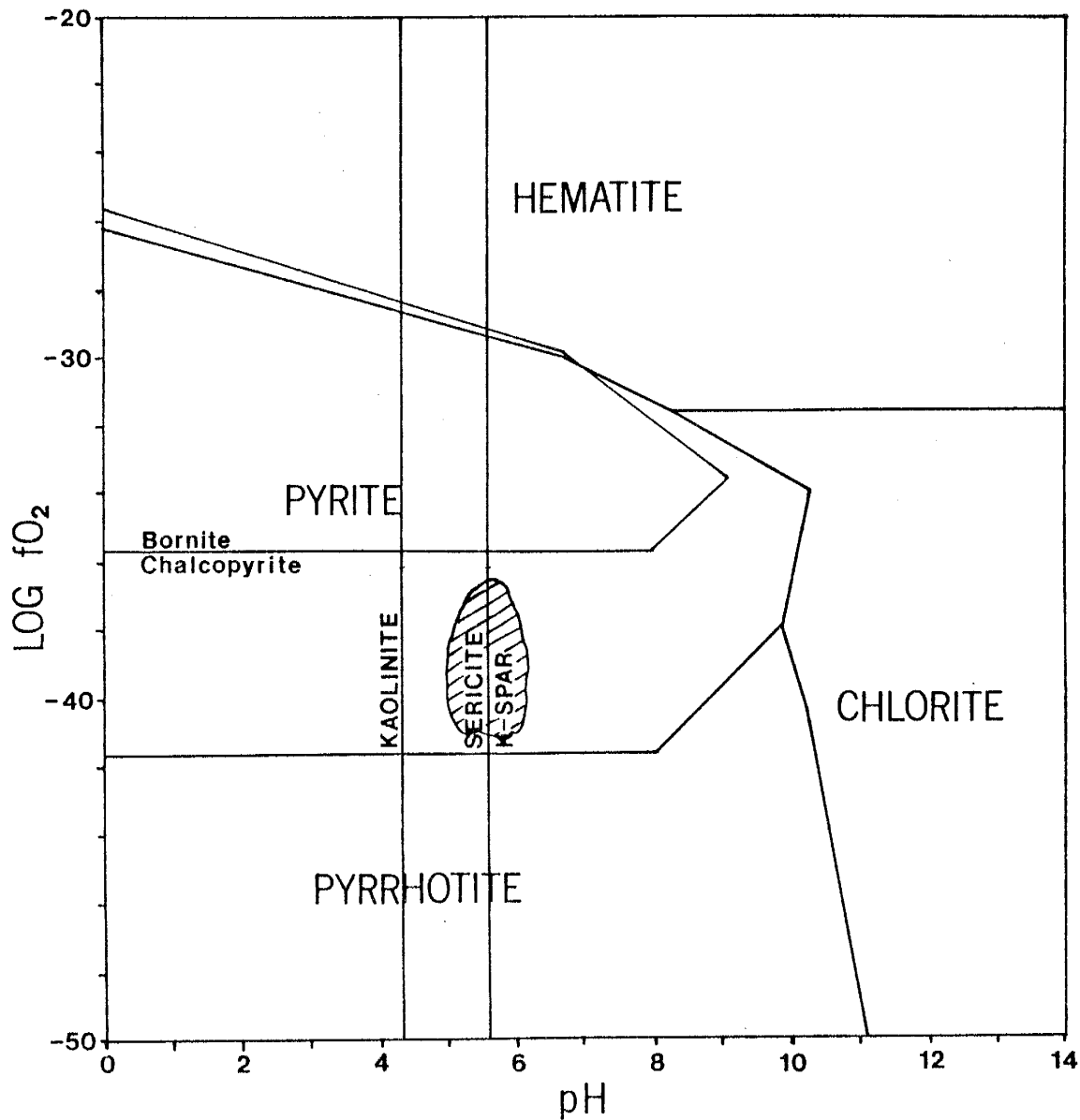


Figure 66-- Oxygen activity-pH diagram calculated at 285 C and 100 bars.  $a_{\text{Na}}/a_{\text{K}} = 6$ ,  $a_{\text{Cl}} = 0.06$ , total S = 0.02 molal. Modified from Klisch, 1989. The cross-hatched area is the environment of L-D main stage fluids.

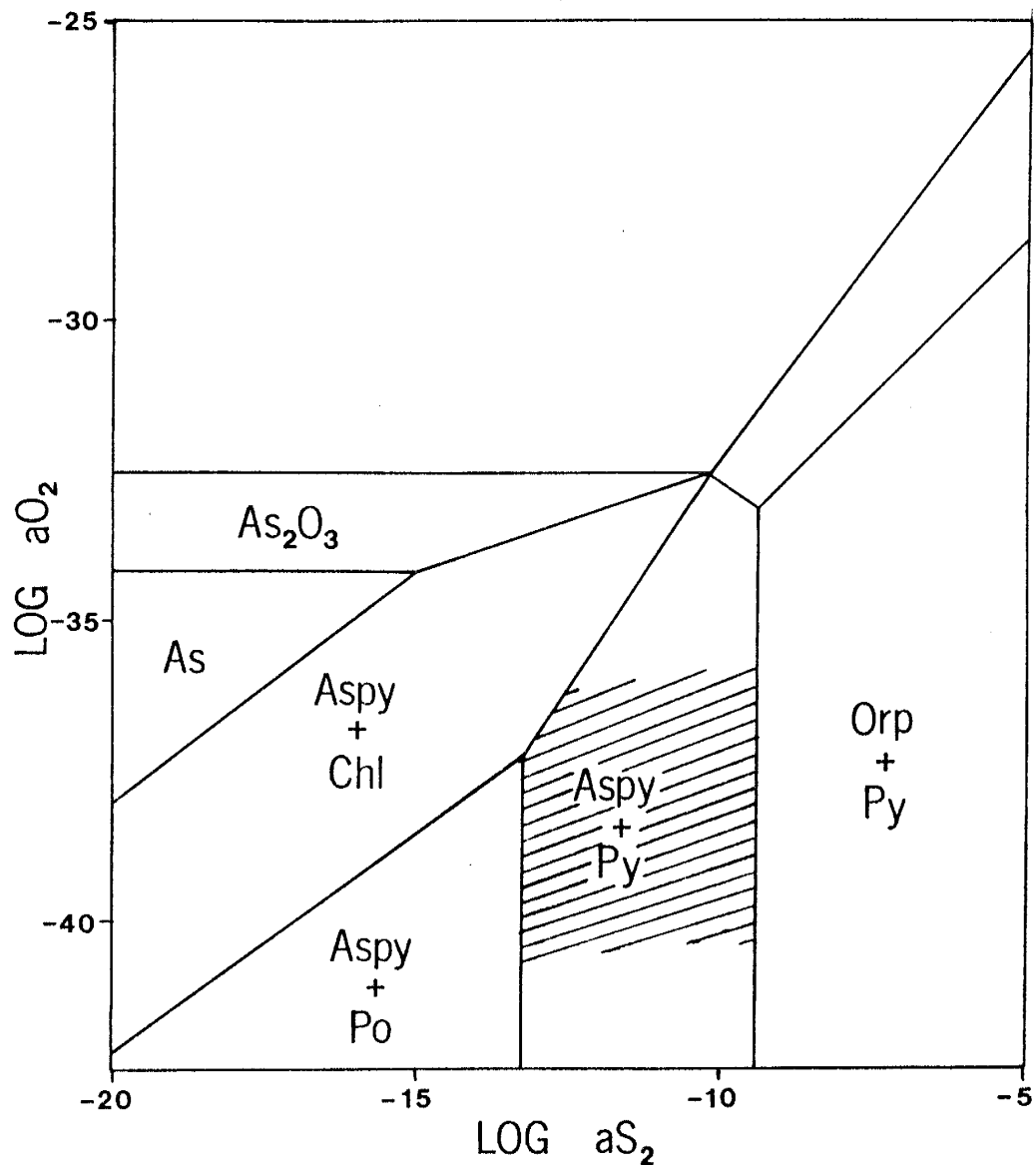


Figure 67-- Calculated oxygen activity-sulfur activity diagram for the system Fe-As-NaCl-S-H<sub>2</sub>O at 250 C, pH = 5, and 1.0 m NaCl. Modified from Romberger, 1988. The cross-hatched area is the environment of L-D main stage fluids.

from the low overall abundance of sulfides and trace-elements. Finally, the presence of large amounts of calcite indicates the fluids contained significant amounts of CO<sub>2</sub> (Brown and Ellis, 1970; Giggenbach, 1980; Fournier, 1985). This environment is favorable for transporting gold, silver and copper as bisulfide complexes (Seward, 1973, 1989; Berger and Henley, 1989). Methane may have also been a component in the system because of the abundance of carbonaceous material in the sediments. Exploration drilling in the Cannon mine often encounters pockets of CH<sub>4</sub>.

#### Supergene processes

Weathering has had a profound effect on the hypogene assemblages. Destruction of pyrite and arsenopyrite in the wall rock is the primary source of acid solutions generated during weathering. In areas of extreme weathering, even sulfides in the quartz veins were altered by descending groundwater. The presence of iron oxides and hydroxides support the observation that the overall sulfide content is low, suggesting only limited mobility of iron (Anderson, 1982). Jarosite is a stable mineral in the normal weathering environment and indicates pH conditions less than 3 (Brown, 1971). Goethite is formed from jarosite by continued leaching of potassium and sulfur, and the coexistence of jarosite with goethite in the L-D mine is due to the sluggishness of the reaction (Brown, 1971; Bladh,

1982) and incomplete leaching. Hematite is formed under less hydrous conditions possibly at a slightly greater depth or under local "dry" conditions in less permeable beds. Figure 68 is an Eh-pH diagram showing the characteristics of the supergene fluids in the L-D mine. Reaction of acid waters with the hypogene silicate assemblage produced kaolinite after illite and sericite in detrital grains and matrix, however, primary detrital textures are preserved. Permeability of the sediments, coupled with the abundance of illite and sericite, and low sulfide content in altered rocks, effectively buffered the pH of the supergene fluids so that mobility of Ag and Cu was minimized, hence no secondary enrichment of either metals. A low Cl<sup>-</sup> content of supergene fluids may have also been a factor (Mann, 1984).

#### Considerations on ore genesis

Gold deposited in a boiling environment is accompanied by finely banded, rapidly precipitated silica, calcite, or its pseudomorphs, adularia and often pyrite (Berger and Henley, 1989). In the L-D mine, precious metals were deposited with banded, fine grained quartz and pyrite. Bladed calcite and quartz pseudomorphs after bladed calcite are abundant, and adularia is present. In addition, coexisting vapor-rich and liquid-rich fluid inclusions are frequently observed in the bladed calcite. Boiling is



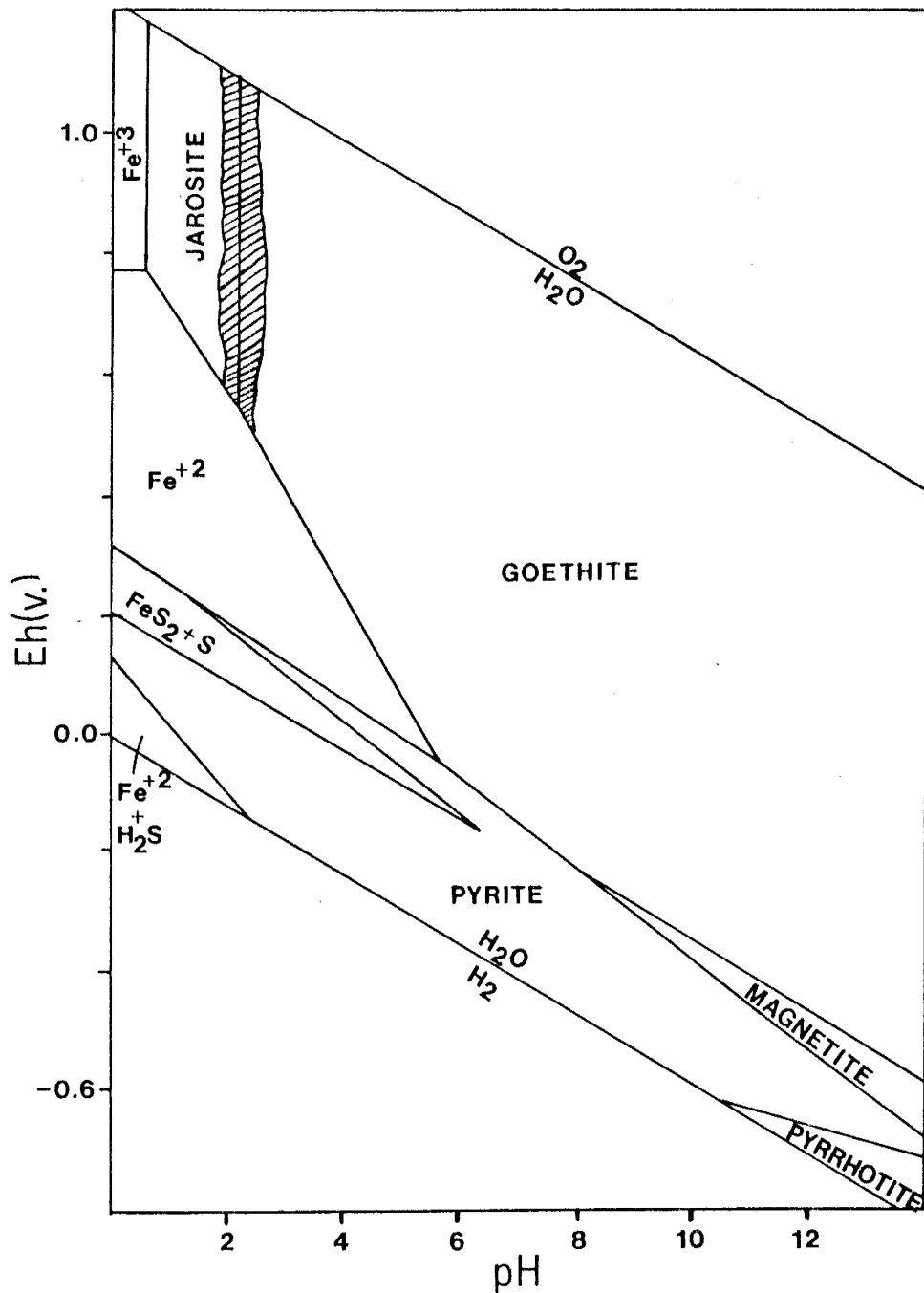


Figure 68-- Eh-pH diagram for some iron compounds at 25 C and 1 atm, calculated from the activities of ions in an acid water (from Brown, 1971). The cross-hatched area is the environment of L-D supergene fluids.

cited as the primary mechanism of gold deposition in the Cannon mine on the basis of fluid inclusion analyses (Klisch, 1989). Therefore, deposition of precious metals by boiling seems a possible mechanism in the L-D mine.

No work has been done to determine the source of the metals in the Wenatchee district. A magmatic contribution to the hydrothermal system is possible considering the spatial and temporal relationship with mineralization, but as demonstrated by Romberger (1988), leaching of large volumes of country rock over a period of time is more than sufficient to accumulate the metals found in these systems. Duration of the hydrothermal system has not been determined, but clustering of age dates around 44 Ma may indicate a span of less than a million years. According to Seward (1989), a typical ore-forming system, such as Ohaaki-Broadlands, can deposit one million ounces of gold in only 600 years with a Au concentration in solution of 11.1 ug/kg. Assuming an average Au concentration in the potential source rocks of 3 ppb (rhyolite, sandstone and gneiss) and 10 % efficiency of extraction, would require leaching of approximately 60 km<sup>3</sup> of rock to deposit 6 million ounces of gold, a volume six times as large as the Wenatchee district. There is a growing body of evidence, however, to support a magmatic contribution for the CO<sub>2</sub>, sulfur as SO<sub>2</sub>, HCl, and Au in these systems (Berger and Henley, 1989; Sillitoe, 1989).

The L-D mine fits the criteria of an epithermal deposit based on the mineralogy, associated elements, alteration, types of mineralization, and mineral textures as defined by Lindgren (1933) (Table 7). Specifically, the L-D mine would fit into Lindgren's "Gold deposits" sub-class. Previous workers have classified the system into Lindgren's "Gold-selenide" sub-class based on the abundance of naumannite (Guilbert, 1963; Margolis, 1987; Ott, 1988), but geochemistry and petrography do not support this conclusion. Despite the sedimentary host rock, mineralization at the L-D mine is comparable to volcanic-hosted deposits and not a Carlin-type system. In terms of modern classification schemes, the L-D and Cannon mines, could be classified as low-sulfur type (Bonham, 1986), also called adularia-sericite type (Heald and others, 1987). Table 8 is a list of the characteristics of low-sulfidation or adularia-sericite type epithermal deposits as defined by Bonham and Heald and others.

It is suggested here and elsewhere (Margolis, 1987) that the L-D and Cannon systems appear to have formed in the outflow plume of a single convective hydrothermal system originating from the Wenatchee Heights area as indicated by mineralogy, alteration, and trace-element geochemistry. As mentioned previously there is a general decrease in the trace-element concentration northward away from Wenatchee Heights (figure 65). Temperature of the

Table 7-- Characteristics that classify a hydrothermal system as being epithermal (after Lindgren, 1933).

---

Depth of formation	Surface to 1000m
Temperature of formation	50 to 300 C
Form of deposits	Thin to large veins, stockworks, disseminations, replacements
Ore textures	Open-space filling, crustification, colloform banding, comb structure, brecciation
Ore elements	Au, Ag, (As, Sb), Hg, [Te, Tl, U], (Pb, Zn, Cu)*
Alteration	Silicification, argillization, sericite, adularia, propylitization
Common features	Fine-grained chalcedonic quartz, quartz pseudomorphs after calcite, brecciation

---

\*[ ] elements rarely present in economic concentration;

( ) elements sometimes present in economic concentrations.

Table 8-- Characteristics of low-sulfur or adularia-sericite type epithermal systems (after Bonham, 1986 and Heald and others, 1987).

---

Depth of formation	0 to 1000 m
Temperature of formation	100 to 320 C
Character of ore fluids	Low salinity; reduced; Meteoric water dominated with possible magmatic contribution; pH near neutral, may become alkaline with boiling; total S content typically low; low base-metal content (Pb, Zn)
Associated alteration	Extensive propylitic alteration in surrounding regions; sericitic; argillization; boiling may produce advanced argillic alteration
Character of mineralization	Open-space and cavity filling; sharp-walled veins; layered vein fillings; multi-stage brecciation; stockworks; disseminations
Characteristic textures	Crustiform banding; comb texture; colloform banding; chalcedonic quartz; drusy cavities; vugs; vein breccia; silica pseudomorphs after bladed calcite (boxwork texture)
Characteristic mineralogy	Chalcedony; adularia

hydrothermal system may also decrease northward (Gill, personal communication, 1990). In addition, alteration type changes from low pH, acidic alteration under Wenatchee Heights (Margolis, 1987) to neutral-weakly acidic conditions in the L-D and Cannon mines. Alteration and mineralization in the F and G-reef areas is very sporadic and not as pervasive, in fact, wall rock at G-reef is not silica flooded. Figure 69 is a proposed model for the formation of the L-D mine. The model is a modification of the one proposed by Margolis (1987) and is similar to the Creede, Colorado system (Bethke and Lipman, 1987).

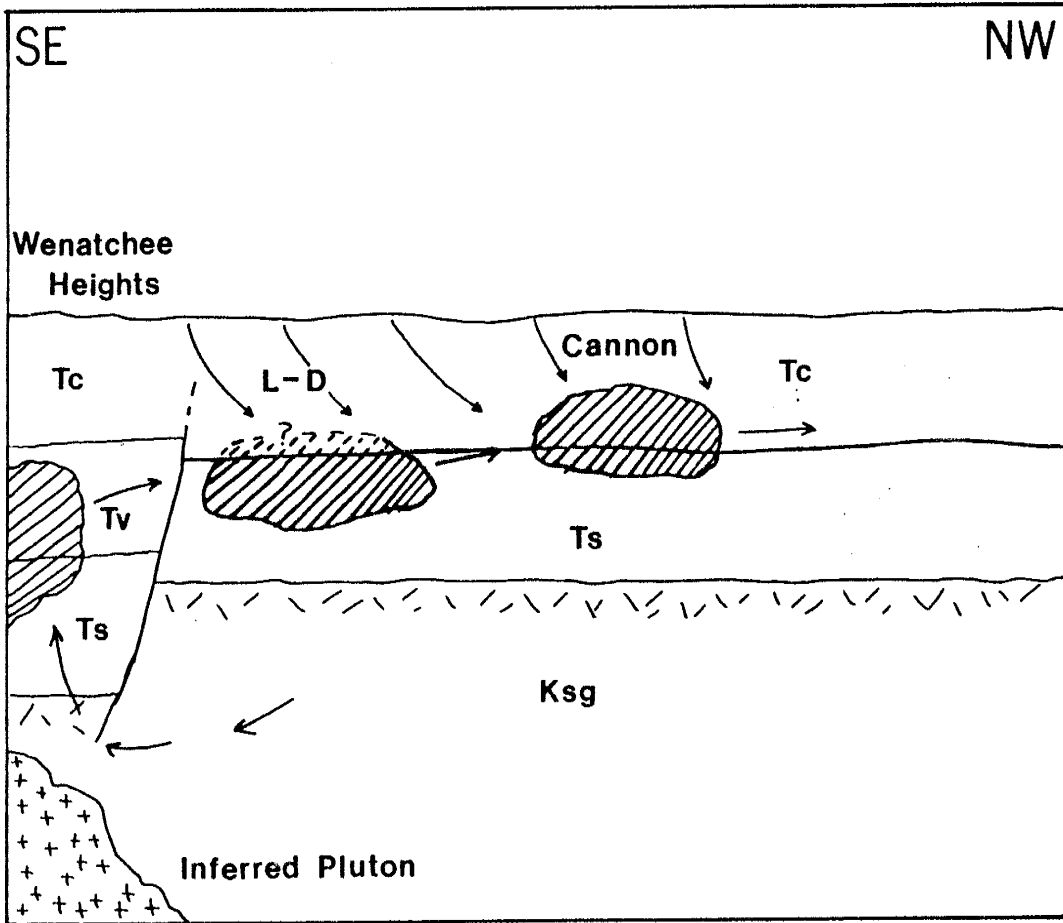


Figure 69-- Conceptual model for the L-D mine. Cross-section is along the Eagle Creek structure. Looking southwest. No scale.

## CONCLUSIONS

1. The Eagle Creek structure is the primary regional control on magmatism and mineralization, and local tensional fracture patterns within the structure are the sites of mineral deposition.
2. Mineralization is spatially and temporally associated with calc-alkalic arc magmatism. This magmatism is represented by the NORCO volcanic complex, a dominantly rhyolitic sequence with caldera affinities. This volcanic center is postulated to be responsible for the elevated geothermal gradient that drove the hydrothermal system.
3. The Eocene Swauk Formation is the host for mineralization in the L-D mine, Compton's Knob, C-reef, F and G-reefs, and possibly some of the Wenatchee Heights mineralization. Cannon mine mineralization is hosted by lower Chumstick Formation.
4. The Footwall Fissure is reinterpreted to be a high-angle reverse fault and not a thrust-fault.
5. Alteration is characteristic of neutral to weakly acidic fluids and is potassium metasomatic. Four types of alteration have been identified: 1) silicification, 2) strong sericitic, 3) weak sericitic (mixed layer zone), and 4) propylitic. Alteration types occur in discrete zones.
6. The mineral assemblage is indicative of low Cl<sup>-</sup>, low total S, low fO<sub>2</sub>, high CO<sub>2</sub>, dilute meteoric



dominated fluids, but a magmatic contribution cannot be ruled out.

7. Textural evidence suggests that boiling is the primary mechanism of precious metal deposition in the L-D mine, but mixing may also play a role.

8. Mineralization can be classified as a low-sulfur type or adularia-sericite type epithermal system.

9. There is enough evidence to speculate that the L-D mine is part of the outflow plume of a large convective hydrothermal system originating under Wenatchee Heights.

10. All mineralization in the district may be the product of a single hydrothermal event.

11. Mineralization dies out to the north, with the sporadically mineralized, sub-economic F and G-reef area being the most proximal portion. The best areas for further exploration are areas south of the NORCO complex along the Eagle Creek structure, the portion of the L-D mine cut-off by the Footwall Fissure, and perhaps areas between the western boundary of the Eagle Creek structure and west of the Cannon and L-D mines.

## REFERENCES

- Albers, J.P. and Kleinhampl, F.J., 1970, Spatial relation of mineral deposits to Tertiary volcanic centers in Nevada: U.S. Geological Survey Professional Paper 700-C, pp. C1-C10.
- Alexander, F., 1956, Stratigraphic and structural geology of the Blewett-Swauk area, Washington: unpub. M.S. thesis, University of Washington, 63 pp.
- Anderson, J.A., 1982, Characteristics of leached capping and techniques of appraisal, in Titley, S.R., ed., Advances in Geology of the Porphyry Copper Deposits: University of Arizona Press, Tucson, pp. 275-295.
- Anonymous, 1953a, Wallace Miner, v. 47, no. 46, p. 4.
- Anonymous, 1953b, Wallace Miner, v. 47, no. 3, p. 1.
- Anonymous, 1962, Wenatchee World, July 4 edition.
- Armstrong, R.L., 1979, Cenozoic igneous history of the U.S. Cordillera from latitude 42 to 49 North, in Smith, R.B., and Eaton, G.P., (eds.) Cenozoic Tectonics and Regional Geophysics of the Western Cordillera: Geological Society of America Memoir 152, pp. 265-282.
- Bagby, W.C. and Berger, B.R., 1985, Geologic characteristics of sediment-hosted, disseminated precious-metal deposits in the western United States, in Berger, B.R. and Bethke, P.M., eds., Geology and Geochemistry of Epithermal Systems: Reviews in Economic Geology, v. 2, pp. 169-202.
- Bayley, E.P., Jr., 1965, Bedrock geology of the Twin Peaks area, an intrusive complex near Wenatchee, Washington: unpub. M.S. thesis, University of Washington, 47 pp.
- Berger, B.R. and Silberman, M.L., 1985, Relationships of trace-element patterns to geology in hot-spring type precious-metal deposits, in Berger, B.R. and Bethke, P.M., (eds.) Geology and Geochemistry of Epithermal Systems: Reviews in Economic Geology, v. 2, pp. 233-247.
- Bethke, P.M. and Lipman, P.W., 1987, Deep environment of volcanogenic epithermal mineralization: proposed research drilling at Creede, Colorado: EOS Transactions, American Geophysical Union, v. 68, no. 13, pp. 458-459.

- Bladh, K.W., 1982, The formation of goethite, jarosite, and alunite during the weathering of sulfide-bearing felsic rocks: *Economic Geology*, v. 77, pp. 176-184.
- Bonham, H.F., 1986, Models for volcanic-hosted epithermal precious metal deposits, in Schafer, R.W., Cooper, J.J. and Vikre, P.G., eds., Bulk minable precious metal deposits of the western United States, Symposium Proceedings: Geological Society of Nevada, pp. 259-271.
- Berger, B.R. and Henley, R.W., 1989, Advances in the understanding of epithermal gold-silver deposits, with special reference to the western United States, in Keays, R.R., Ramsay, W.R.H. and Groves, D.I., eds., *The Geology of Gold Deposits: The Perspective in 1988*: Economic Geology Monograph 6, pp. 405-423.
- Brown, J.B., 1971, Jarosite-goethite stabilities at 25 C, 1 ATM: *Mineralium Deposita*, v. 6, pp. 245-252.
- Browne, P.R.L. and Ellis, A.J., 1970, The Ohaki-Broadlands hydrothermal area, New Zealand: Mineralogy and related geochemistry: *American Journal of Science*, v. 269, pp. 97-131.
- Buza, J.W., 1977, Dispersal patterns of lower and middle Tertiary sedimentary rocks in portions of the Chiwaukum graben, east-central Cascade Range, Washington: unpub. M.S. thesis, University of Washington, 40 pp.
- Chappell, W.M., 1936, Geology of the Wenatchee quadrangle, Washington: unpub. Ph.D dissertation, University of Washington, 249 pp.
- Christiansen, R.L. and Lipman, P.W., 1972, Cenozoic volcanism and plate tectonic evolution of the western United States, part 2, Late Cenozoic: *Philosophical Transactions of the Royal Society of London*, ser. A, v. 271, pp. 249-284.
- Coombs, H.A., 1950, Spherulitic breccias in a dome near Wenatchee, Washington: *American Mineralogist*, v. 37, pp. 197-206.
- , 1950, Granitization in the Swauk arkose near Wenatchee, Washington: *American Journal of Science*, v. 248, pp. 369-377.
- Engebretson, D.C., Cox, A. and Thompson, G.A., 1984, Correlation of plate motions with continental tectonics: Laramide to Basin-Range: *Tectonics*, v. 3, no. 2, pp. 115-119.

- Evans, J.E., 1988, Depositional environments, basin evolution and tectonic significance of the Eocene Chumstick Formation, Cascade Range, Washington: unpub. Ph.D dissertation, University of Washington, 325 pp.
- and Johnson, S.Y., 1989, Paleogene strike-slip basins of central Washington: Swauk Formation and Chumstick Formation, in Joseph, N.L. and others, (eds.), Geologic guidebook for Washington and adjacent areas: Washington Division of Geology and Earth Resources Information Circular 86, pp. 215-223.
- Ewing, T.E., 1980, Paleogene tectonic evolution of the Pacific Northwest: *Journal of Geology*, v. 88, no. 6, pp. 619-638.
- Fournier, R.O., 1985, Carbonate transport and deposition in the epithermal system, in Berger, B.R. and Bethke, P.M., eds., *Geology and Geochemistry of Epithermal Systems: Reviews in Economic Geology Volume 2*, pp. 63-72.
- Frizzell, V.A., Jr., 1979, Petrology and stratigraphy of Paleogene nonmarine sandstones, Cascade Range, Washington: U.S. Geological Survey Open-File Report 79-1149, 151 pp.
- Giggenbach, W.F., 1980, Geothermal gas equilibria: *Geochimica et Cosmochimica Acta*, v. 44, pp. 2021-2032.
- , 1981, Geothermal mineral equilibria: *Geochimica et Cosmochimica Acta*, v. 45, pp. 393-410.
- Greenwood, N.N. and Earnshaw, A., 1984, *Chemistry of the Elements*: Pergamon Press, Oxford, 1542 pp.
- Gresens, R.L., 1976a, A new Tertiary Formation near Wenatchee, Washington: *Geological Society of America Abstracts with Programs*, v. 8, no. 3, pp. 376-377.
- , 1976b, Unusual structural features associated with mid-Tertiary deformation near Wenatchee, Washington: *Geological Society of America Abstracts with Programs*, v. 8, no. 9, pp. 892-893.
- , 1979, Timing of Cenozoic igneous and tectonic events on the western flank of the Cascade Range in central Washington: *Geological Society of America Abstracts with Programs*, v. 11, no. 1, p. 80.

- , 1980, Deformation of the Wenatchee Formation and its bearing on the tectonic history of the Chiwaukum graben, Washington, during Cenozoic time, Summary: Geological Society of America Bulletin, pt. 1, v. 91, no. 1, pp. 4-7.
- , 1982a, Early Cenozoic geology of central Washington state: I. Summary of sedimentary, igneous, and tectonic events: Northwest Science, v. 56, pp. 218-229.
- , 1982b, Early Cenozoic geology of central Washington state: II. Implications for plate tectonics and alternatives for the origin of the Chiwaukum graben: Northwest Science, v. 56, pp. 259-264.
- , 1983, Geology of the Wenatchee and Monitor quadrangles, Chelan and Douglas Counties, Washington: Washington Division of Geology and Earth Resources Bulletin 75, 75 pp.
- , Whetten, J.T., Tabor, R.W., and Frizzell, V.A., Jr., 1977, Tertiary stratigraphy of the central Cascade Mountains, Washington state, in Brown, E.H. and Ellis, R.C., eds., Geologic Excursions in the Pacific Northwest: Western Washington University Press, Bellingham, Washington, pp. 84-126.
- , Naeser, C.W. and Whetten, J.T., 1981, Stratigraphy and age of the Chumstick and Wenatchee Formations, Tertiary fluvial and lacustrine rocks, Chiwaukum graben, Washington, Summary: Geological Society of America Bulletin, pt. 1, v. 92, no. 5, pp 233-236.
- Guilbert, J.M., 1963, Report on selected specimens from the Gold King mine, Wenatchee, Washington: unpub. report for Day Mines Inc., Wallace, Idaho, 27 pp.
- Heald, P., Foley, N.K. and Hayba, D.O., 1987, Comparative anatomy of volcanic-hosted epithermal deposits: Acid-sulfate and adularia-sericite types: Economic Geology, v. 82, no. 1, pp. 1-26.
- Heller, P.L., Tabor, R.W. and Suczek, C.A., 1987, Paleogeographic evolution of the United States Pacific Northwest during Paleogene time: Canadian Journal of Earth Science, v. 24, pp. 1652-1667.

- Henneberger, R.C., 1986, Ohakuri fossil epithermal system, in Henley, R.W., Hedenquist, J.W. and Roberts, P.J., (eds.), Guide to the Active Epithermal (Geothermal) Systems and Precious Metal Deposits of New Zealand: Monograph Series on Mineral Deposits, no. 26, Gebruder-Borntraeger, Berlin, pp.121-128.
- Johnson, S.Y., 1984, Evidence for a margin-truncating transcurrent fault (pre-Late Eocene) in western Washington: *Geology*, v. 12, pp. 538-541.
- , 1985, Eocene strike-slip faulting and nonmarine basin formation in Washington, in Biddle, K.T. and Christie-Blick, N., eds., Strike-slip deformation, basin formation, and sedimentation: Society of Economic Paleontologists and Mineralogists, Special Publication 37, pp. 283-302.
- Kisch, H.J., 1983, Mineralogy and petrology of burial diagenesis (burial metamorphism) and incipient metamorphism in clastic rocks, in Larsen, G. and Chilinger, G.V., eds., *Developments in Sedimentology 25B: Diagenesis in Sediments and Sedimentary Rocks, 2*: Elsevier Scientific Publishing Co., Amsterdam, pp. 289-493.
- Klisch, M.P., 1989, A study of fluid inclusions and geochemical mechanisms for gold deposition, Cannon mine, Wenatchee, Washington: unpub. M.S. thesis, Western Washington University, 124 pp.
- and Roberts, T.T., 1989, Summary of surface mapping project: Summer 1989: unpub. internal report, Asamera Minerals (U.S.) Inc., 6 pp.
- Levinson, A.A., 1974, *Introduction to Exploration Geochemistry*: Applied Publishing Ltd., Calgary, 612 pp.
- Lindgren, W., 1933, *Mineral Deposits*, 4th ed.: McGraw-Hill, New York, 930 pp.
- Lipman, P.W., Prostka, H.J. and Christiansen, R.L., 1971, Evolving subduction zones in the western United States, as interpreted from igneous rocks: *Science*, v. 174, pp. 821-825.
- , 1972, Cenozoic volcanism and plate tectonic evolution of the western United States, part 1, Early and middle Cenozoic: *Philosophical Transactions of the Royal Society of London*, ser. A, v. 271, pp. 217-248.

- Lipman, P.W., Fisher, F.S., Mehnert, H.H., Naeser, C.W., Leudke, R.G., and Steven, T.A., 1976, Multiple ages of mid-Tertiary mineralization and alteration in the western San Juan Mountains, Colorado: *Economic Geology*, v. 71, pp. 571-588.
- Lovitt, E.H. and McDowall, V., 1954, The Gold King mine: *Western Miner*, v. 27, no. 3, pp. 37-39.
- and Skerl, A.C., 1958, Geology of the Lovitt gold mine, Wenatchee, Washington: *Mining Engineering*, v. 10, pp. 963-966.
- Mann, A.W., 1984, Mobility of gold and silver in lateritic weathering profiles: Some observations from western Australia: *Economic Geology*, v. 79, pp. 38-49.
- Margolis, J., 1987, Structure and hydrothermal alteration associated with epithermal Au-Ag mineralization, Wenatchee Heights, Washington: unpub. M.S. thesis, University of Washington, 90 pp.
- McClincey, M., 1986, Tephrostratigraphy of the Chumstick Formation: unpub. M.S. thesis, Portland State University, 122 pp.
- McKee, E.H., 1979, Ash-flow sheets and calderas: Their genetic relationship to ore deposits in Nevada: *Geological Society of America Special Paper* 180, pp. 205-211.
- Meyer, C. and Hemley, J.J., 1967, Wallrock alteration, in Barnes, H.L., ed., *Geochemistry of hydrothermal ore deposits*: New York, Holt, Rinehart and Wilson, pp. 166-235.
- Miller, R.B., 1985, The ophiolitic Ingalls complex, north-central Cascade Mountains, Washington: *Geological Society of America Bulletin*, v. 96, pp. 27-42.
- Mitchell, A.H.G. and Garson, H.S., 1981, *Mineral deposits and global tectonic settings*: Academic Press, New York, 405 pp.
- Moody, D.W., 1958, An examination of the ore minerals of the Lovitt mine, Wenatchee, Washington: unpub. B.S. thesis, University of Washington, 22 pp.

- Ott, L.E., Groody, D., Follis, E.L., and Siems, P.L., 1986, Stratigraphy, structural geology, ore mineralogy, and hydrothermal alteration at the Cannon mine, Chelan County, Washington, U.S.A., in Macdonald, A.J., ed., Proceedings. Gold '86, an international symposium on the geology of gold deposits, Toronto, Canada, pp. 425-435.
- , 1988, Economic geology of the Wenatchee mining district, Chelan County, Washington: unpub. Ph.D dissertation, University of Idaho, 270 pp.
- Patton, T.C., 1967, Economic geology of the L-D mine, Wenatchee, Washington: unpub. M.S. thesis, University of Washington, 29 pp.
- and Cheney, E.S., 1971, L-D gold mine, Wenatchee, Washington--new structural interpretation and its utilization in future exploration: Transactions of the Society of Mining Engineers, AIME, v. 250, pp. 6-11.
- Roberts, T.T., 1988, Report on surface exploration drilling: unpub. internal report for Asamera Minerals (U.S.) Inc., 20 pp.
- Romberger, S.B., 1988, Geochemistry of gold in hydrothermal deposits: U.S. Geological Survey Bulletin 1857-A, pp. A9-A25.
- Russell, I.C., 1900, A preliminary report on the geology of the Cascade Mountains in northern Washington: U.S. Geological Survey, 20th Annual Report, part II, pp. 85-210.
- Rytuba, J.J., 1981, Relation of calderas to ore deposits in the western United States: Arizona Geological Society Digest v. 14, pp. 227-236.
- Sanger-von Oepen, P., Friedrich, G. and Vogt, J.H., 1989, Fluid evolution, wallrock alteration, and ore mineralization associated with the Rodalquilar epithermal gold-deposit in southeast Spain: Mineralium Deposita, v. 24, pp. 235-243.
- Schmidt, K.W., 1983, Summary of Geology, Wenatchee Project: unpub. internal report, United Mining Corp., Virginia City, NV, 44 pp.
- Seward, T.M., 1973, Thio complexes of gold and the transport of gold in hydrothermal ore solutions: Geochimica et Cosmochimica Acta, v. 37, pp. 379-399.



- , 1989, The hydrothermal chemistry of gold and its implications for ore formation: Boiling and conductive cooling as examples, in, Keays, R.R., Ramsay, W.R.H. and Groves, D.I., eds., The Geology of Gold Deposits: The Perspective in 1988: Economic Geology Monograph 6, pp. 398-404.
- Siddeley, G. and Araneda, R., 1986, The El Indio-Tambo gold deposits, Chile, in Macdonald, A.J., ed., Proceedings Gold '86, an international symposium on the geology of gold deposits, Toronto, Canada, pp. 445-456.
- Silberman, M.L., Stewart, J.H. and McKee, E.H., 1976, Igneous activity, tectonics, and hydrothermal precious-metal mineralization in the Great Basin during Cenozoic time: Transactions of the Society of Mining Engineers, AIME, v. 260, pp.253-263.
- and Berger, B.R., 1985, Relationship of trace-element patterns to alteration and morphology in epithermal precious-metal deposits, in Berger, B.R. and Bethke, P.M., eds., Geology and Geochemistry of Epithermal Systems: Reviews in Economic Geology, v. 2, pp. 203-232.
- Silling, R.M., 1979, A gravity study of the Chiwaukum graben, Washington: Unpub. M.S. thesis, University of Washington, 79 pp.
- Sillitoe, R.H., 1977, Metallic mineralization affiliated to subaerial volcanism: A review, in Volcanic processes in ore genesis: London Institute of Mining and Metallurgy-Geological Society of London, pp. 99-116
- , 1989, Gold deposits in western Pacific island arcs: The magmatic connection, in Keays, R.R., Ramsay, W.R.H. and Groves, D.I., eds., The Geology of Gold Deposits: The Perspective in 1988: Economic Geology Monograph 6, pp. 274-291.
- Smith, G.O. and Calkins, F.C., 1904, A geological reconnaissance across the Cascade range near the 49th parallel: U.S. Geological Survey Bulletin 235, pp. 3-103.
- Swanson, D.A., Wright, T.L., Hooper, P.R., and Bentley, R.D., 1979, Revisions in stratigraphic nomenclature of the Columbia River Basalt Group: U.S. Geological Survey Bulletin 1457-G, 59 pp.

- Tabor, R.W., Waitt, R.B., Frizzell, V.A., Jr., Swanson, D.A., Byerly, G.R., and Bentley, R.D., 1982, Geologic map of the Wenatchee 1:100,000 quadrangle, central Washington: U.S. Geological Survey Miscellaneous Investigations Map I-1311.
- , Frizzell, V.A., Jr., Vance, J.A. and Naeser, C.W., 1984, Ages and stratigraphy of lower and middle Tertiary sedimentary and volcanic rocks of the central Cascades, Washington: Application to tectonic history of the Straight Creek fault: Geological Society of America Bulletin, v. 95, pp. 26-44.
- , Frizzell, V.A., Jr., Whetten, J.T., Waitt, R.B., Swanson, D.A., Byerly, G.R., Booth, D.B., Hetherington, M.J., and Zartman, R.E., 1987, Geologic map of the Chelan 30-minute by 60-minute quadrangle, Washington: U.S. Geological Survey Miscellaneous Investigations Map I-1661.
- Taylor, S.B., Johnson, S.Y., Fraser, G.T., and Roberts, J.W., 1988, Sedimentation and tectonics of the lower and middle Eocene Swauk Formation in eastern Swauk Basin, central Cascades, central Washington: Canadian Journal of Earth Science, v. 25, pp.1020-1036.
- Tingley, J.V. and Berger, B.R., 1985, Lode gold deposits of Round Mountain, Nevada: Nevada Bureau of Mines and Geology Bulletin 100, 62 pp.
- Vance, J.A., 1979, Early and middle Cebozoic arc magmatism and tectonics in Washington state: Geological Society of America Abstracts with Programs, v. 11, p. 132.
- Van Houten, F.B., 1961, Maps of Cenozoic depositional provinces, western United States: American Journal of Science, v. 259, pp. 612-621.
- Waters, A.C., 1930, Geology of the southern half of the Chelan quadrangle, Washington: unpub. Ph.D dissertation, Yale University, 256 pp.
- , 1962, Basalt magma types an their tectonic associations: Pacific Northwest of the United States: American Geophysical Union, Geophysical Monograph 6, pp. 158-170.
- Wells, R.E., Engbretson, D.C., Snavely P.D., Jr., and Coe, R.S., 1984, Cenozoic plate motions and the volcano-tectonic evolution of western Oregon and Washington: Tectonics, v. 3, pp. 275-294.

- Whetten, J.T., 1976, Tertiary sedimentary rocks in the central part of the Chiwaukum graben, Washington: Geological Society of America Abstracts with Programs, v. 8, no. 3, p. 420.
- , 1977, Sedimentology and structure of part of the Chiwaukum graben, Washington: Geological Society of America Abstracts with Programs, v. 9, no. 4, p 527.
- White, N.C. and Hedenquist, J.W., 1990, Epithermal environments and styles of mineralization: variations and their causes, and guidelines for exploration: Journal of Geochemical Exploration, v. 36, pp. 445-474.
- Wilcox, R.E., Harding, T.P. and Seely, D.R., 1973, Basic wrench-fault tectonics: American Association of Petroleum Geologists Bulletin, v. 57, no. 1, pp. 74-96.
- Willis, C.L., 1958, The Chiwaukum graben, a major structural feature of central Washington: American Journal of Science, v. 251, pp. 789-797.

APPENDIX 1  
THIN-SECTION SAMPLE LOCATION MAP



Table 1. Thin-section samples collected from Block 1.

Drill Holes	Survey Stations
C87-1j 178'	0 vein 1250 level
C87-1q 5'	No. 1 1250 level
C87-1q 23'	No. 3 1250 level
C87-1q 83'	2.5 vein 1250 level
C87-1q 105'	5-20
C87-1s 4'	8-4
C87-1s 20'	8-6
C87-1s 42'	DR 9 1250 level
C87-1s 188'	9-23
C87-1s 230'	10-0
C87-1s 261'	10-6
C87-2b 6'	10-9
C87-2b 28'	10-60
C87-2b 80'	10-116
C87-2b 86'	11-7
C87-2b 122'	12-34
C87-2b 145'	13b-1
C87-2b 175'	13b-42
C87-2b 208'	13e-20
C87-2b 232'	6-20 1450 level (3)
C87-2b 254'	6-29 1450 level
C87-2c 95'	6-40 1450 level
C87-2d 177'	7-10 1450 level
C87-2k 149'	
C87-2o 80'	
C87-2v 293'	
C87-2x 115'	
C87-2z 42'	
C87-3a 98' (2)	
C87-3a 99'	
C87-3a 110'	
C87-3a 112'	
C87-4m 33' (2)	
C87-5n 5'	
C87-5n 33'	
C87-5n 93'	
C87-5n 118'	
C87-5n 160'	
C87-5n 188'	
C87-5n 397'	
C88-7k 34'	
C88-7k 56'	
C88-7m 97'	
C88-7m 190'	
C88-7m 256'	
C88-7m 380' (3)	
C88-7n 16'	

Table 1. cont'd

Drill Holes

C88-7n 48'  
 C88-7n 101'  
 C88-7n 224'  
 C88-8a 21'  
 C88-8a 67'  
 C88-8a 137'  
 C88-8a 150'  
 C88-8a 245'  
 C88-8b 47'  
 C88-8b 121'  
 C88-8c 273'  
 C88-8d 109'  
 C88-8g 150'  
 C88-8g 203'  
 C88-9a 92'  
 C88-9a 188'  
 C99-9b 174'

Table 2. Thin-section samples collected from Block 2.

Drill Holes	Survey Stations
C88-6a 3'	19-52
C88-6a 50'	20-99
C88-6a 81'	22-31 (2)
C88-6a 111'	22-52
C88-6a 133'	22-68
C88-6a 163'	22-101
C88-6a 192'	LHS
C88-6a 220'	24-23
C88-6a 222'	25-5
	28-10 (2)
	29-0
	29-10
	31-30
	37a-18
	38-0 (4)
	LRCS
	FD
	FDE
	B3-0
	B3-1
	B3-2

Table 2. cont'd.

=====  
Rib and outcrop

B3-3  
B3-4  
B3-5  
LHS-15  
A-LHS-1550 level (2)  
LHS-1550 level (2)  
1550-ws  
1550 (3)  
1550-1  
1550-2  
1550-3 (2)  
TB2

Table 3. Thin-section samples collected from Block 3.

=====  
Rib and outcrop

1645 (4)  
CCB3 (2)  
WF

Table 4. Thin-section samples collected from other parts of the district.

=====  
Drill Holes

I88-2a 32'  
I88-2a 169'  
I88-2a 187'  
SR-1a 717'  
SR-2b 707'  
SR-4a 646'

Outcrop

CR (C-reef)  
SR (Saddle Rock)  
OB-1 (Old Butte)



1

Samples numbered in the #-# format are underground rib samples and labeled as follows:

Survey station-Distance in feet from Point  
Ex. 22-101= Sample taken 101 feet  
north from survey station 22.

2

Drill hole samples are listed with the station and hole designation followed by the footage down hole.

3

All other samples are numbered according to the nearest permanent physical marker, feature, or geographic point.

Table 5. Samples collected for X-ray diffraction analyses.

SAMPLE NO.	DRILL HOLE	FOOTAGE
190850	C87-1j	100'-105'
190900	C87-1j	350'-355'
190910	C87-1j	400'-405'
190920	C87-1j	450'-455'
190930	C87-1j	500'-505'
198678	C87-5n	145'-150'
198688	C87-5n	195'-200'
198698	C87-5n	245'-250'
198710	C87-5n	305'-310'
198196	C88-6a	50'-55'
198255	C88-6a	95'-100'
198267	C88-6a	155'-160'
198275	C88-6a	195'-200'

APPENDIX 2  
GEOCHEMICAL SAMPLES

# 1250 CHIP SAMPLES

Asamera Minerals

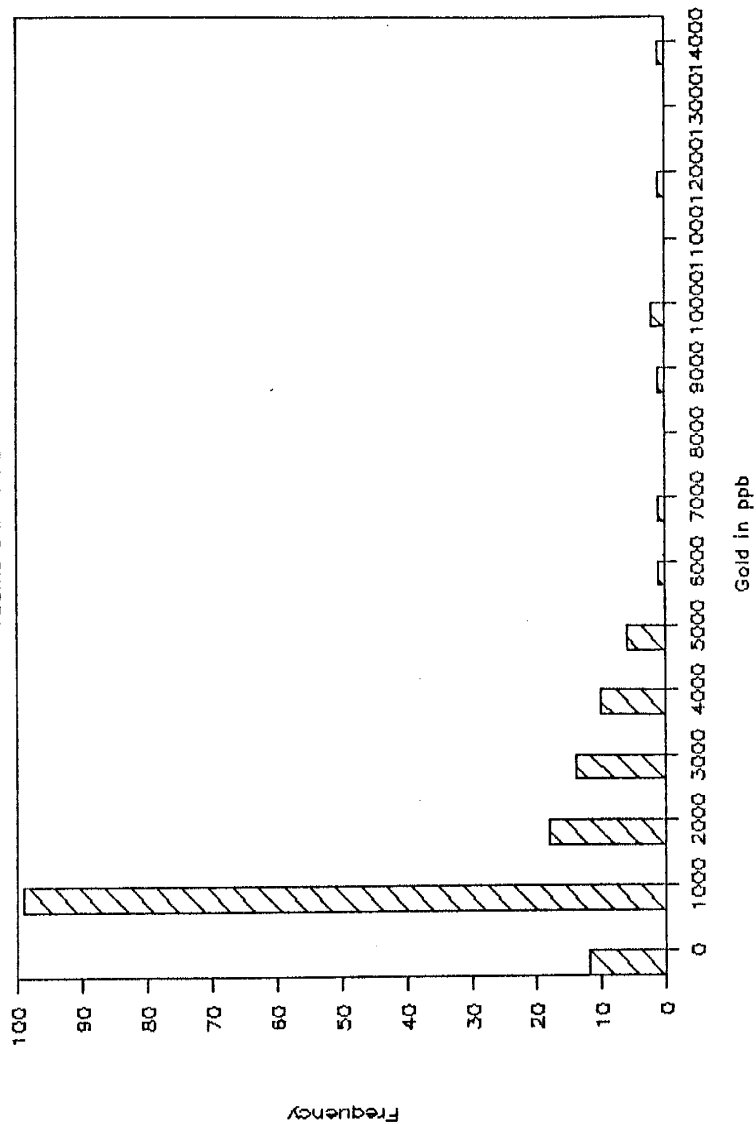


Figure 1-- Histogram plot of gold values in channel samples from the 1250 level in Blocks 1 and 2. Sampling by Asamera Minerals. n = 167.

# 1250 CHIP SAMPLES

Asamera Minerals

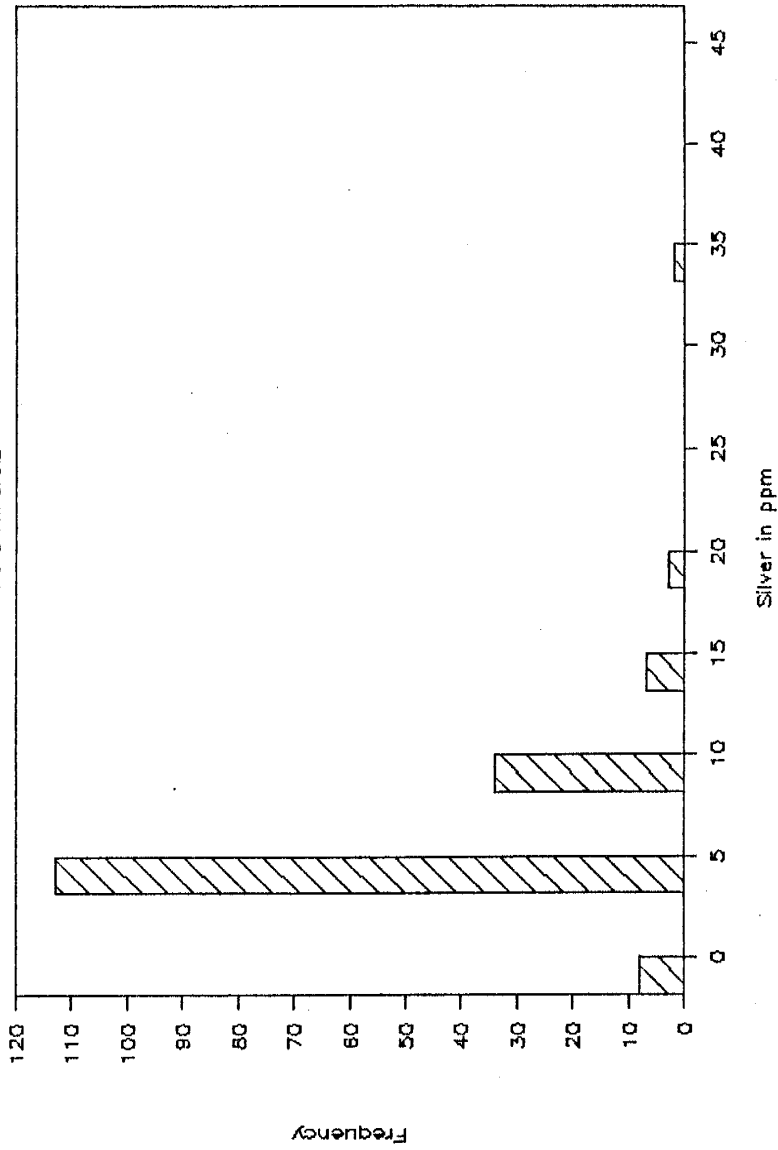


Figure 2-- Histogram plot of silver values in channel samples from the 1250 level in Blocks 1 and 2. Sampling by Asamera Minerals. n = 167.

# 1250 LEVEL SAMPLES

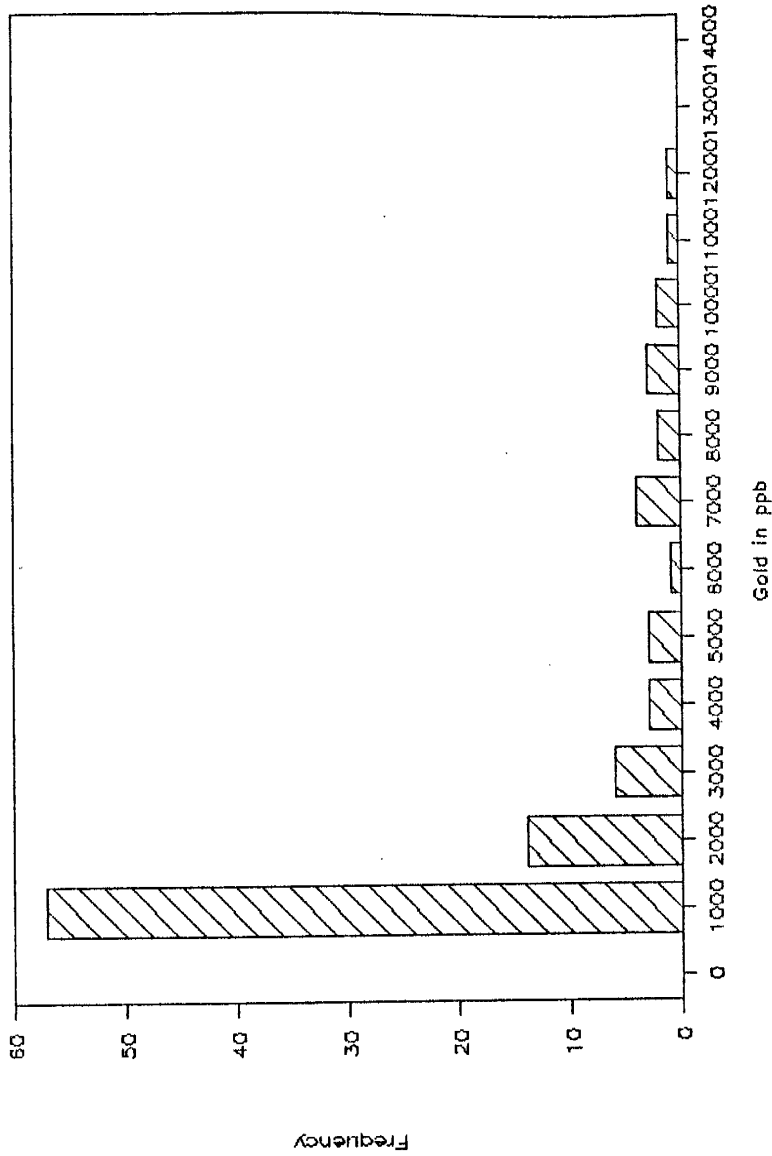


Figure 3-- Histogram plot of gold values in channel samples from the 1250 level of Block 1. Sampling by United Mining Corporation. n = 99.

1250 LEVEL SAMPLES

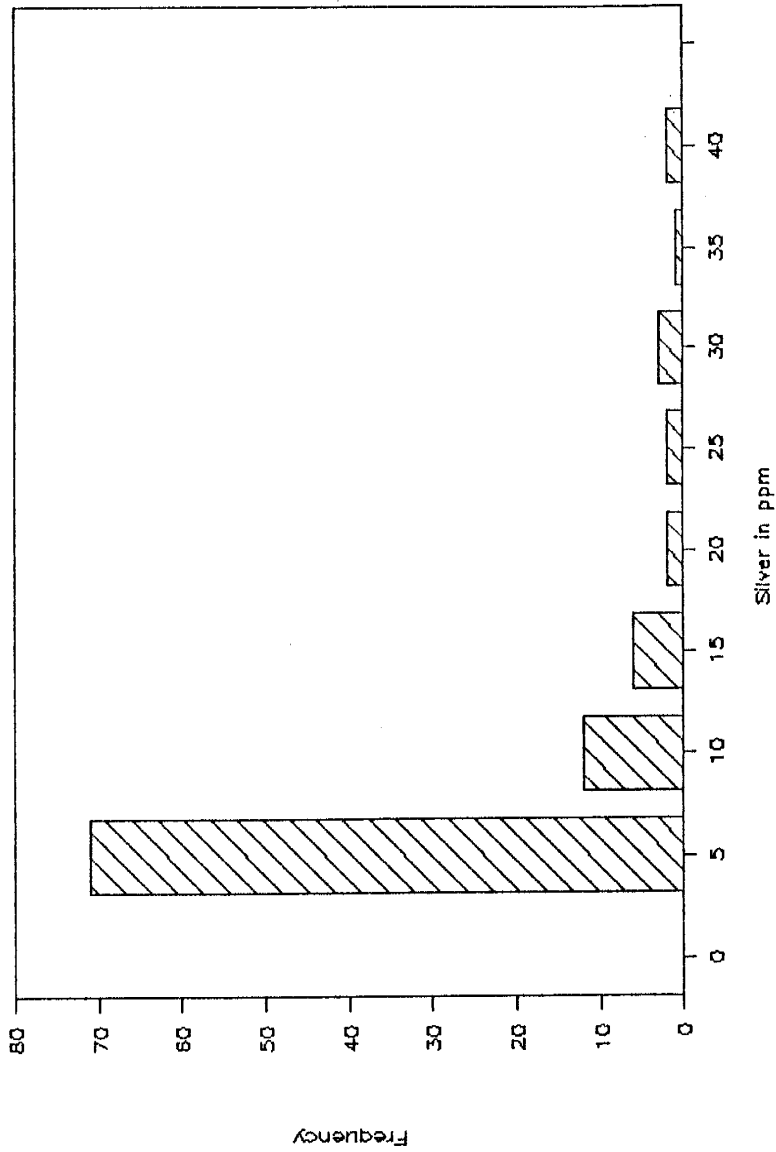


Figure 4-- Histogram plot of silver values in channel samples from the 1250 level of Block 1. Sampling by United Mining Corporation. n = 99.

1250 BLOCK 2  
Asamera Minerals

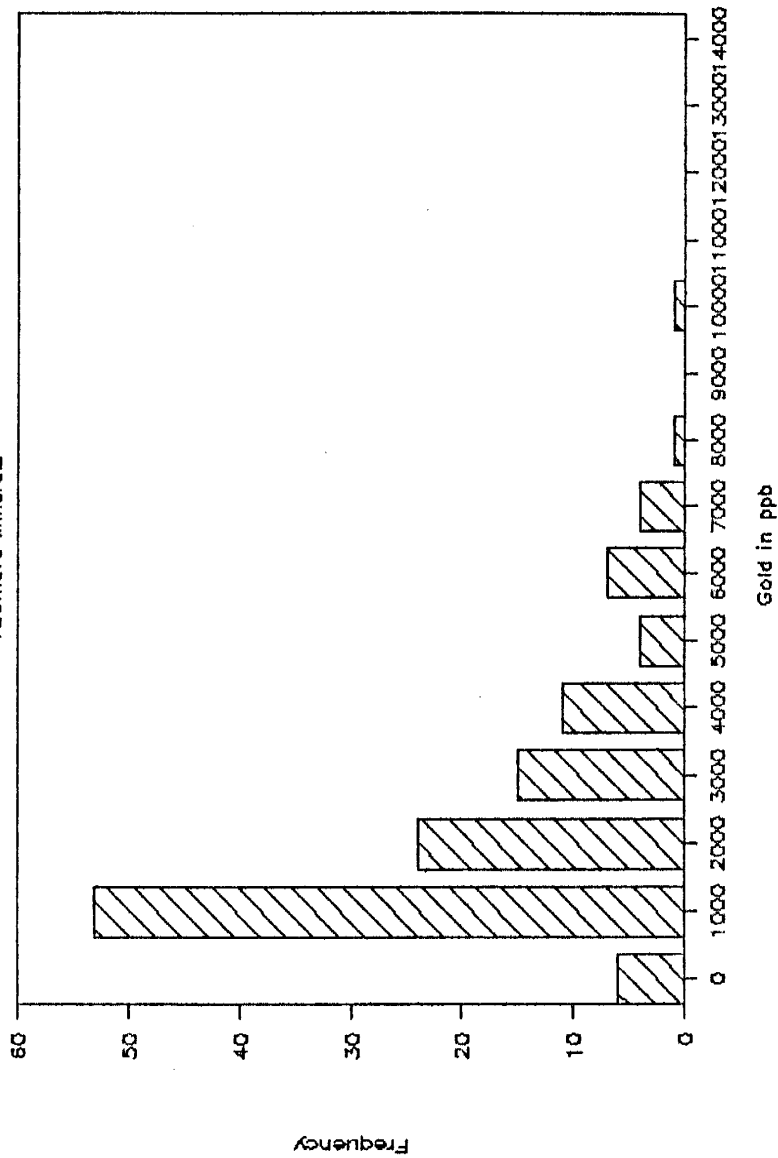


Figure 5-- Histogram plot of gold values in diamond drill holes from Block 2. Sampling by Asamera Minerals. n = 131.

1250 BLOCK 2  
Asamera Minerals

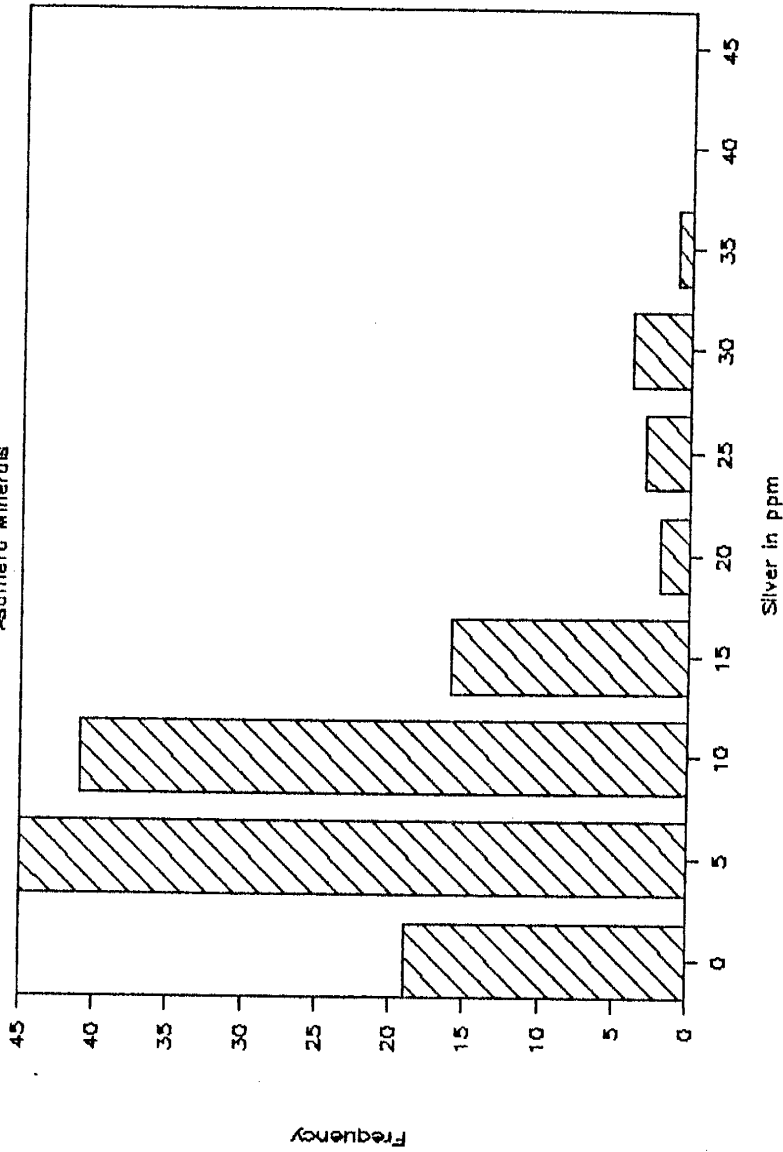


Figure 6-- Histogram plot of silver values in diamond drill holes from Block 2. Sampling by Asamera Minerals. n = 131.



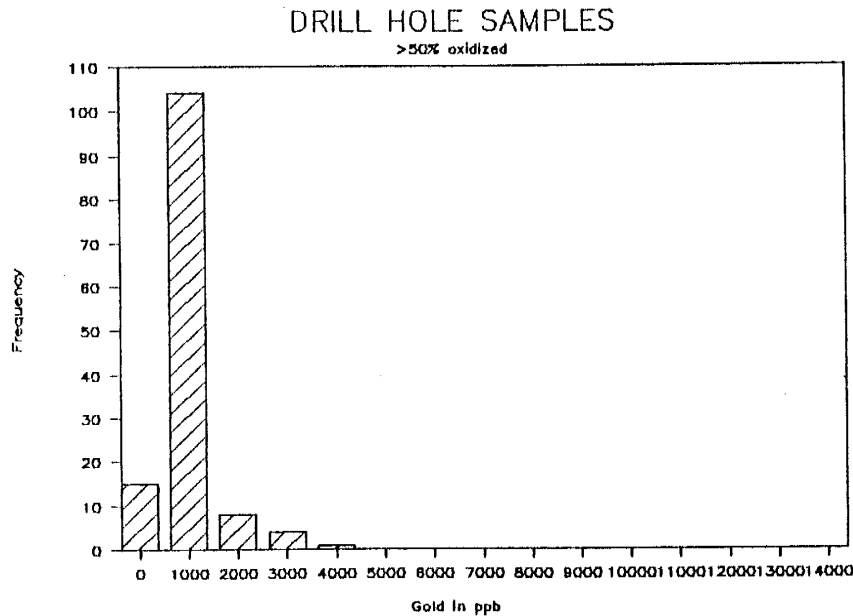
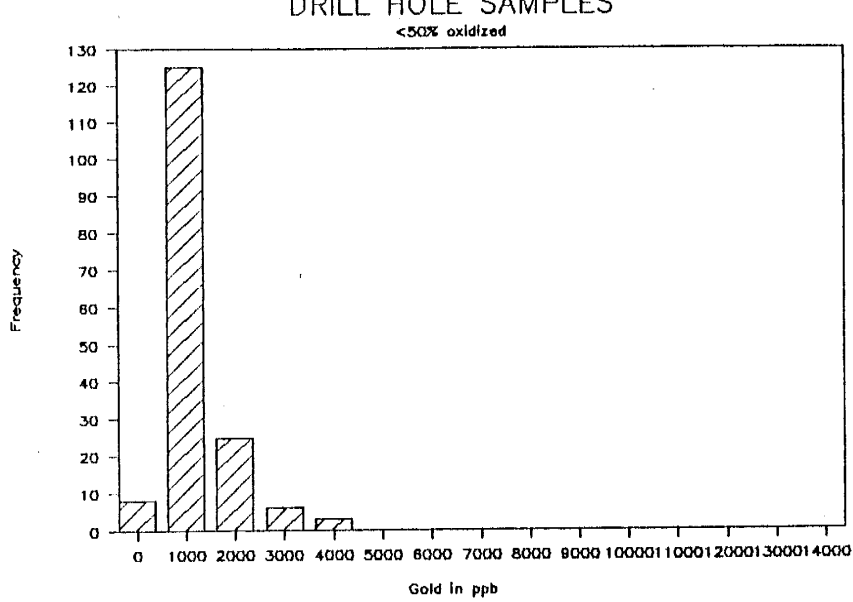


Figure 7-- Histogram plot of gold values in diamond drill holes from Block 1. Sampling by Asamera Minerals. n = 299.

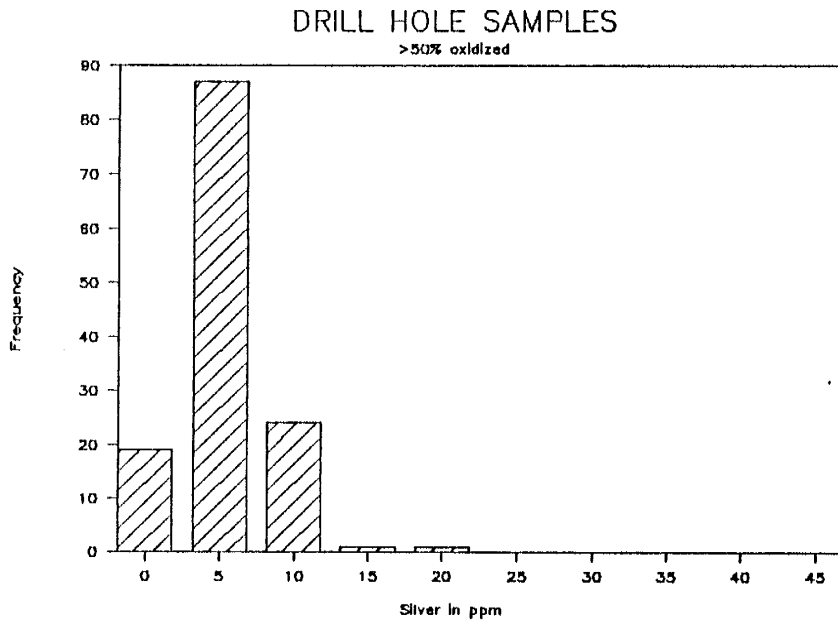
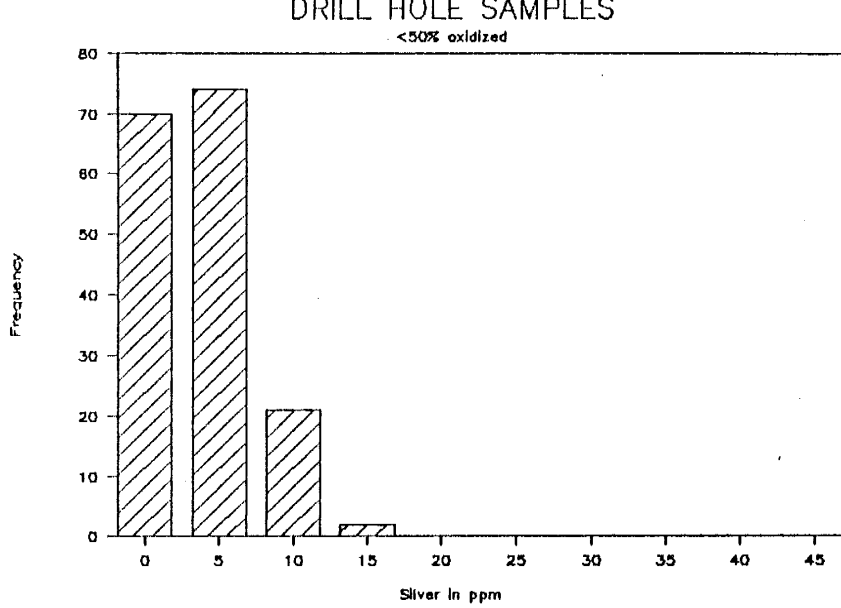


Figure 8-- Histogram plot of silver values in diamond drill holes from Block 1. Sampling by Asamera Minerals.  
n = 299.

1250 LEVEL SAMPLES

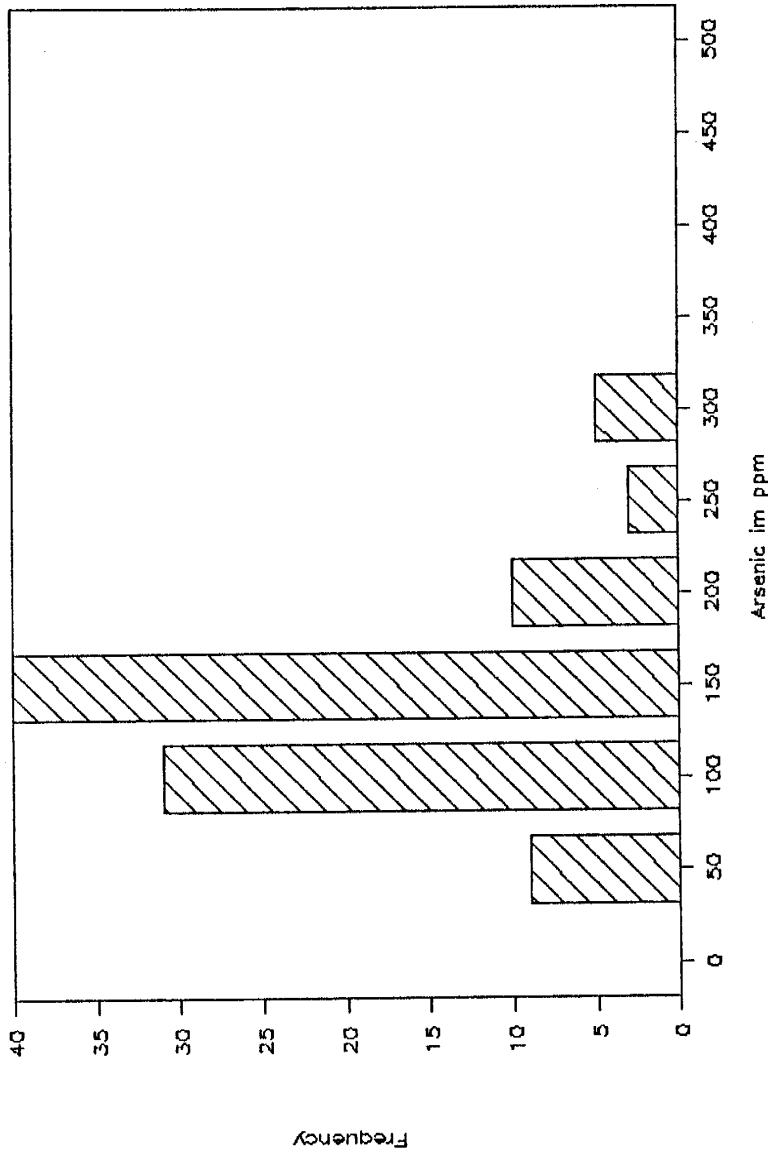


Figure 9-- Histogram plot of arsenic values from the 1250 level of Block 1. Sampling by United Mining Corp. n = 99.

1250 LEVEL SAMPLES

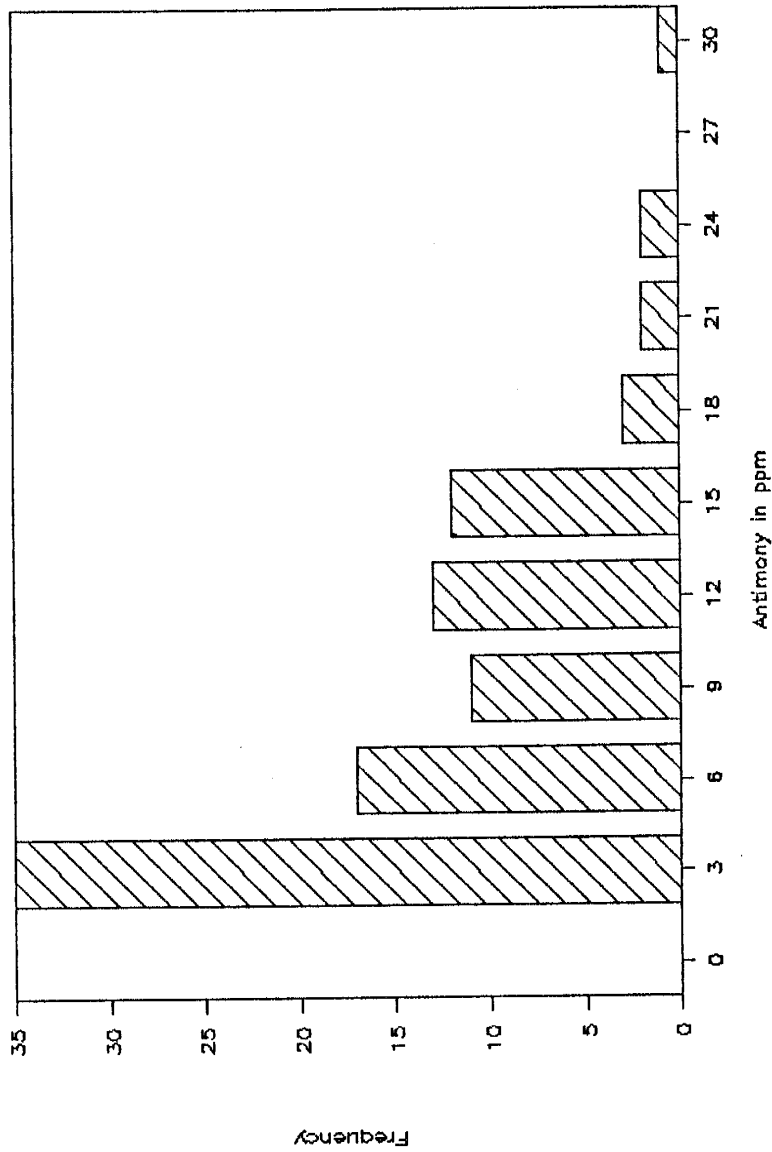


Figure 10-- Histogram plot of antimony values from the 1250 level of Block 1. Sampling by United Mining Corp. n = 99.

# 1250 LEVEL SAMPLES

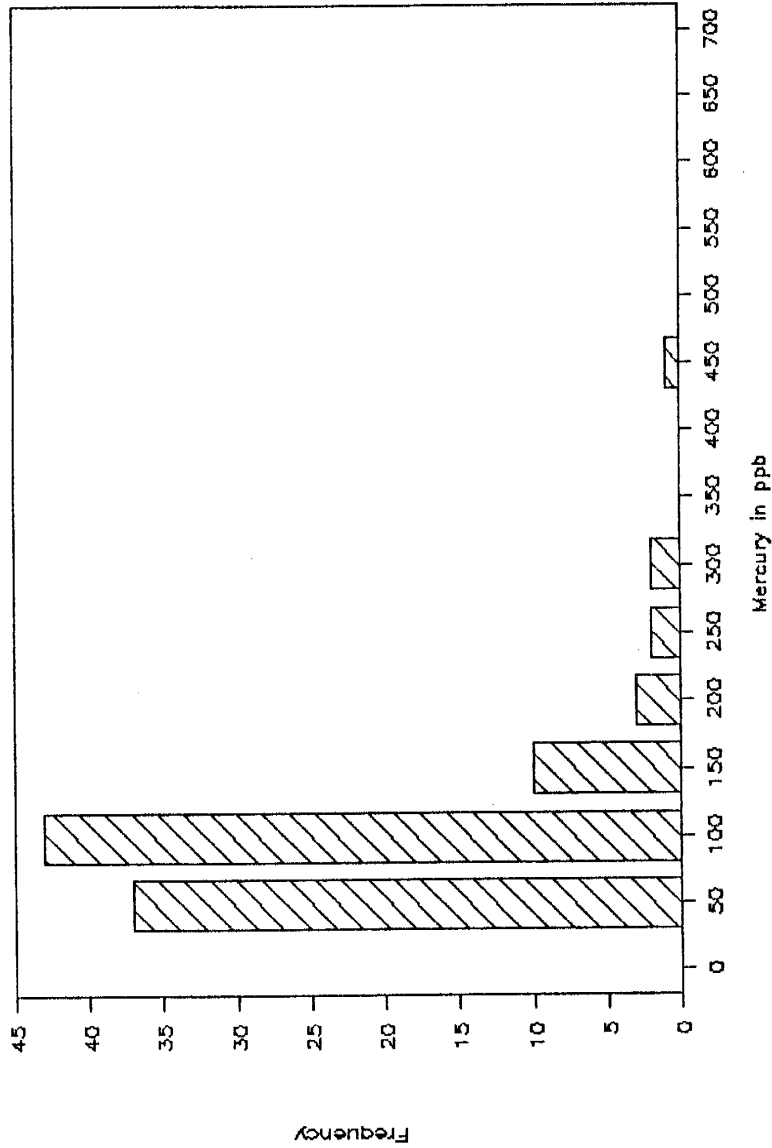


Figure 11-- Histogram plot of mercury values from the 1250 level of Block 1. Sampling by United Mining Corp. n = 99.

1250 LEVEL SAMPLES

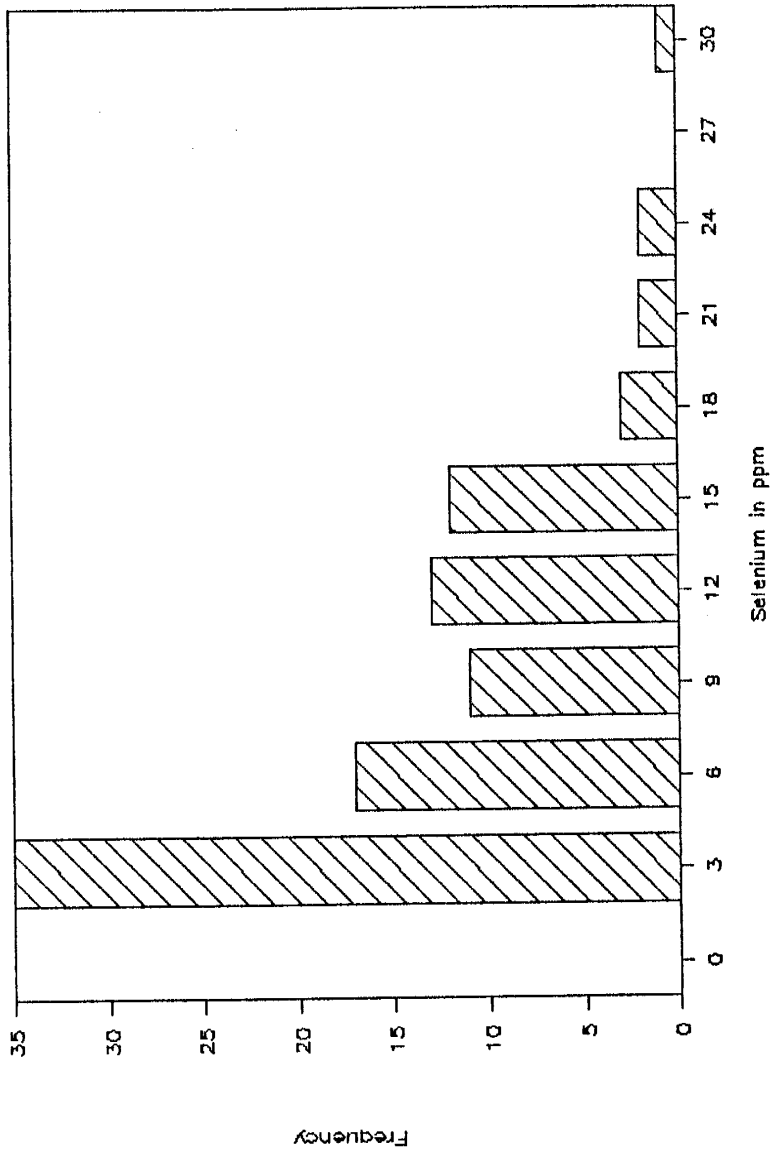


Figure 12-- Histogram plot of selenium values from the 1250 level of Block 1. Sampling by United Mining Corp. n = 99.

# 1250 LEVEL SAMPLES

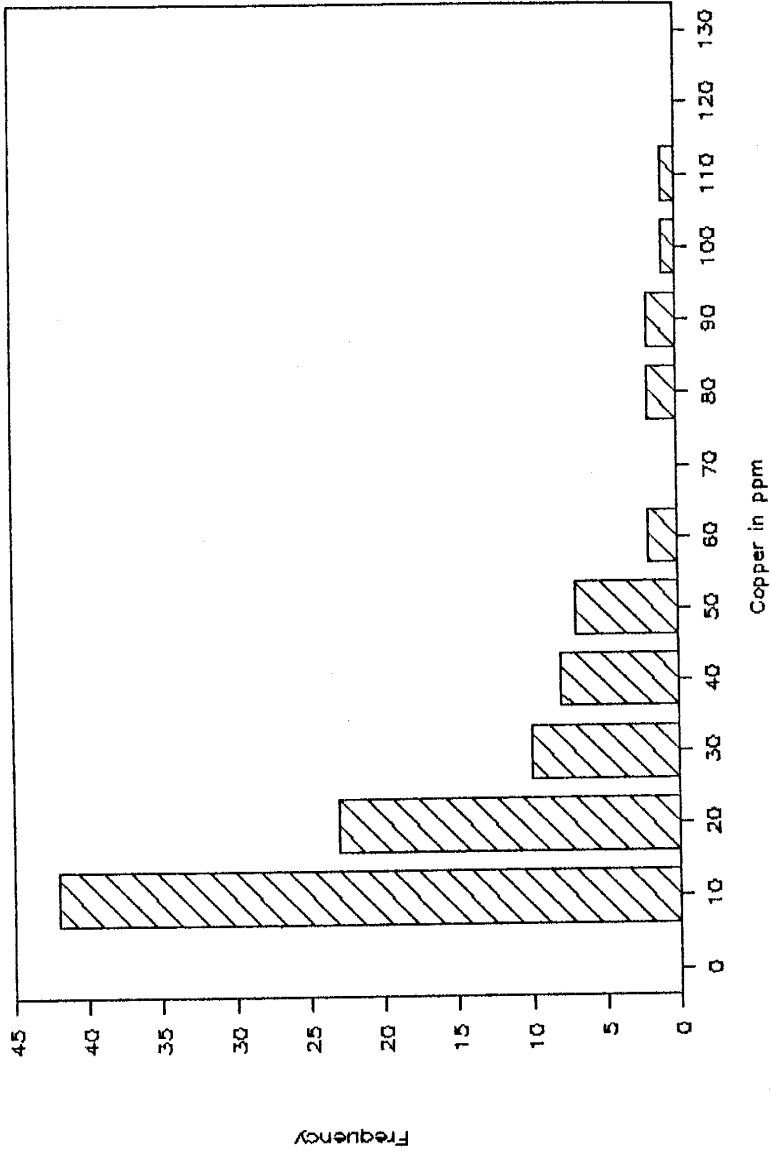


Figure 13-- Histogram plot of copper values from the 1250 level of Block 1. Sampling by United Mining Corp. n = 99.

# 1250 LEVEL SAMPLES

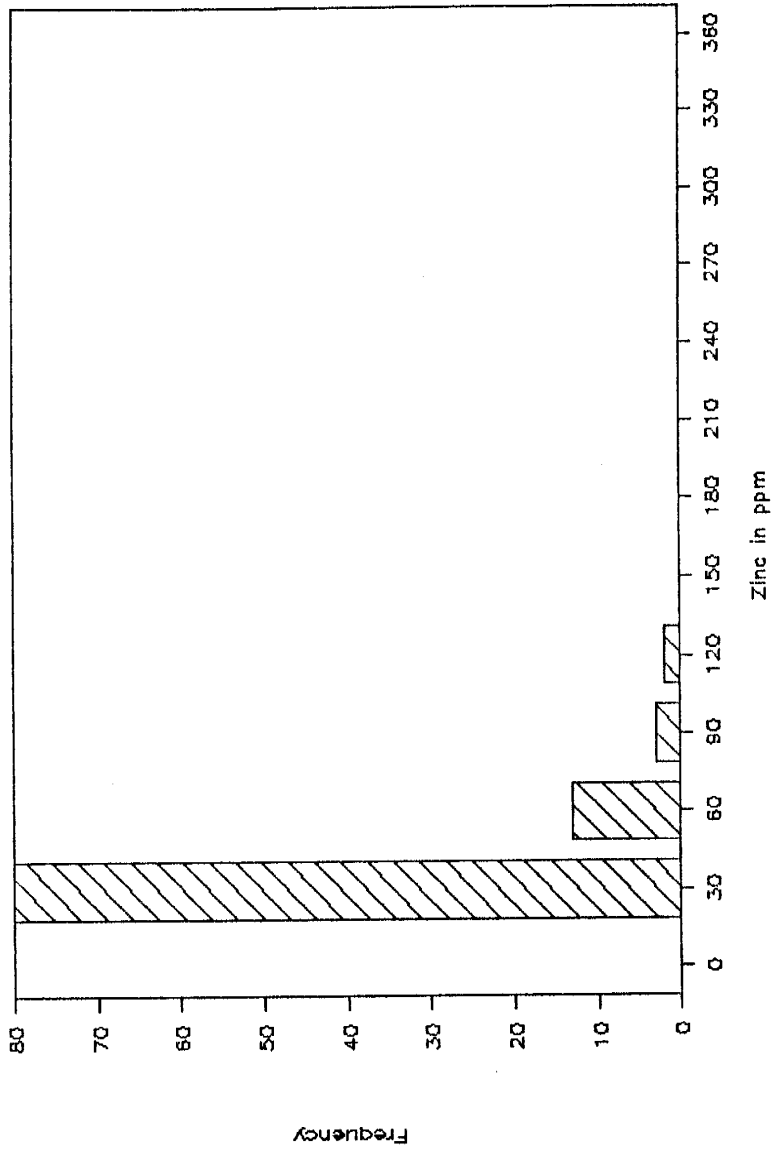


Figure 14-- Histogram plot of zinc values from the 1250 level of Block 1. Sampling by United Mining Corp. n = 99.



1250 LEVEL

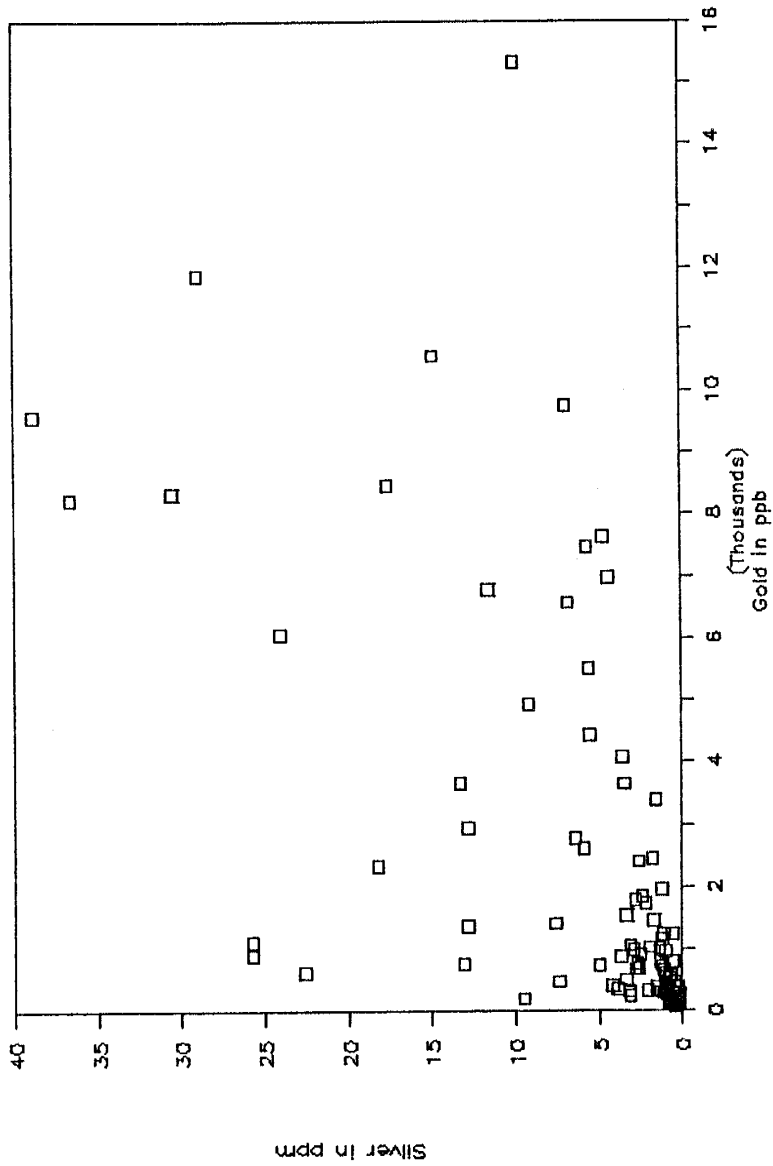


Figure 15-- Linear plot of silver vs. gold in channel samples taken by United Mining on the 1250 level. n = 99.

# 1250 BLOCK 2

Asamera Minerals

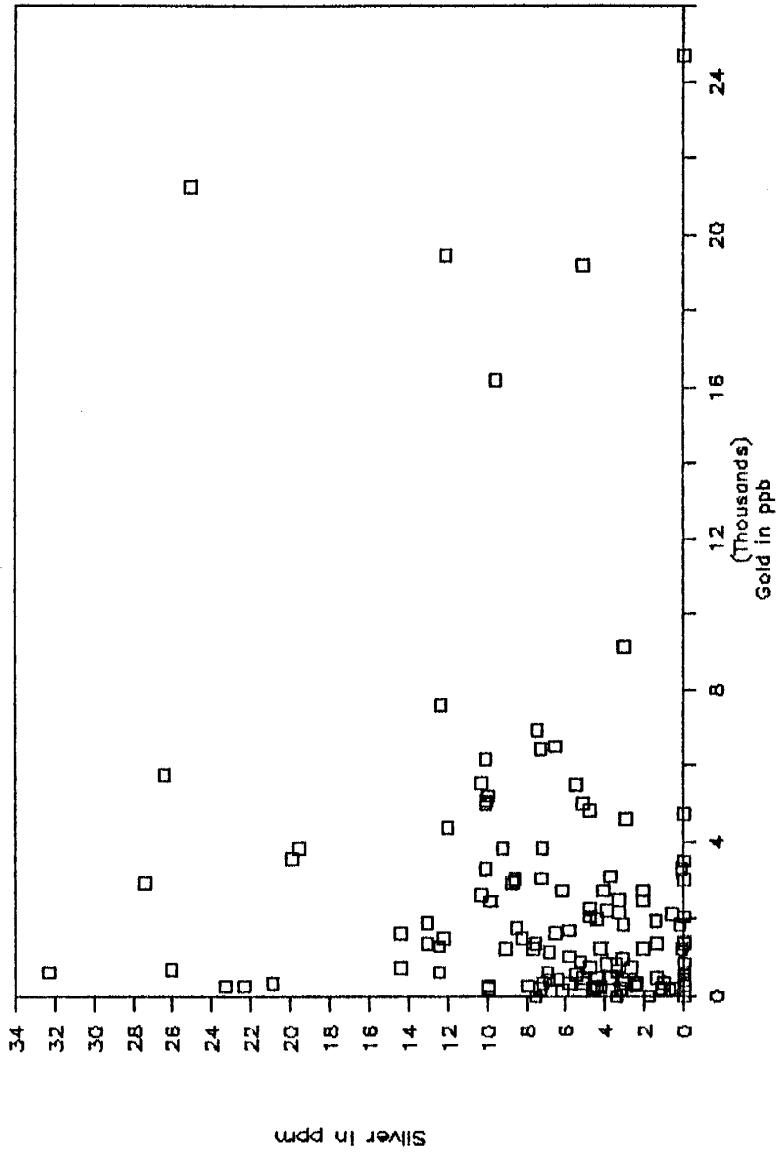


Figure 16-- Linear plot of silver vs. gold in drill hole samples from Block 2 taken by Asamera Minerals. n = 131.

# 1250 CHIP SAMPLES

Asamera Minerals

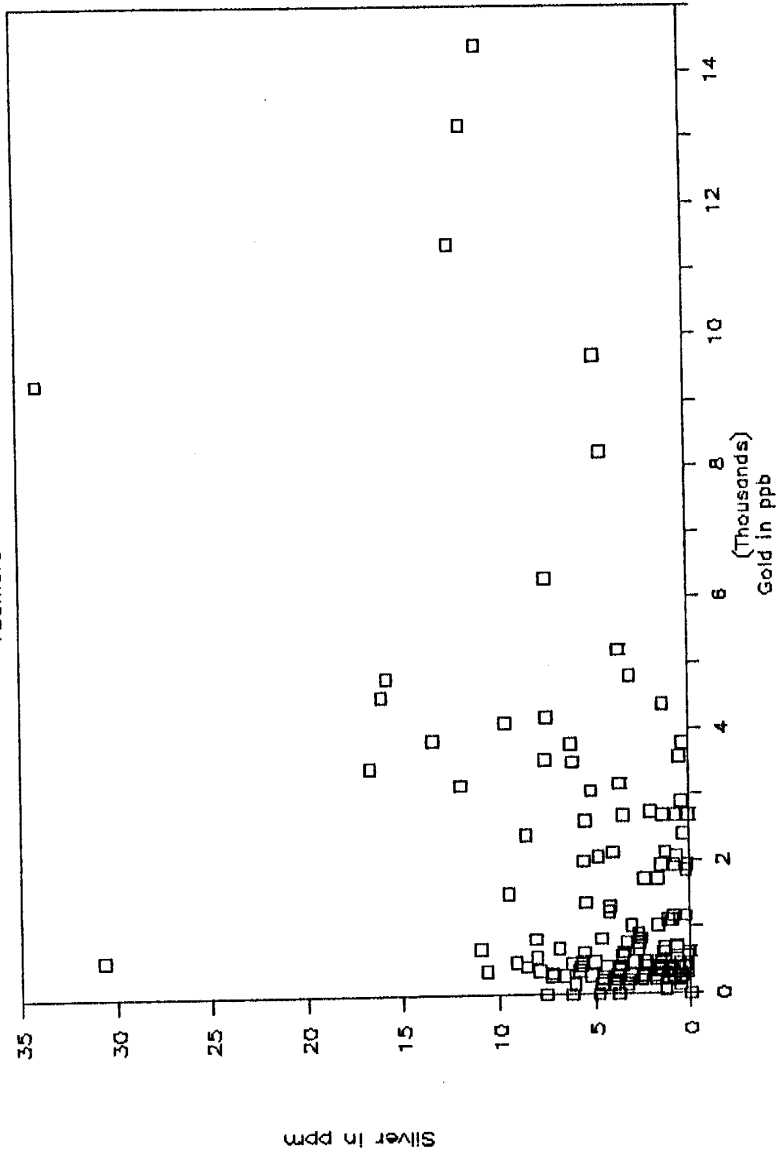


Figure 17-- Linear plot of silver vs. gold in channel samples taken by Asamera Minerals from the 1250 level in Blocks 1 and 2. n = 167.

1250 LEVEL

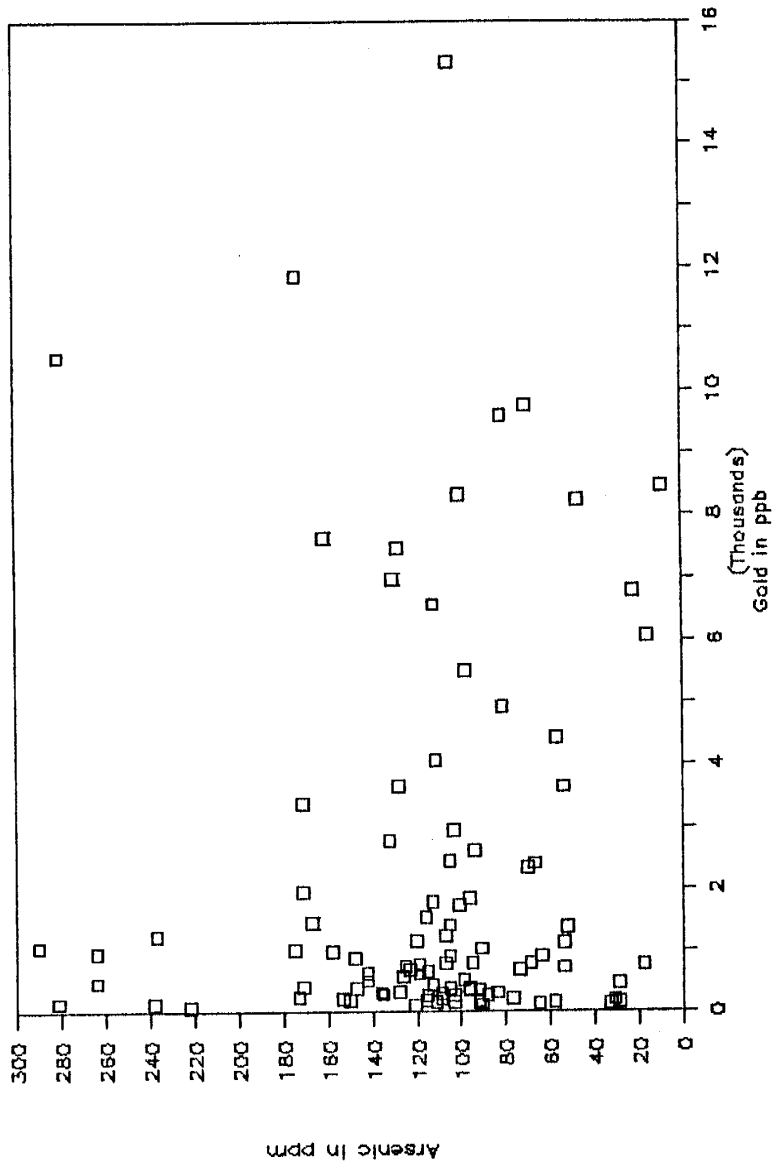


Figure 18-- Linear plot of arsenic vs. gold in samples from the 1250 level in Block 1. Sampling by United Mining. n = 99.

1250 LEVEL

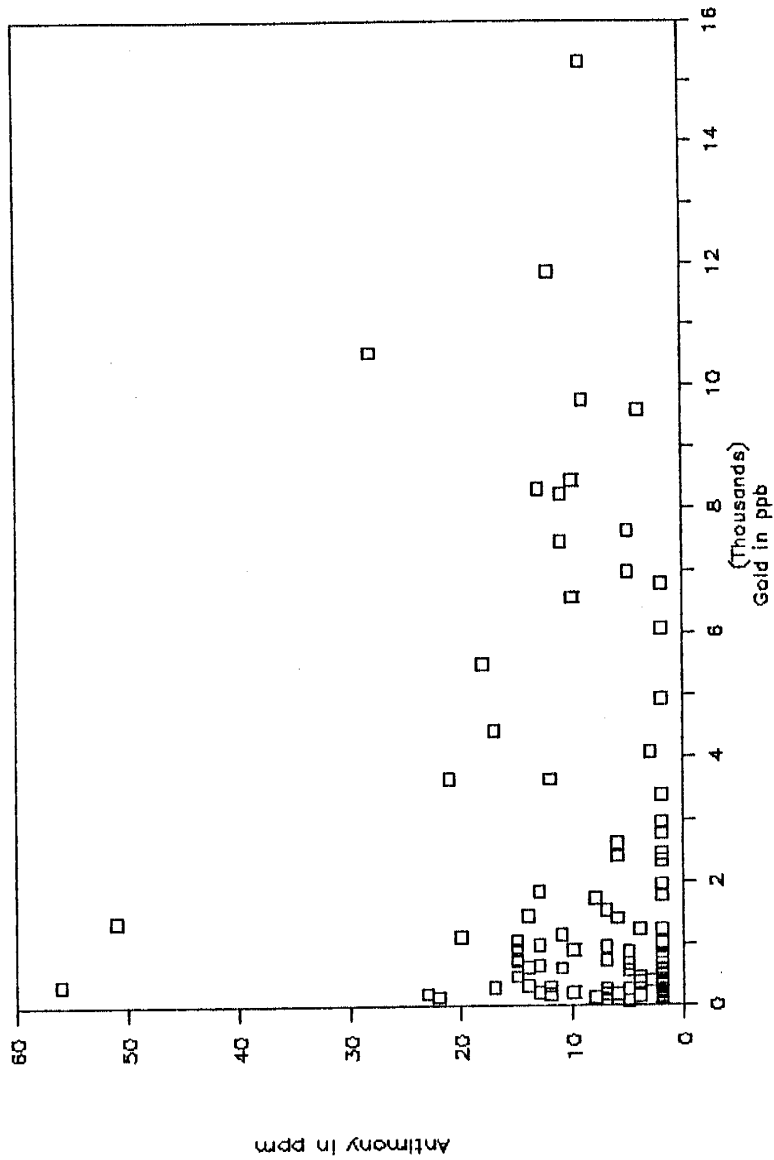


Figure 19-- Linear plot of antimony vs. gold in samples from the 1250 level in Block 1. Sampling by United Mining. n = 99.

1250 LEVEL

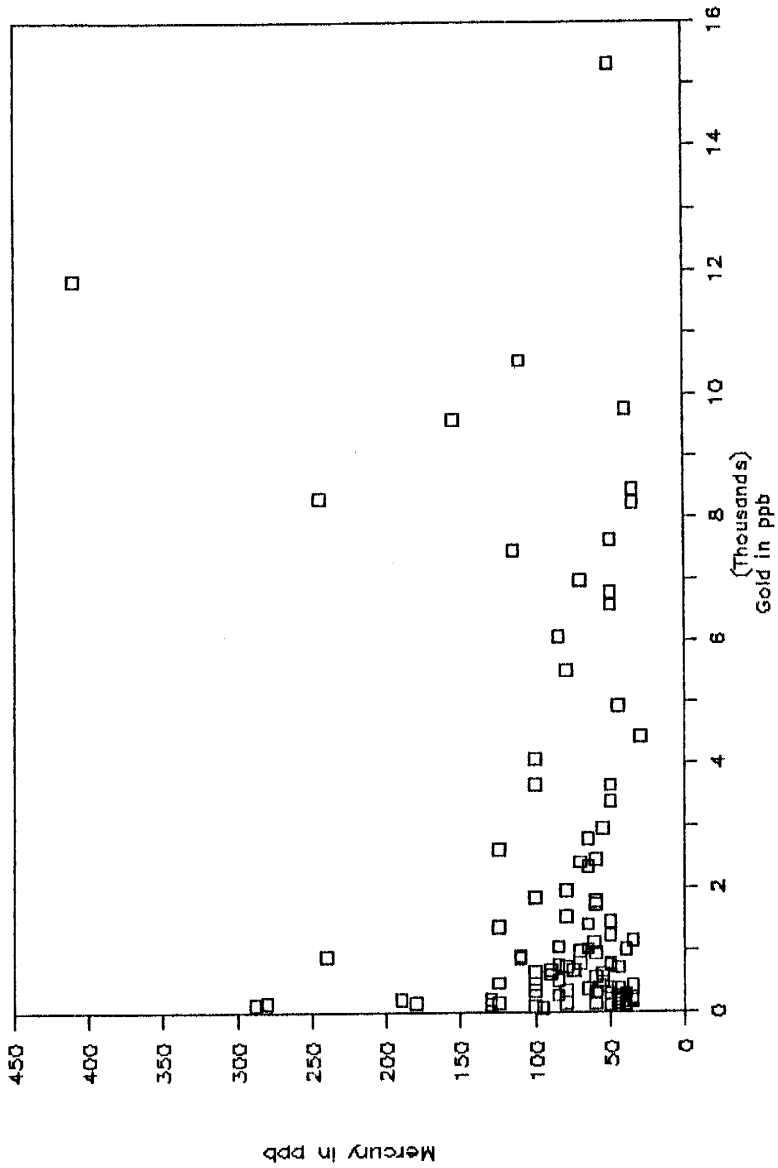


Figure 20-- Linear plot of mercury vs. gold in samples from the 1250 level in Block 1. Sampling by United Mining. n = 99.

1250 LEVEL

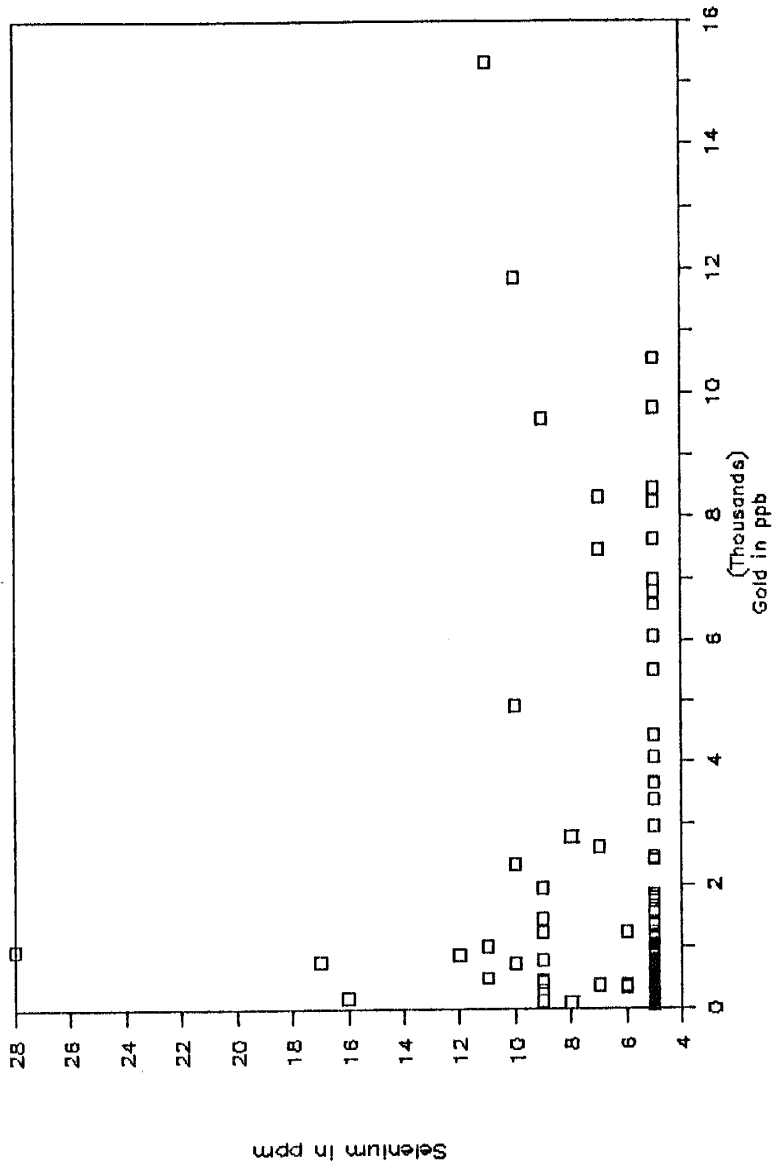


Figure 21-- Linear plot of selenium vs. gold in samples from the 1250 level in Block 1. Sampling by United Mining. n = 99.

1250 LEVEL

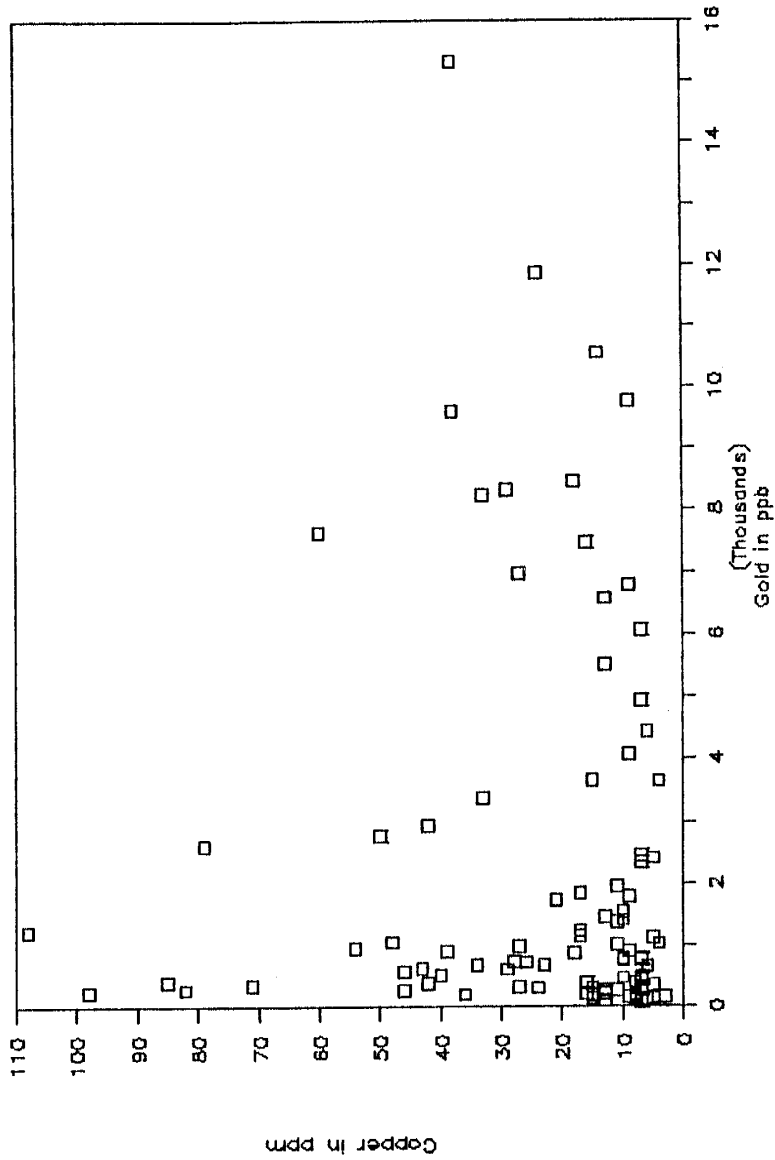
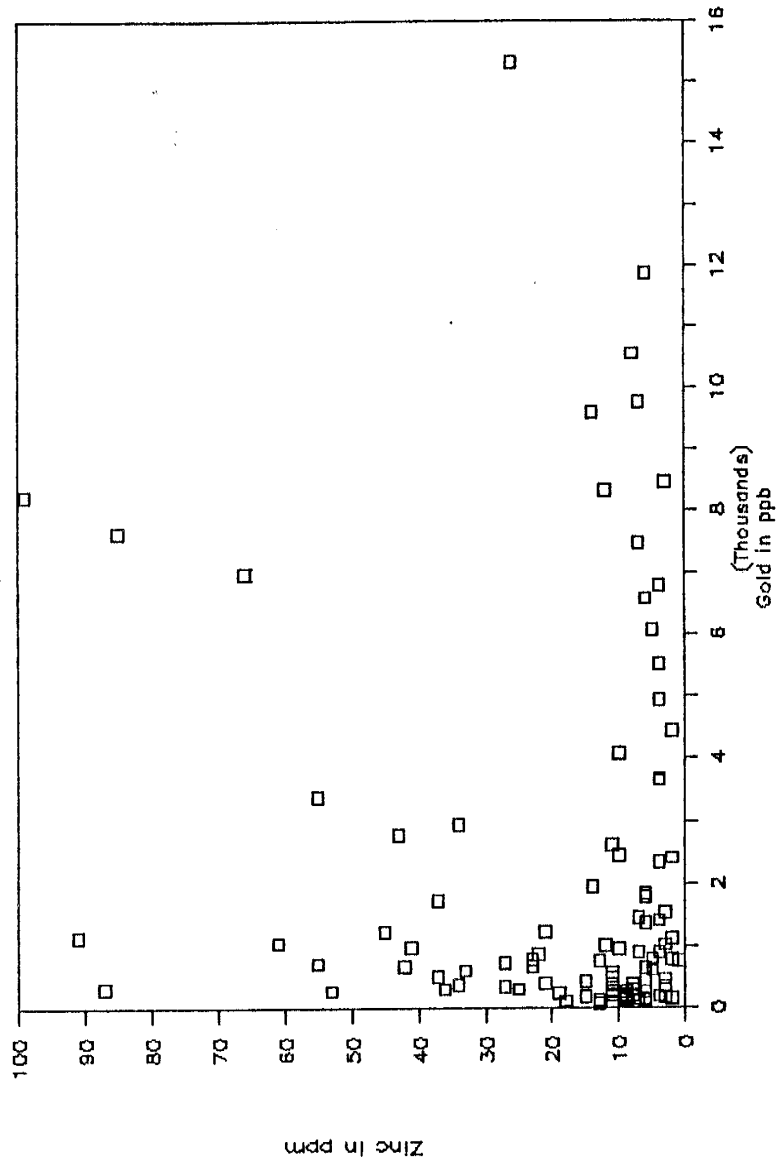


Figure 22-- Linear plot of copper vs. gold in samples from the 1250 level in Block 1. Sampling by United Mining. n = 99.



1250 LEVEL



This thesis is accepted on behalf of the faculty  
of the Institute by the following committee:

*William X. Keenan, Jr.*

Advisor

*Andrew Campbell*

*David L. Norman*

*May 7, 1990*

Date